Camber-Car Design & Dynamics

Tristan French, E.I.T.
tristan.french@gmail.com

Alissa Roland, E.I.T.
alissaroland3@gmail.com

Subsystem Lead:
Maximilian Sluiter, E.I.T.
maximiliansluiter@gmail.com

Mechanical Engineering Department

California Polytechnic State University

San Luis Obispo

2013

Contents

List of Figures

Abstract & Background

The purpose of this project was to design a suspension that would improve the performance of the Cal Poly SAE Formula Electric car around a racing track. Performance would be quantified through skidpad, slalom, and straight-line acceleration tests as well as autocross lap times. The approach to meeting the objective was to increase the steady-state lateral acceleration and quicken the transient response while maintaining predictable handling so that the driver could extract maximum performance from the car.

The Cal Poly Formula Electric car has used a "camber car" configuration for the past several years. This design is characterized by the tops of the tires leaning inwards towards the chassis and was first proposed in 1949 by William F. Milliken, though it was not actually tested until 1968 and his evaluations lasted until the early 1980's. Results were not widely publicized so the camber car is still a relatively unknown concept.

Further testing of the concept was still necessary to fully understand the benefits and drawbacks of cambered tires, and to compare them directly to conventional car racing tires. As a result, the team was looking for someone to design a new suspension for the 2013 car with these goals in mind. Maximilian Sluiter volunteered for this task and proposed the senior project during the summer. Alissa Roland and Tristan French then joined the team.

Max was responsible for designing the suspension in CAD and did extensive background research. Alissa and Tristan were responsible for sizing wheel bearings, analyzing the old suspension, and doing most of the load and stress analysis before the design freeze. They also spearheaded the manufacturing.

According to research, maximum lateral grip is achieved at a high-negative camber angle (-40 degrees) but best longitudinal acceleration is had with no camber. The original design for the suspension was a passive, dynamic camber system which varied the camber in order to provide maximum grip in a straight line as well as in turns. The scale of this design was deemed to be too large for the time, resources, and manufacturing skill of the Formula Electric team this year. Therefore, it was decided to produce a highly adjustable static camber suspension that could be tuned best performance as well as adjusted to allow for testing of the dynamic camber concept.

The final design used the "5 link" concept on each corner of the car, with 6 simple-to-manufacture tension-compression members per wheel. Analysis consisted primarily of pseudo-statics to find forces in the links so that they could be sized for minimum weight and adequate strength. Component testing and validation consisted of Instron testing for link buckling, link thread pullout, link tensile strength, and rod end buckling. Testing on the suspension as a whole will involve skidpad tests to find the maximum steady state lateral acceleration from various camber configurations as well as acceleration tests to find the effect of camber on longitudinal acceleration. The goal will be to find the best static camber setup and determine if a dynamic camber system, active or passive, would actually provide a significant advantage if the manufacturing resources were available to build it.

Fundamental Tire & Vehicle Dynamics

Tires generate the majority of the forces necessary for accelerating, decelerating, and turning a ground vehicle (aerodynamic devices which could provide additional maneuvering forces as well as downforce to increase tire grip will not be covered in this report). A vehicle's suspension system links the four tires to the "sprung mass", which is essentially the chassis and everything rigidly mounted to it. The term "unsprung mass" is applied to the tires, wheels, and some fraction of the inertia of each component of the suspension mechanism. Those fractions are based on the kinetic energy of the particular piece of the mechanism with respect to a single, simpler variable – usually the vertical displacement of the wheel. The unsprung mass on each corner of the car is separated from the ground by the compliant tire, modeled as a spring of between 100 and 350 kN/m stiffness[1] and sometimes a weak damper. It is separated from the sprung mass by the suspension spring(s), damper(s), and in some cases inerter(s).

Suspension Basics

The purposes of a suspension system are as follows:
- Transfer forces from the tires to the sprung mass.
- Put the tire in the correct orientation to the road for maximum grip.
- Isolate the sprung mass from road irregularities.
- Manage the load on each tire to provide the best grip.

While meeting the requirements stated above, the suspension should also have as little inertia as possible. This not only reduces the total car mass but more importantly reduces the effective unsprung mass. Reducing the ratio of unsprung to sprung mass helps keep the load on each tire closer to optimal and improves the ride (isolates the sprung mass) from high frequency road inputs because the highly-underdamped wheel-tire system then has a higher natural frequency. This higher "wheel hop" frequency means that the unsprung mass is not excited as much by inputs from bumps in the road. Since the unsprung masses' motions are the forcing functions for the sprung mass, less unsprung mass excitation means less disruption of the sprung mass. The components with the largest effect on unsprung mass in most suspension systems are the uprights (which hold the wheel bearings and hubs), the wheels, the tires, and any brake components that may be mounted outboard. Lighter wheels and tires have the added benefit of reducing the inertia that the drivetrain must accelerate and reducing gyroscopic forces (which are usually not a significant factor in four-wheeled vehicle dynamics). For these reasons, lighter wheels are one of the best upgrades for any car.

Tire Basics

Tires generate forces through their interaction with the road surface. The normal load (weight) on a tire causes it to deform out of round and form a "contact patch" or "footprint" which grips the road via several mechanisms. These include mechanical interlocking, whereby the soft rubber is squeezed into small crevices in the road surface and acts like teeth in a rack and pinion gear mesh, and chemical bonding. Deformation of the contact patch is resisted by a distributed force arising where the rubber meets the road. This force pushing back on the tire is

---

[1] Cossalter, Vittore: <u>Motorcycle Dynamics</u>, 2nd ed., page 56

transferred through the suspension to the sprung mass in order to accelerate, turn, and brake the car as a whole. The objective of the suspension design in this report was to improve both steady-state lateral acceleration and transient response for better handling. Therefore, lateral force and the mechanisms to generate it will be the focus of the following discussion, with less explanation given for the source of tractive (acceleration and braking) forces since they also arise from a deformation of the contact patch, just in a different direction.

There are two main methods to deform the tire for the purpose of generating lateral force: slip angle and inclination angle. To understand what these terms mean, please refer to Figure 1. Slip angle results when a tire is steered about an axis normal to the road. Inclination angle is a tilting of the tire about an axis parallel to the plane of the road and orthogonal to both the slip angle axis and the axis about which the wheel rotates (the axis defined physically by the wheel bearings in the upright). In the figure, "direction of wheel travel" can be thought of as the direction the car is moving (in reality it takes into account both rotation and translation and so is a local velocity vector on the car) and "direction of wheel heading" is the direction the wheel is pointing or being steered towards. Slip angle is given the symbol of the Greek letter alpha (α) and inclination angle gamma (γ). Inclination angle is shown measured from the vertical axis passing through the contact point (or the center of the contact patch) to the dotted line which is in the plane of the wheel and passes through both the contact point and the axis of rotation (rotation is called "spin" in the diagram).

Positive Inclination Angle

γ

Aligning Torque M_z

Wheel Plane

Direction of Wheel Heading (Wheel Plane) +x

Longitudinal (Tractive) Force F_x

Rolling Resistance Moment M_y

α

Direction of Wheel Travel

Positive Slip Angle

Road Plane

R_ℓ

Torque $T = F_x R_\ell + M_y \cos \gamma + M_z \sin \gamma$

Spin Axis

Center of Tire Moment (Origin 0)

Overturning Moment M_x

Lateral Force F_y

+y

+z

Normal Force F_z
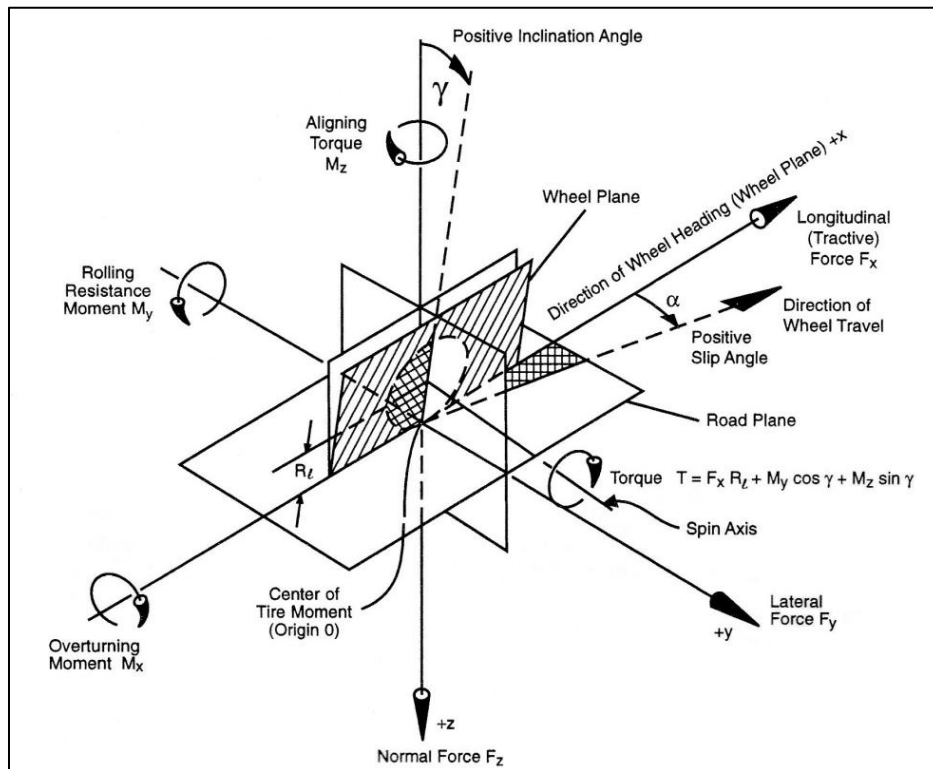
Figure 1: SAE Tire Axes[2]

[2] Milliken, William F. & Douglas L.: <u>Race Car Vehicle Dynamics</u>, page 62

Slip Angle

The manners in which slip angle and inclination angle deform the contact patch are different. With slip angle, the tire is twisted. As shown in the diagram of Figure 1, this comes about because the wheel is restrained to rotate about the axis defined by the wheel bearings, but the velocity of the upright in which the wheel bearings are mounted does not align with the plane of the wheel. Therefore, when a tread element (which can be infinitesimally small) makes contact with the road it adheres and stays in place while the wheel rolls over it and the next tread element enters the contact patch and sticks. The first tread element is now directly behind the second, with the tread elements aligned to the velocity vector of the upright (direction of wheel travel) rather than the tangential velocity on the bottom of the wheel (direction of wheel heading). This means that the tire must distort in the section of sidewall and carcass between the wheel rim and contact patch. The distortion of the tire combined with its stiffness causes both a lateral force and a restoring moment (which attempts to remove the twisting deformation and align the wheel heading to the direction of travel). The force and moment are reacted through the tire's grip on the road (which is the fixed reference frame) and the compliment of that force causes the car to accelerate laterally in response. A diagram of this deformation can be seen in Figure 2, which is from a viewpoint of an observer below a transparent road surface and with the plane of the wheel along the x-axis. The curved line to the left of point A is the result of the lateral stiffness of the tire carcass (in the range of 100 to 200kN/m)[3] causing the deflection in the contact patch to propagate forward. The tread element makes contact at A, proceeds through B and H, and leaves the road at D.[4]

---

[3] Cossalter, Vittore: Motorcycle Dynamics, 2nd ed., page 56
[4] Milliken, William F. & Douglas L.: Race Car Vehicle Dynamics, page 22
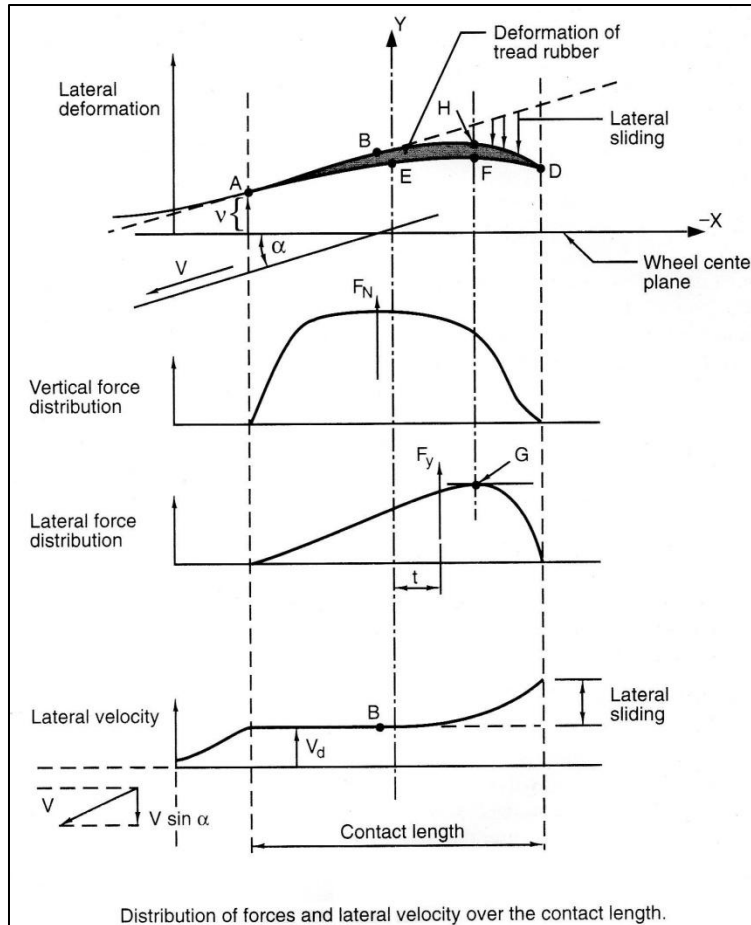
Figure 2: Tire Vertical Load, Lateral Force, and Contact Patch Deformation Distribution for Slip Angle[5]

The diagram also shows that, due to the roughly parabolic distribution of normal force within the contact patch and the linearly-increasing trend of deformation, the limit of static friction is reached before the end of the contact patch. Sliding occurs in the lightly-loaded aft portion of the patch and this region increases in area as slip angle increases until the whole footprint is sliding. A noteworthy point is that the maximum lateral force occurs behind the center of the contact length. The line labeled F_y is the resultant of the distributed lateral force and therefore passes through the centroid of the area under the lateral force curve. The length "t" denotes how far behind the center of the contact patch the lateral force resultant occurs and is called the pneumatic trail. Pneumatic trail causes a moment which attempts to reduce slip angle, aligning the tire with the direction of travel. As slip angle increases the sliding fraction of the contact patch grows from the rear forward and the force resultant moves forward because sliding friction is less than static friction. The lateral force resultant grows in magnitude but the pneumatic trail decreases, causing the restoring moment to peak, usually just before maximum lateral force, and fall off afterwards. The self-aligning moment is felt by the driver through the steering system and gives useful feedback about how close to the limit of performance the car is.[6]

---

[5] Milliken, William F. & Douglas L.: <u>Race Car Vehicle Dynamics</u>, page 23
[6] Milliken, William F. & Douglas L.: <u>Race Car Vehicle Dynamics</u>, page 404

For small values of α, lateral force is directly proportional to slip angle and the proportionality constant is called cornering stiffness. At larger slip angles the rate of change of lateral force with respect to slip angle decreases to zero at the peak lateral force and becomes negative past it, which means a polynomial curve fit is necessary for modeling the behavior of tires at higher slip angles. Cornering stiffness is actually a partial derivative because the lateral force produced by a tire also varies with the vertical load on it. It is possible, however, to normalize the lateral force to the vertical force and produce a graph of "lateral force coefficient". Plots of this quantity for three different loads are shown in Figure 3. The beginnings of the curves are linear, with a slope equal to the normalized cornering stiffness (to obtain cornering stiffness, multiply by the vertical load). At higher slip angles the curves roll off and reach a peak, past which the tire is mostly sliding.
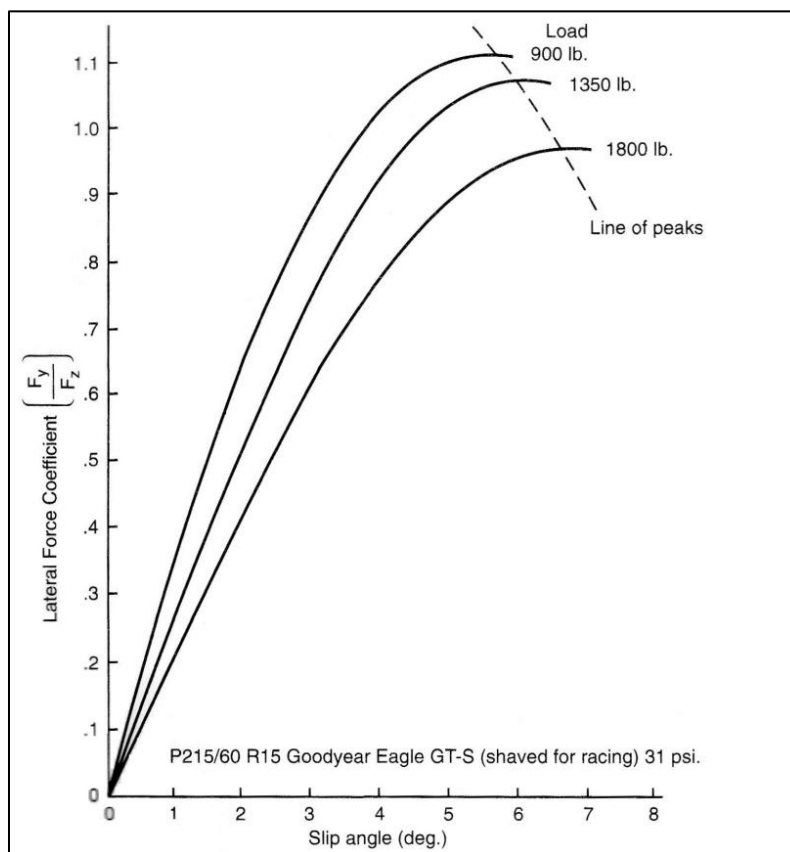
Figure 3: Typical Load Sensitivity Behavior[7]

It can be seen in Figure 3 that the peak lateral force coefficient decreases as vertical load increases. This is known as load sensitivity. If this trend were extrapolated to zero load, there would be maximum lateral force without the tire contacting the road so it is reasonable to speculate that the peak lateral force coefficient reaches a maximum at some light load, different for every type of tire, before again falling to zero with no load. Load sensitivity is a very important concept and dictates much of the design of racing cars. Conventional racing cars aim

---

[7] Milliken, William F. & Douglas L.: Race Car Vehicle Dynamics, page 27

to have a low center of mass and a wide track (lateral spacing between the wheels). This reduces the lateral load transfer which results from the tire forces arising in the ground plane but being transferred to the mass center, which must be above the ground. This creates a roll moment that, in the absence of aerodynamic devices, must be reacted by a redistribution of the vertical load on the four tires. Less lateral weight transfer is desired for tires utilizing slip angle for lateral force because the peak lateral force coefficient decreases on the more heavily loaded, outside tire, meaning that combined lateral force capability is lost when weight is distributed unequally across an axle. In other words, more grip is lost from the inside tire than is gained from the outside.

Inclination

The deformation due to inclination is shown in Figure 4. Depicted are the shapes which the contact patch of a motorcycle tire and car tire would assume when placed on a frictionless surface, inclined, and under a vertical load. The round, motorcycle tire has more curvature (seen in the black line running through each patch) than the car tire and this results in more camber thrust (lateral force due to inclination). On a real road the curvature is suppressed by friction and this produces a lateral force. The greater curvature of the motorcycle tire gives one explanation for the greater camber stiffness of round-section tires compared to square-section car tires.[8] Camber stiffness is the partial derivative of lateral force with respect to camber angle and at a particular vertical load. Bias-ply tires with stiffer sidewalls generally have greater camber stiffness than radial tires, which let the contact patch deform too easily under the road load.[9] Camber is similar to inclination angle but its sign depends on which side of the vehicle the tire is on. Negative camber means that the tops of the tires lean in – towards the sprung mass, while positive camber means they lean outward. An excellent example of negative camber is the Milliken MX-1, which will be discussed later in this report and is shown in Figures 8 and 9.

---

[8] Pacejka, Hans B.: Tire and Vehicle Dynamics, 3rd ed., page 77
[9] Milliken, William F. and Douglas L.: Race Car Vehicle Dynamics, page 47
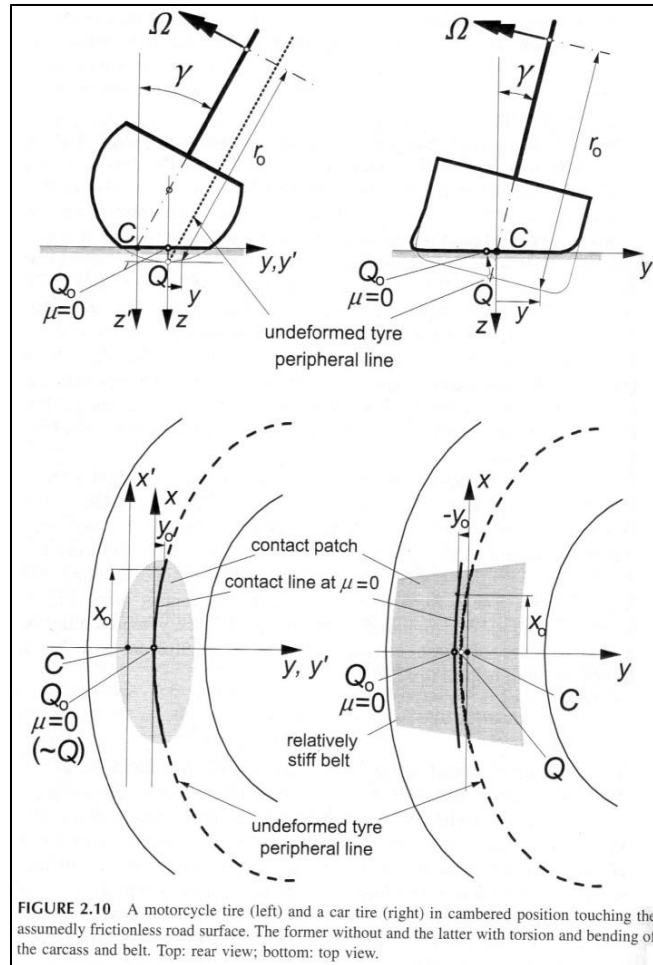
FIGURE 2.10 A motorcycle tire (left) and a car tire (right) in cambered position touching the assumely frictionless road surface. The former without and the latter with torsion and bending of the carcass and belt. Top: rear view; bottom: top view.

Figure 4: Shape of Deformed Contact Patch for Frictionless Road[10]

Also apparent in Figure 4 is that the lateral deformation of the contact patch is symmetrical about the y-axis (positioned halfway back from the front of the contact area). This curvature more closely matches the distribution of normal load on the tire seen in Figure 2 and results in less sliding of the tire on the road.[11] The symmetry also results in much less (or even negative) self-aligning moment (pneumatic trail) than for slip angle.[12]

Figure 5 is a clearer look at how a motorcycle tire's contact patch changes shape as inclination angle increases.

[10] Pacejka, Hans B.: Tire and Vehicle Dynamics, 3rd ed., page 76
[11] Milliken, William F. and Douglas L.: Race Car Vehicle Dynamics, page 47
[12] Milliken, William F. and Douglas L.: Race Car Vehicle Dynamics, page 47

Fig. 2-34 The effect of camber angle on contact patch shape.
[Rear tire $Fz = 2000\ N$ and $p = 2\ bar$].
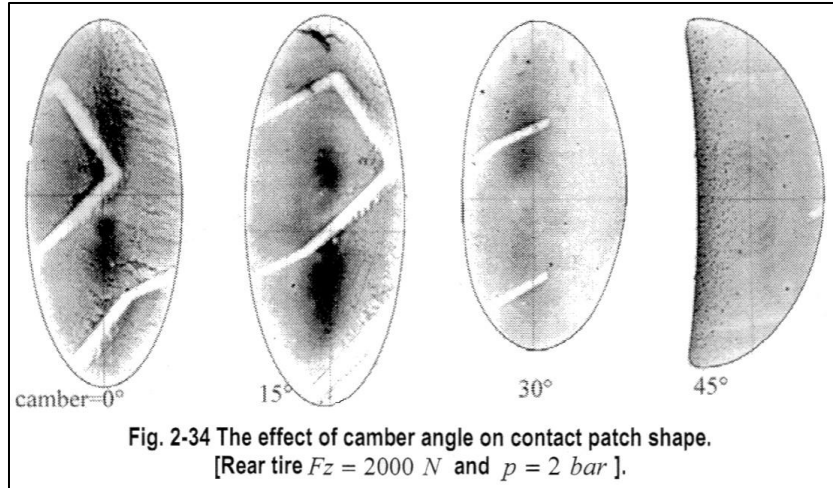
Figure 5: Changes in Contact Patch Area and Shape due to Camber and Tread Blocks[13]

Camber thrust behaves very differently than slip angle. It has an approximately linear relationship to both vertical load and inclination angle, even up to and beyond 45 degrees of inclination, as seen in Figure 6. The linear relationship to vertical load is evidenced by the normalized camber thrust data all falling on the same trend line even when the vertical load was increased five-fold, from 500N (112lb.) to 2500N (561lb.); thus the tire tested does not show camber thrust load sensitivity for the range of loads that would be seen on a lightweight racecar such as an FSAE car. From the two graphs it can be seen that this lack of load sensitivity is not simply due to the round section and construction of the particular motorcycle tested, since the tire does show load sensitivity when subjected to slip angle deformation but does not do so when inclined. The slip angle plots show curvature similar to that seen in the plots for car tires, although there is no peak to them because the range of slip angle tested is not as large as for car tires because motorcycles do not usually use large slip angles.
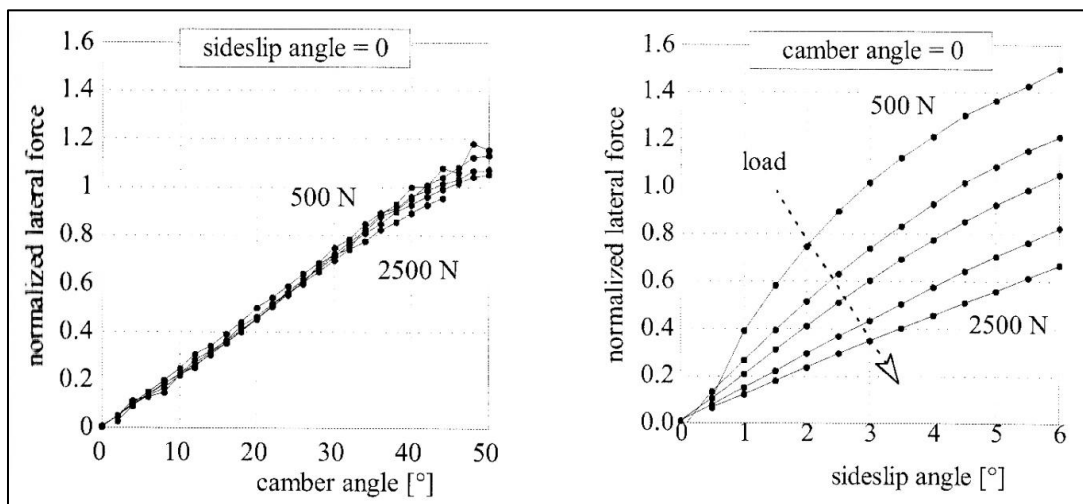
Figure 6: Load Sensitivity of Motorcycle Tires with Slip Angle but None for Inclination[14]

---

[13] Cossalter, Vittore: Motorcycle Dynamics, 2nd ed., page 67
[14] Cossalter, Vittore: Motorcycle Dynamics, 2nd ed., page 55

Combining Inclination & Slip Angle

The linearity of camber thrust holds true even when there is a small slip angle present, as is the case in Figure 7, where the right side plot shows it most clearly. The left side plot shows the saturation (leveling off of lateral force) of the tire at large inclination angles and small slip angles, with maximum lateral force occurring at lower slip angles when the inclination is increased. In the left-side plot of Figure 7 it is apparent that 40 degrees of inclination produces slightly more peak grip than 50 degrees, suggesting 40 degrees is possibly the optimum negative camber angle. The maximum lateral force at 40 degrees of inclination also occurs at a reasonable slip angle of about six degrees, similar to where most car tires (as opposed to round-section, motorcycle tires) produce maximum lateral force without inclination. The amount of slip angle required means that a car using 40 degrees of negative camber for maximum grip could still be controlled by the conventional method of steering via altering the toe angle of the front wheels (rotation about an axis normal to the road). If the maximum lateral force occurred at a nearly zero slip angle then a more complex steering system on both front and rear would be needed to eliminate slip angle and to control inclination in order to initiate the turn.
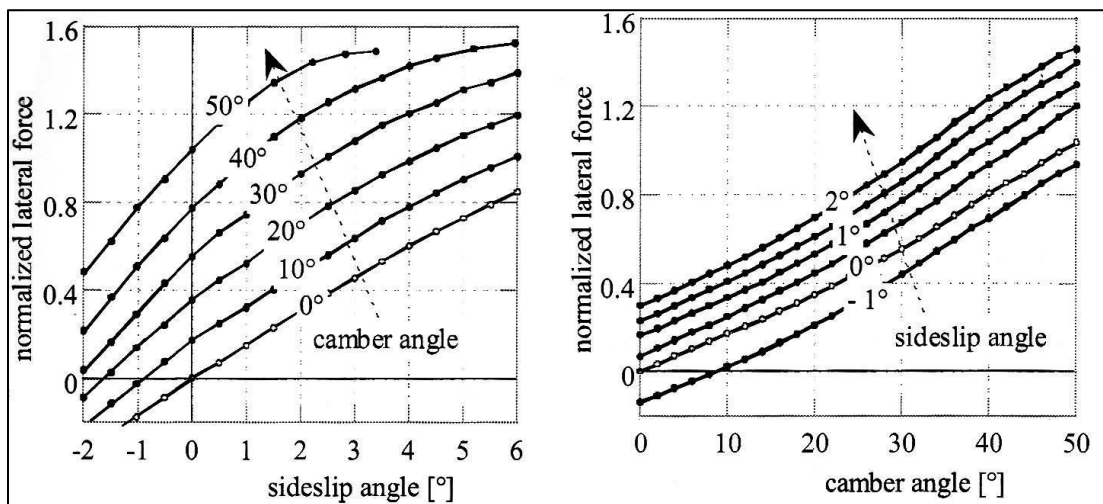
Figure 7: Lateral Force of Motorcycle 120/70-17 Front Tire at Combined Slip and Inclination Angles[15]

The plots of Figure 7 were made at a single vertical load. A more comprehensive test of combined inclination and slip angle was performed under the guidance of William F. Milliken while he was working on his MX-1 camber car and the vehicle dynamics behind it. This innovative test vehicle is shown in figures 8 and 9, showing its large negative camber angle and round-section tires, making it look like no other car on the road. With older, lower-performance tires (relative to modern tires) it achieved greater than 1g lateral acceleration consistently, and with more modern Dunlop radials it achieved about 1.3g[16], an impressive result for a pure test machine with many compromises for the sake of adjustability. This was achieved with a negative camber angle of just more than 23 degrees and a curb weight of 1,555 pounds with 52% of that weight distributed on the rear track. Results from tests of the original MX-1 bias-ply tires can be seen in figures 10 and 11.

---

[15] Cossalter, Vittore: Motorcycle Dynamics, 2nd ed., page 49
[16] Milliken, William F.: Equations of Motion, page 520

Figure 8: Milliken MX-1 Front View[17]

Figure 9: Milliken MX-1 Side View[18]

Figure 10 shows the lateral force generated by a motorcycle tire at a lighter load, while Figure 11 is at a 66% higher load. These plots show the increased lateral grip due to the addition of negative camber to slip angle at higher vertical loads. Camber values are reported as positive but represent the magnitude of the negative camber on the outside wheel. The dotted line represents the equilibrium state for a motorcycle without the rider hanging off to the inside of the bike and does not pertain to this discussion of four-wheeled vehicle dynamics.

---

[17] Photo from ultimatecarspage.com via Google Images
[18] Photo from joefenstermaker on flickr
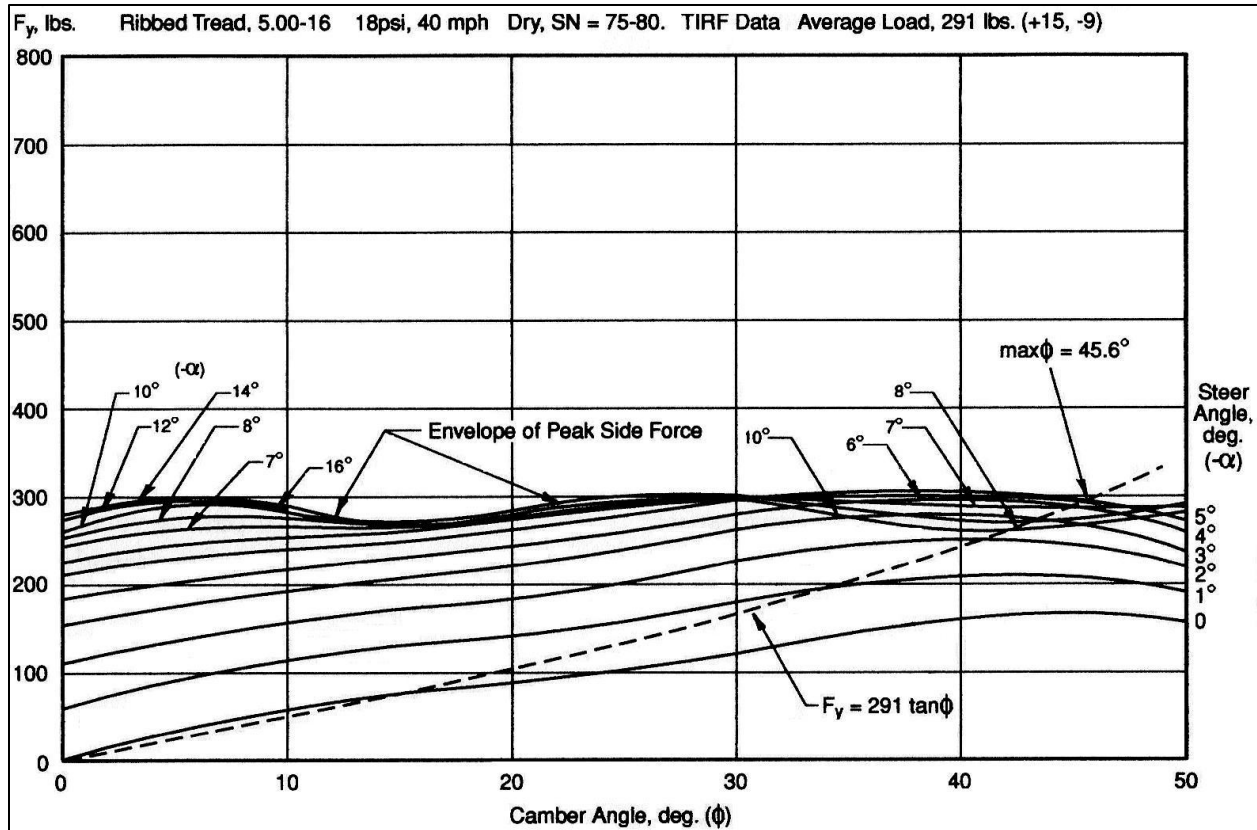
Figure 10: Lateral Force for Combined Camber and Slip Angles at Low Load (291 pounds) for 5.00-16 Bias-Ply, Ribbed-Tread Goodyear Eagle Motorcycle Tires[19]

The nonlinearity of the envelope of peak side force, particularly the decrease in grip between 5 and 25 degrees of inclination, is interesting. Based on the trend of lateral force against slip angle, one would expect a single peak, but the maximum lateral force increases again after 15 degrees of inclination and actually surpasses the first peak (near 5 degrees) at about 35 to 40 degrees of inclination. Since these tires had "ribbed tread" it may be due to the effects of tread blocks on the contact patch shape and area, as seen in Figure 5.

In Figure 11 there is only one peak but there is a distinct change in slope and curvature just after 25 degrees of camber. The peak grip still occurs at 40 degrees, similar to the highest peak in Figure 10. At 40 degrees of inclination the addition of slip angle increases maximum lateral force by more than 40%. The most significant point illustrated is that the addition of 40 degrees of inclination increases the maximum grip by 25% compared to a vertical tire.

---

[19] Milliken, William F.: Equations of Motion, page 521

12
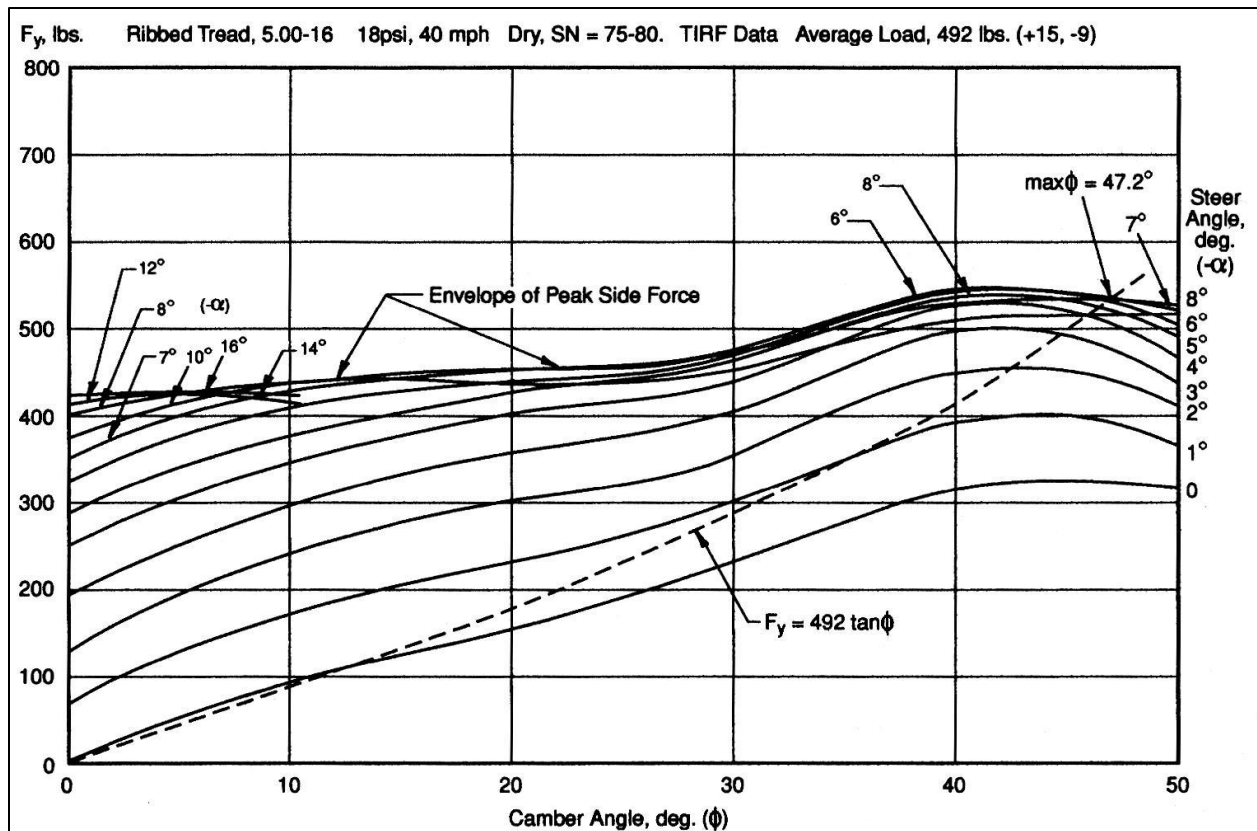
Figure 11: Lateral Force from 5.00-16 Bias-Ply, Ribbed-Tread Goodyear Eagle Motorcycle Tires at Combined Inclination and Slip Angles with Vertical Load of 492 pounds[20]

Based on figures 7, 10, and 11, the optimal inclination for the outside tire in a turn is about 40 degrees. It should be noted, however, that the MX-1 tires are out-dated and modern sport motorcycle tires should outperform them handily, but the trends of camber thrust and maximum grip should still be relevant. 40 degrees appears as optimal for more models of tire than just those old Goodyears, so it is reasonable to expect modern motorcycle tires to peak at around the same inclination, with the further reasoning that since motorcycles depend on camber thrust for stability in a way that cars do not the tires will only have gotten better in terms of camber stiffness and grip. Tests should still be done on modern rubber before constructing a vehicle to determine which tire is best suited to a camber car, and whether 40 degrees is the best for a tire in isolation. Whether static, negative camber equal to the optimal inclination for a single tire is best for a camber car is not immediately clear because those figures do not show what the inside tire is doing. To determine the optimal camber, the behavior of tires under adverse inclination and light loads must be known.

If the trend of the maximum side force against camber angle in Figure 11 is extrapolated and assumed to be oddly symmetric about the intercept with the lateral force axis, then the inside tire looses as much lateral force coefficient (compared to zero camber) as the outside tire gains. Figure 10 shows, however, that at lower loads the effect of camber on maximum lateral grip is smaller. This behavior agrees with the way in which camber and slip angle distort the contact

---

[20] Milliken, William F.: Equations of Motion, page 522

13

patch. Camber relies on vertical force to deform the tire out of round while the deformation due to slip angle is independent of load (though the amount of friction available to counteract that deformation does vary). Therefore, the inside tire gains lateral force coefficient when weight transfers off of it because the camber thrust is not fighting the slip angle force as much. Continuing the trend of peak side force seen in Figure 10 would mean that *the inside tire is not significantly hampered by adverse camber* and would likely not benefit enough from inclination into the turn to make a variable-camber system worth its weight and complexity. The load below which the leveling-off of maximum side force occurs is dependent on the particular model of tire but if it is true for the case of positive camber it would mean that a static camber configuration would corner just as well as a tilting machine such as a motorcycle, even with less than 100% lateral weight transfer.

As found by William F. Milliken, lateral weight transfer increases the amount of lateral force which a pair of negatively-cambered tires can produce. This is the opposite behavior to traditional, vertical tires but is intuitive if one understands that the camber thrust of a tire is proportional to load. With a pair of negatively-cambered tires, even rolling straight-ahead, there will be a net lateral force if a disturbance causes one tire to be loaded more than the other since the camber thrust on one side increases and the thrust on the other side which opposes it will reduce. This net lateral force works to increase the lateral load transfer because of the mass center of the system being above ground level. As described above, however, the inside tire does not need to be completely unloaded to achieve maximum grip because at some point its lateral force becomes oriented into the turn. More load increases the force but less load increases the coefficient, so there should be an optimal, non-zero, load for the inside tire, unless the outside tire gains significant amounts of lateral force coefficient with more load, which is the opposite behavior of a normal car tire at small camber angles.

Interestingly, the maximum lateral force coefficient for a single tire at -40 degrees of camber increases by more than 5% (from 1.05 to 1.11) when vertical load is increased by 66% (from 291 pounds to 492 pounds). Those numbers are taking into account the tolerance on the load measurement and so may be higher or lower but still show positive load sensitivity. This means that the outside tire experiences a greater gain in potential lateral force than the increase in vertical load, the opposite of the conventional car tire behavior shown in Figure 3. Even if the increasing trend is weak, it is at least better than the decrease in lateral force coefficient with vertical tires. The vertical loads in Figure 3 are more than double those in Figure 11, however, so it is not conclusive whether normal tires would behave similarly to the cambered tires at lighter loads and if the camber tires would experience negative load sensitivity at much higher loads. The 900 pound load in Figure 3 would represent a small, road-legal sports car without aerodynamic downforce undergoing a high-lateral-acceleration turn which was causing nearly full lateral weight transfer.

It is clear from Milliken's work with the MX-1 and his subsequent analysis of the data that the gains in grip on the outside tire due to negative camber overwhelm the losses in grip on the inside tire due to its adverse camber, and if the loads are in the right range for the tires the inside tire likely gains grip. Fascinatingly, the beneficial effect of camber appears to be true even for the hypothetical case of zero load transfer. This conclusion is based on simulations which William F. Milliken and his associates performed after the extensive tests during the MX-1

program. The results of three simulations are shown in figures 12 and 13. The main point they convey is that a pair of negatively-cambered tires can produce more net lateral force with more lateral load transfer, while vertical wheels show the opposite trend (negative load sensitivity). Also apparent is that the normalized lateral force is higher at -40 degrees of camber than at -20 degrees, even at zero lateral load transfer (h/T=0).
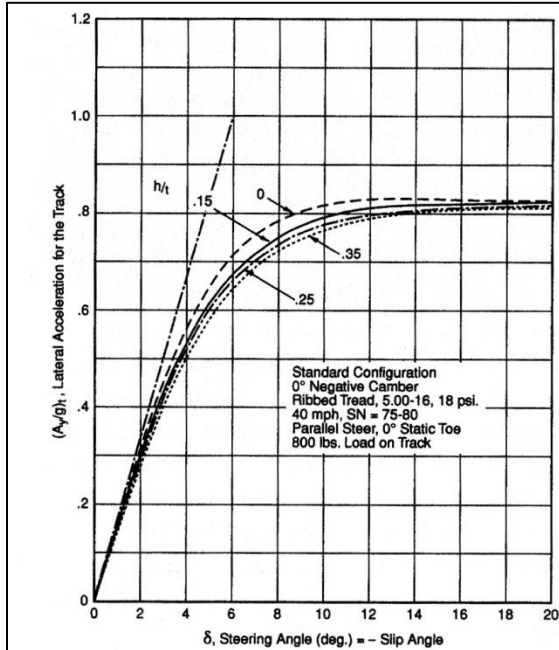
Fig. 23-47
This figure is a plot of normalized lateral force for a pair of vertical wheels on a single track vs. steer angle (or, slip angle). It is the cornering force curve for a pair of wheels with various lateral load transfers, as represented by *h/t* (see text). It shows that with vertical wheels (no camber), the lateral force for the wheel pair decreases both the cornering stiffness and peak force. This is well known and accounts for the use of an antiroll bar for adjusting the over/understeer characteristic.
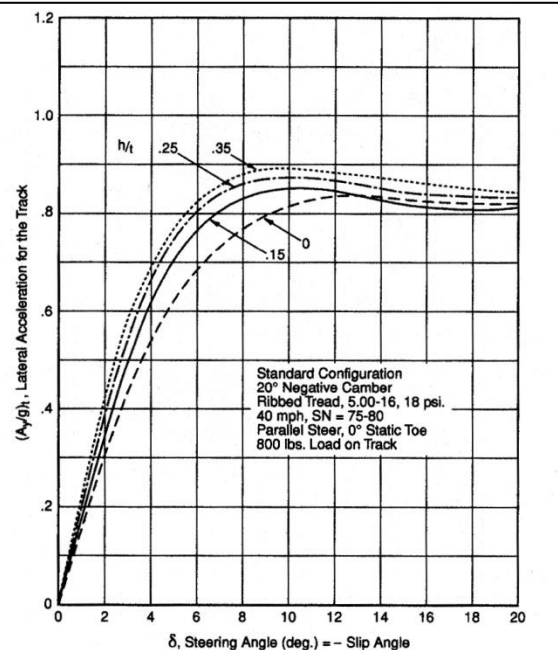
Fig. 23-48
This plot is similar to that of Fig. 23-47 except for a pair of negatively cambered wheels (–20° camber). It will be noted that the cornering stiffness and lateral force increase with lateral load transfer. This remarkable result is the only configuration we know of where lateral weight transfer is desirable. It accounts for the high lateral accelerations (over 1g) of MX-1 and its exceptional limit behavior.

Figure 12: Simulation Comparing Effect of Lateral Weight Transfer on Total Lateral Force from A Pair of Tires With and Without Negative Camber

It can be seen by comparing the plots in Figure 12 and in Figure 13 that the lateral acceleration increases from about 0.825g to 0.925g when going from -20 degrees and -40 degrees, even without lateral load transfer. That is a difference of 12% and that difference increases to 15.5% at when lateral weight transfer is added, even though that transfer of load is only about 75% complete for the highest lateral acceleration in Figure 15, meaning there is still a decent safety margin against overturning. This supports the theory that -40 degrees of camber is best for lateral acceleration, despite Milliken using only -23 degrees on the MX-1, a value which was the most the MX-1 could achieve.
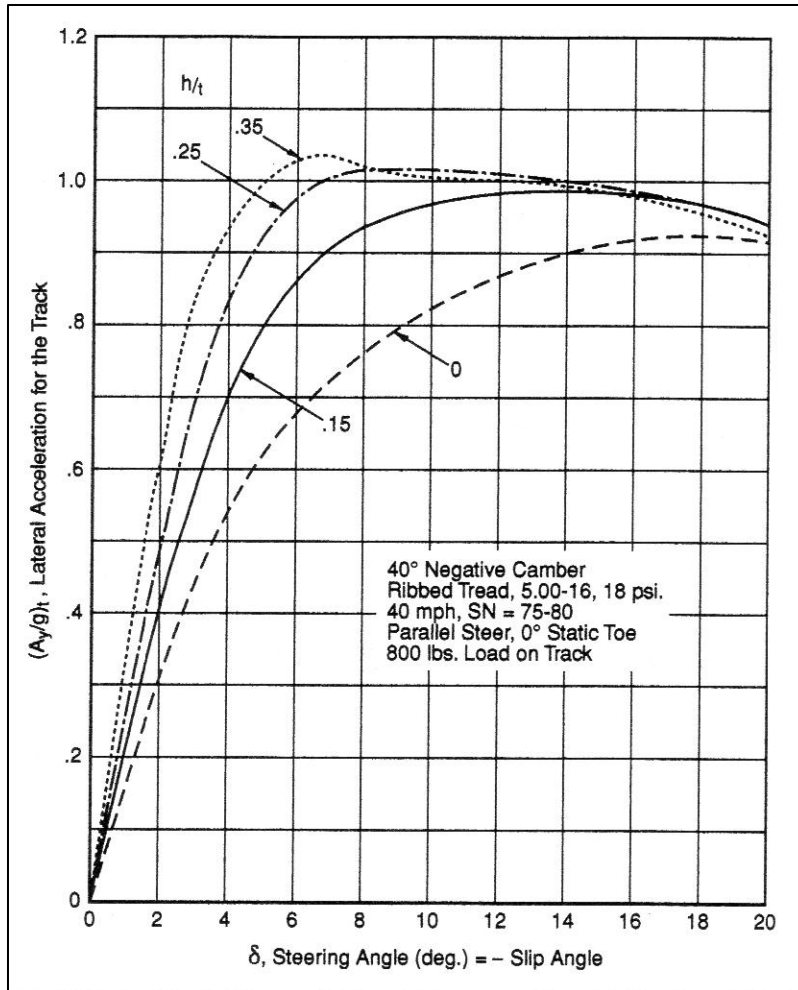
Figure 13: Simulation of Lateral Force for Pair of Tires at -40 Degrees of Camber Showing More Lateral Force than -20 Degrees

Round-Section Tires vs. Square-Shouldered Tires

The beneficial effect of camber appears to be associated most strongly with motorcycle (round-section) tires since large camber angles are necessary for significant gains and car tires with their rectangular section are not suited to camber angles much greater than 5 degrees. Figure 14 shows car tire data which show load sensitivity for small negative camber angles (5 degrees or less) and neutral load sensitivity for 10 degrees of negative camber. This data was taken at 7 degrees of slip angle, which produced nearly the peak lateral force at each camber angle. The tires in that test were 225/70R15 car tires, which are radial tires with relatively high aspect ratios (tall sidewalls which would be less stiff than short ones) and so would be more tolerant to large camber angles than wider, lower-profile tires. Extrapolating the trend, one would expect positive load sensitivity above -10 degrees of camber but car tires cannot use larger camber angles because the tire ends up riding on the stiffer shoulder, shrinking the contact patch and putting more pressure on it, which decreases grip. This is evidenced by the reduction in peak lateral force coefficient at -10 degrees of camber versus -5 degrees of camber, though -10 degrees produced more lateral force than 0 degrees at high loads and equal force at low load.

16
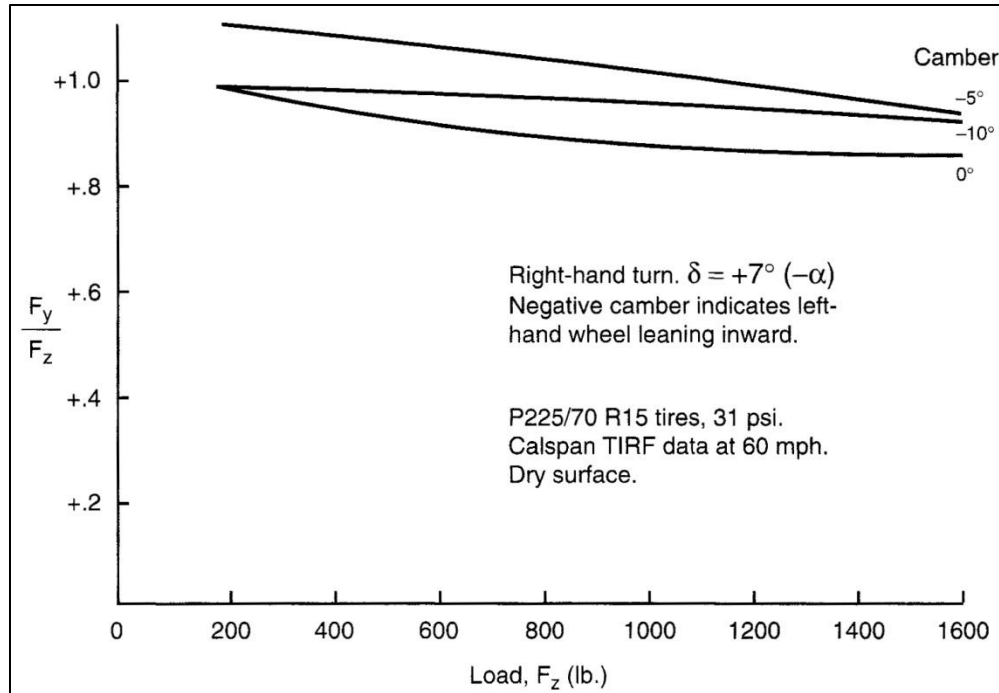
Figure 14: Load Sensitivity for Various Camber Angles at 7° Slip Angle[21]

Figure 15 is a plot of maximum lateral force versus camber angle at high load for three different round-section tires. This data was recorded by Albert G. Fonda, who made a sort of tilting go-kart which had the rider lean into the turn. William F. Milliken was impressed by its high lateral acceleration (1.2g) but wanted to avoid its shortcoming: what motorcyclists term "high-siding". If the kart was turning and encountered a lower-friction spot it would benignly "lay down" and slide with increased inclination, but when it encountered a high-friction surface again it tended to capsize to the outside of the turn and throw the rider out.[22] The tires Fonda tested for his 1956 paper "Tire Tests and Interpretation of Data" (published just after William F. Milliken proposed to Cornell Aeronautical Laboratory that they patent his camber car idea) were not for the kart, however, being much too large for it but suitable for an automobile. These tires are not specified as motorcycle tires in the paper and it is mentioned in the conclusion that an expanded test could include motorcycle tires at 30 to 50 degrees of inclination, leading to the deduction that these are simply 1955 vintage automobile tires which were narrower and more rounded in section than today's "high performance" rubber. Once shaved of their tread (in order to remove the effects of tread pattern seen in Figure 5) these tires (shown in Figure 16) appear to have a similar section to tires specifically made for motorcycles and the tires are also bias-plies, which are generally stiffer than radials in certain modes and so see more benefits from camber.[23] These car tires should therefore have behaved similarly to motorcycle tires, however the high load of more than 900 pounds at which the tires were tested is not representative of motorcycle loading.

---

[21] Milliken, William F. & Douglas L.: <u>Race Car Vehicle Dynamics</u>, page 54
[22] Milliken, William F.: <u>Equations of Motion</u>, pages 496,497
[23] Milliken, William F. & Douglas L.: <u>Race Car Vehicle Dynamics</u>, page 405
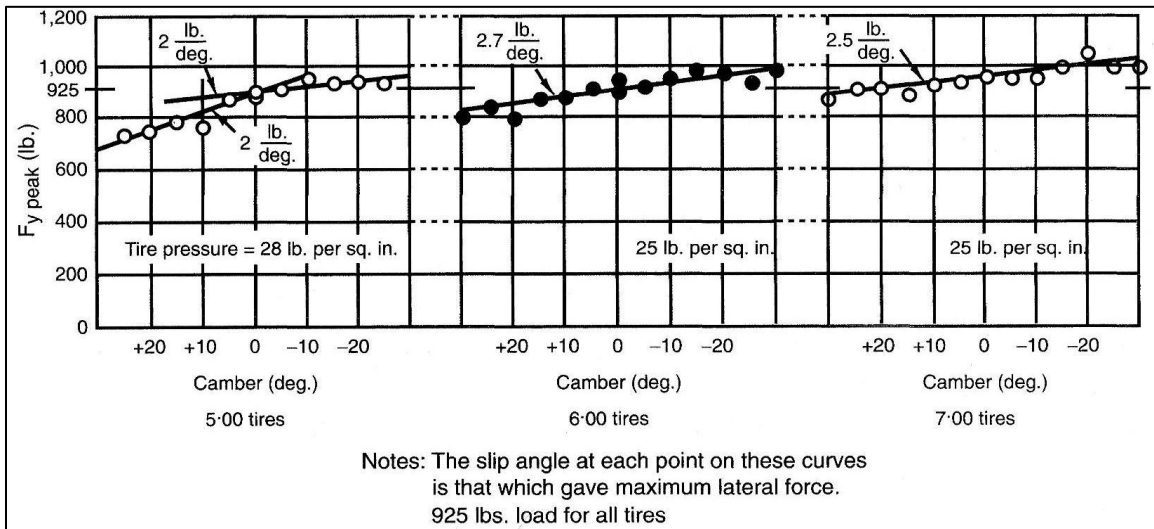
Figure 15: Peak Lateral Force vs. Inclination Angle[24]

Fig. 59. Dunlop Smooth, Round, Treadless Tyres
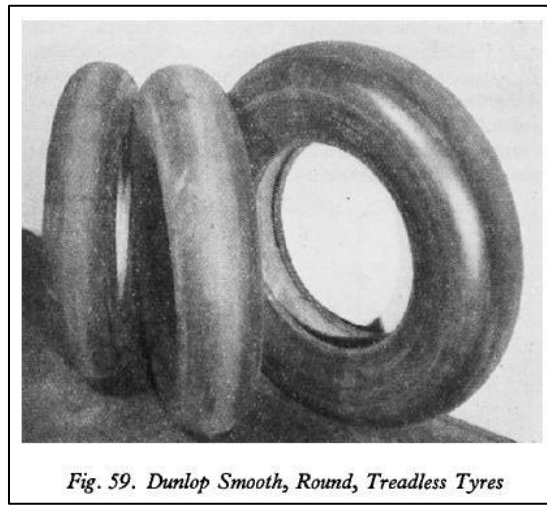
Figure 16: Tires Used to Generate Data for Figure 9[25]

The slip angle varies between data points in Figure 15 because the steering angle was adjusted for maximum lateral force at the specified camber angle. The plots show that the benefits of camber extend to tires not specifically for motorcycles, as extrapolating the trend lines to 40 degrees of camber produces a gain in lateral force coefficient of more than 10 percent. The plots also show that the trend of increasing lateral force with negative camber extends to the case of positive camber when the load is high enough. Lateral grip appears to be degraded by positive camber by about the same amount as negative camber improves it, though some tires may show a more nonlinear trend and have a steeper reduction in side force with positive camber, as seen in the leftmost plot of Figure 15.

---

[24] Graph as presented: Milliken, William F. & Douglas L.: <u>Race Car Vehicle Dynamics</u>, page 49
    Original data and graph: Fonda, Albert G.: "Tire Tests and Interpretation of Data"
[25] Fonda, Albert G. "Tire Tests and Interpretation of Data"

18

Identically-sized 100/85-R10 PMT racing scooter rear tires are being used on all four corners of the 2013 Formula Electric car as have been used previously. Being round-section, they can support larger camber angles. The PMT's are about three pounds lighter than the smallest Hoosier square-section racing tires available and have less aerodynamic drag than the wider Hoosiers or taller, full-sized motorcycle tires.

The scooter tires are radials, which Milliken says shows less of the effects of camber than bias-plies[26] due to their greater lateral compliance, but being made for motorcycles should be stiffer than car radial tires, since the lateral stiffness and camber stiffness of the tires significantly affects the stability, safety, and performance of a motorcycle.

Fig. 2-20 An example of lateral force as a function of the camber angle φ (left) and of the sideslip angle λ (right) for different front (top) and rear (bottom) tires.
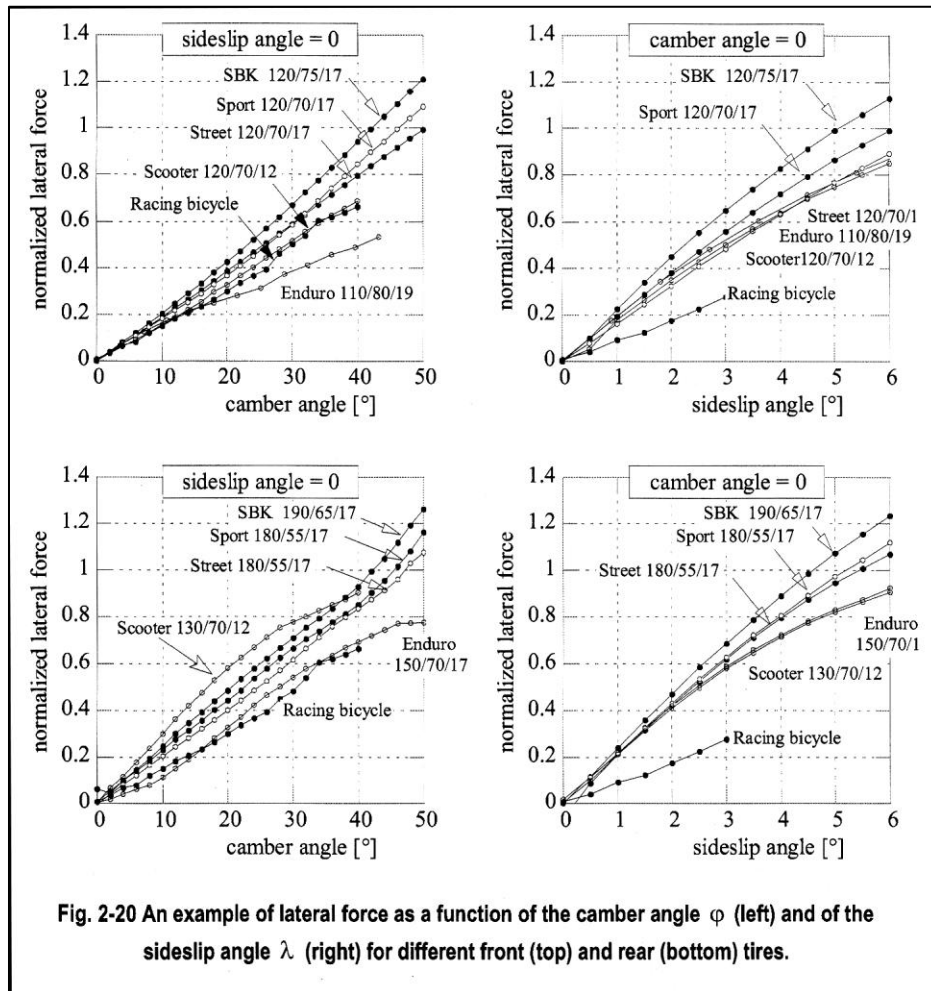
Figure 17: Lateral Force Characteristics for Various Round-Shouldered Tires[27]

The scooter tires can be expected to behave similarly to the other round-section tires which generated the data used to develop the camber tire model used here. Figure 17 shows that ordinary scooter tires generally have a linear relationship between camber thrust and slip angle

---

[26] Milliken, William F. & Douglas L.: <u>Race Car Vehicle Dynamics</u>, page 405
[27] Cossalter, Vittore: <u>Motorcycle Dynamics</u>, 2nd ed., page 54

similar to motorcycle tires. Due to the more intense use which racing scooters receive, they would logically be closer to the motorcycle or racing motorcycle (SBK) tires than the treaded scooter tires. The deviations of the enduro tires can be put down to their greater siping allowing tread blocks to squirm and because of the change in number of tread blocks in contact with the road as camber increases, as seen in Figure 5. The rear tire data for the enduro, scooter, and racing bicycle are further from the motorcycles' than the front tire data for those vehicles are. This may be due to construction (ply orientation and composition) and rubber compound. The slip angle data does not extend far enough to show a peak and drop-off in lateral force because single-track vehicles do not typically corner at slip angles greater than those shown in the figure.

Square-shouldered, wide tires have an advantage in being able to have larger contact patches, which due to load sensitivity effects increases grip. When the tire is deformed under vertical load the contact patch is formed and the integral over the patch of the pressure on each differential piece of area must equal the normal load on the tire. Stiffer sections of the tire bear more pressure for an equal displacement. With wide, square-shouldered tires the contact patch ends up with the same area as a narrower tire with the same tire pressure and stiffness would have but the footprint is wide and short instead of circular or long and thin. The shorter patch means there is less deformation out-of-round and so less heating of the rubber. This, in turn, means that softer rubber can be used which increases grip even further. Lower pressures could also be run to return to the same level of deformation out-of-round but with a larger contact area.

Because round-shouldered tires can make more use of the benefits of camber, they are preferred for best lateral grip. Conventional, wide car tires are expected to be better for longitudinal grip.

Longitudinal Force

Longitudinal forces (for propulsion and braking) arise, like lateral forces, from the deformation of the contact patch. In this case the deformation is in line with the wheel heading and velocity vector. Because there is a limit to the amount of distortion in any direction the contact patch can support, there is a limit to the amount of force the tire can produce in any direction. This means that the magnitude of the ground-plane force vector from the tire is limited such that maximum lateral force and maximum longitudinal force cannot happen at the same time. This is visually represented by a "friction circle" or g-g diagram, which is usually more elliptical than circular. Such a diagram is shown in Figure 18, which is distorted by unequal scales on the two axes. Of note is that this data was recorded from the ace driver Ayrton Senna during practice for the Australian Grand Prix in 1987.
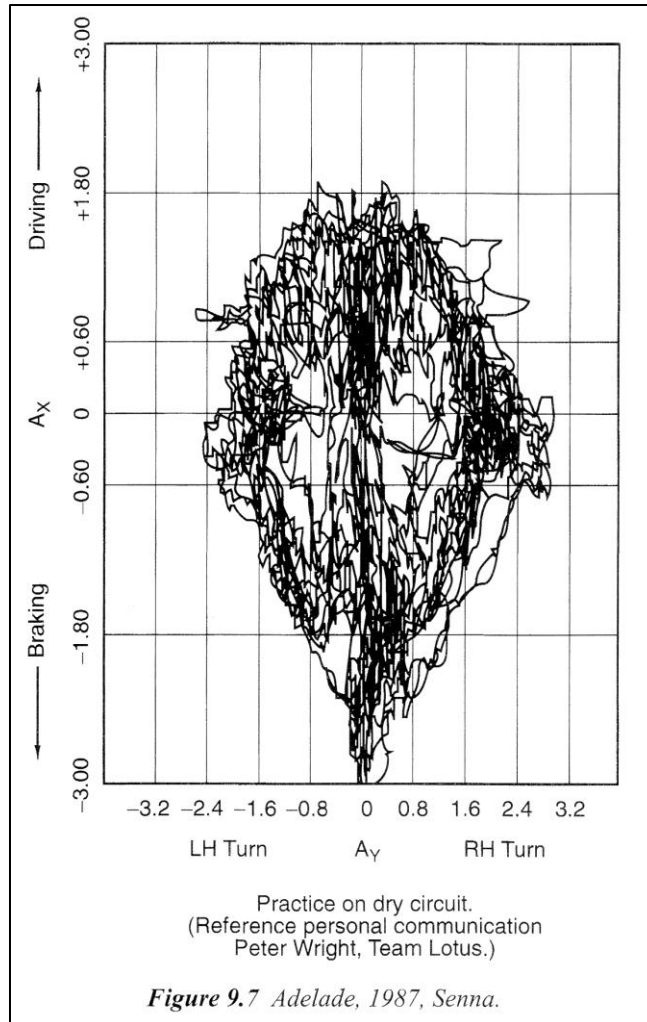
Figure 18: Friction "Circle" from Senna's Lotus at 1987 Australian GP[28]

In g-g diagrams, the longitudinal acceleration is graphed versus the lateral acceleration. The points are each simply the outputs from an accelerometer at the center of mass (or corrected to reflect the accelerations at the center of mass) at an instant in time. They give an idea for how much total performance a tire and vehicle can achieve. A tire or vehicle with a more rounded outer envelope to the graph should be easier to drive and more forgiving. The maximum lateral and longitudinal forces can have the theoretical advantage depending on the track, but generally the tire with the most area inside the "circle" will perform best over a lap of a race track.

Static camber reduces the maximum acceleration and braking which the car can achieve because lateral force is always being produced, even when there is no slip angle or lateral load transfer. In Figure 10 and Figure 11 it can be seen that slip angle adds about 40% more lateral force at 40 degrees of negative camber, but this means that 60% of maximum lateral force is still being produced at zero slip angle.

---

[28] Milliken, William F. & Douglas L.: Race Car Vehicle Dynamics, page 355

This force is present on each tire of a negatively-cambered pair, one opposing the other to achieve a net lateral force of zero. If the tire is producing so much lateral force then it is leaving significant amounts of longitudinal grip unavailable. This could be a non-issue for low-power cars which rely on maintaining momentum by maximizing cornering speed, but this still means that a car with sufficient power would be hampered by the camber on straight sections of track. All-wheel-drive could be used to regain some traction, but this is at the cost of extra weight and still the camber would be outperformed by an all-wheel drive car with vertical tires.

Induced Drag

Generating lateral force by means of slip angle has a drawback in the form of induced drag, which comes about because the lateral force produced is perpendicular to the wheel heading and not the direction of wheel travel. Therefore, a component (sine of the slip angle) of the lateral force is directed opposite the velocity vector, and only the remaining portion (cosine of the slip angle) is actually useful for lateral acceleration. The component opposing the velocity slows the car down or requires engine power to overcome, using more fuel and reducing lateral grip on the drive wheels through the friction circle effect. Induced drag is a significant problem, as seen by a sample calculation which appears in Race Car Vehicle Dynamics for the induced drag on an Indy car. This force turns out to be 225 pounds, which requires 132 horsepower to overcome at the 220 mph speed it is travelling.[29]

Camber thrust does not cause induced drag because the wheel heading aligns with the wheel velocity and, thus, all the lateral force is used for turning and less engine power is needed to maintain speed, which saves fuel and increases the grip on the driving wheels. All this could be offset if the rolling resistance of a tire increases with inclination, however. Fortunately, this does not appear to be the case.

The moment which opposes the rolling of a non-driven, non-braked wheel varies with the cosine of the inclination angle, meaning that rolling resistance actually decreases with camber angle. This is true for small inclination angles up to 10 degrees, where there is less than 2% difference compared to setting the value of the cosine function equal to unity. This is well within the scatter in tire data from test machines. Slip angle also causes similarly small changes in rolling resistance.[30] If the cosine trend continues to large camber angles, or even if the rolling resistance stays nearly the same, then the elimination of induced drag stands as a great benefit to using inclination to achieve high lateral force while reducing slip angle.

Effects of Camber on Vehicle & Suspension Design

In Figure 3 it can be seen that the slip angle at which peak lateral force occurs increases at higher loads. This is the reason reverse Ackermann steering systems exist. Geometrically, the inside front wheel in a turn is on a smaller radius than the outside and should be steered more. This condition is called Ackermann steering, diagrammed in Figure 16. Because of the lateral weight transfer and load sensitivity effects, however, reverse Ackermann produces more lateral

---

[29] Milliken, William F. & Douglas L.: Race Car Vehicle Dynamics, pages 67-69
[30] Milliken, William F. & Douglas L.: Race Car Vehicle Dynamics, page 73

acceleration for conventional cars than normal Ackermann but comes at the expense of high rolling resistance at low lateral accelerations due to scrubbing the inside tire across the road.[31]
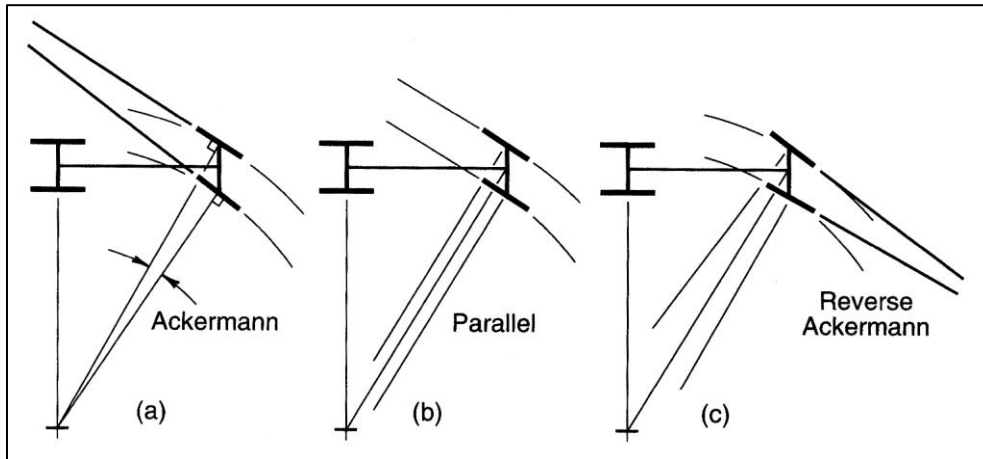
Figure 19: Ackermann Steering Geometry[32]

It should be noted that the geometry that Ackermann is calculated from only applies to very low lateral accelerations, as slip angles in the rear mean that the turning center shifts forward and is no longer perpendicular to the rear tires. When the rear tires have a larger slip angle than the front, this is called oversteer. When the front tires have the larger slip angle the car is said to be understeering. The slip angles depend on the cornering stiffness of the car and the required lateral force at either end of the car. In steady-state cornering, the moments of the front and rear lateral forces about the mass center must be balanced. If the mass center is not at mid-wheelbase, then one of the forces (rear if weight is rear-biased, front if the opposite) must be larger to account for the unequal moment arms. Therefore, when the tires have equal cornering stiffnesses, a car with a rear weight bias needs more rear slip angle to make more rear lateral force and maintain equilibrium. When there is no rear-wheel steering the rear slip angle can only come about by the heading of the car as a whole being yawed relative to the direction of travel. This increased sideslip angle causes the car to corner more "nose-in", or in other words it oversteers. Reduced sideslip angle causes cars with forward weight biases to understeer (if no other changes are made) and cars with equal front-to-rear weight distributions to be neutral steer.

A camber car should use conventional Ackermann because the inside wheels needs more slip angle to counteract the adverse camber. Increased slip angle does result in more induced drag but the inside wheel generates less force than the outside due to the lateral weight transfer so the extra drag is insignificant. The need for more slip angle at low camber is seen in Figure 10, and the trend can reasonably be expected to continue to the case of inclination out of the turn.

Since slip angle is very hard to measure on a car, a measurable quantity called understeer gradient is used to quantify understeer instead of a difference in slip angles. This gives the

---

[31] Milliken, William F. & Douglas L.: <u>Race Car Vehicle Dynamics</u>, page 404
[32] Milliken, William F. & Douglas L.: <u>Race Car Vehicle Dynamics</u>, page 714

amount of steering required on the front wheels in terms of the Ackermann angle plus a modifier term equal to a constant times the lateral acceleration. If this is positive, the car understeers and if negative, the car oversteers. The Ackermann angle depends only on turn radius and wheelbase, so the understeer gradient can be measured by recording the steering wheel angle while negotiating a constant-radius turn, such as during a skidpad test, and gradually building up speed (and later accounting for compliance in the suspension). If the wheel must be turned into the turn more as speed and lateral acceleration increases, then the car understeers. If the steering angle must be reduced then the car oversteers, and if no change is required it is neutral-steer. Understeer means that the car is more stable than if oversteer or neutral and also has a quicker response time than an oversteer car under normal conditions. Oversteer cars have a "critical speed" above which they become divergently unstable. Above this speed they (most likely) cannot be controlled by a human pilot but much like modern jet fighter planes they would have exceptional quick responses if computer stability augmentation was used.

Most race cars are close to neutral steer because of limit plow/spin effects. A front weight bias brings understeer but also causes the front tires to reach their grip limit before the rears if the tires are the same. Therefore, neutral-steer cars have the highest maximum steady-state lateral acceleration as well as acceptable response times and favorable subjective handling (most racing drivers do not like much understeer). Not all race cars have their mass centers at mid-wheelbase, however. This is because oversteer/understeer can be changed by redistributing the lateral load transfer, which is done by changing the proportion of total roll stiffness taken by the front and rear tracks. Changing the roll couple distribution, as this is called, takes grip from one end and adds it to the other, therefore a car that is balanced for neutral steer will achieve the most lateral acceleration that it can for a given mass center location. A mass center forward of mid-wheelbase speeds the lateral acceleration response at the center of mass[33] because the initial yaw into the turn causes more acceleration at the mass center, but the unequal weight distribution also reduces the maximum steady-state lateral grip if the lateral force coefficient follows any trend other than concave-up and increasing with vertical load. Normal load sensitivity (lateral force coefficient decreasing with increasing load) means that the heavy end does not gain as much grip as the light end looses, therefore the total grip decreases and maximum lateral acceleration suffers when the weight distribution is not 50% rear (with the same tires on each corner)[34] Ideally, one would use the best tires on all four corners to maximize the grip, so simply using softer tires on one end is not the best approach to avoid limit plow or spin.

Aerodynamic downforce can also be used to alter the oversteer/understeer balance by applying more load to one track, thereby affecting cornering stiffness but most significantly increasing the maximum grip and controlling plow/spin behavior. The narrower track (relative to wheelbase and general vehicle size) of a camber car, combined with the narrower, round-section tires reduces frontal area and drag coefficient compared to a conventional car. This makes a camber car more fuel efficient and/or able to reach higher speeds and accelerate better out of high speed turns for a given weight and engine power. The narrower, round-section tires also do not obstruct under-floor ground-effect aerodynamic devices as much as square-shouldered, wide

---

[33] Milliken, William F. & Douglas L.: Race Car Vehicle Dynamics, page 401
[34] Milliken, William F. & Douglas L.: Race Car Vehicle Dynamics, page 394,401

tires do.[35] Therefore, the narrower area under a camber car due to the narrower track regains some "effective area" through "cleaner" airflow (less turbulence and loss of total pressure) and less tire obstruction.

With normal load sensitivity, an equal dynamic front-to-rear weight distribution is best for braking performance[36] if the car has brakes on all four wheels (as most cars do) but this requires a rearward static weight bias to counteract the forward weight transfer. When the car only drives the rear wheels the rearward static weight bias also helps acceleration because there is more grip available and the rearward weight transfer during acceleration adds to this by taking weight off the front wheels which are not contributing forward thrust. This weight transfer affects the oversteer/understeer balance, however, so a road-racing car should not be designed to transfer too much weight longitudinally.

The effect of scrub radius combined with caster angle causes a load transfer from one diagonal to another when steering is applied. Scrub radius and caster angle definitions are shown in Figure 20. Scrub radius is the distance from where a line projected along the steering axis intersects the ground and the centroid of the contact patch. It is the lever arm for longitudinal forces such as those from an impact with a bump in the road. A larger scrub radius decreases steering effort at slow speeds because the tire is able to roll around the steering axis rather than the contact patch twisting. Caster angle is the tilt of the steering axis in side view and is usually used to increase a quantity called the mechanical trail, which is the lever arm with which the lateral force from the tire exerts a torque through the steering system that tries to force the steering wheel back to the straight-ahead position. Trail causes the steering weight to increase with lateral acceleration and increases the self-centering effect as speed increases, which are effects that most drivers expect and desire. Caster also adds inclination to both the inside and outside wheel when steering is applied.
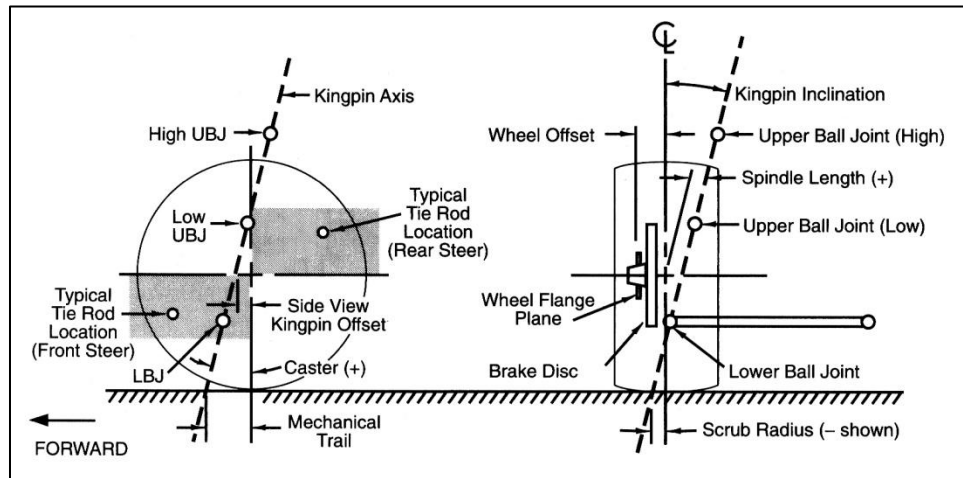

Figure 20: Steering Geometry Definitions[37]

[35] Milliken, William F.: Equations of Motion, page 524,525
[36] Milliken, William F. & Douglas L.: Race Car Vehicle Dynamics, page 391
[37] Milliken, William F. & Douglas L.: Race Car Vehicle Dynamics, page 710

The weight transfer caused by the caster and scrub radius creates either an understeer or oversteer yaw couple, depending on how much camber is used and whether the scrub radius is negative or positive. Because this is a couple and not a simple moment due to an unbalanced increase in lateral force at one end of the car, there is no significant benefit to caster jacking other than tuning turn entry behavior, and to a lesser degree steady-state, behavior to suit driver preferences. The magnitude of this yaw moment is limited by the arm strength of the driver unless a slow steering ratio or power steering is/are used. The sense of the yaw couple is affected by how much the car relies on camber, since lateral weight transfer degrades the lateral force of vertical tires but increases the grip for camber tires.

A major issue that must be considered when designing a camber-car steering system is the kingpin inclination, shown in the diagram on the right of Figure 20. Kingpin inclination causes the contact patch to move relative to the upright as steering angle is increased. It is easier to visualize this as if the highly-cambered tire had been reduced to a thin, circular disc resting on a frictionless surface and prevented from rolling. The contact patch would then "orbit" the tire's circumference as it was steered. Continuing with the visualization of the simplified, highly-cambered tire, the steering axis, which is normally a yaw axis, becomes a pitch axis and causes the wheel to pitch "nose-up" or "nose-down", like an airplane wing, and causing either the "nose" or "tail" to hit the ground. With the circular shape and camber angle less than 90 degrees the contact patch moves smoothly along the circumference as steering angle is increased. This motion is different from the forward/backward motions caused by scrub radius (in the absence of kingpin inclination) because in that case the contact patch stays in the same position relative to the upright and would stay in the same place on the circumference if the tire was on the frictionless surface.

The motion of the contact patch relative to the upright causes a change in mechanical trail in the case of dual A-arm or strut suspensions. The lateral force vector is perpendicular to line of intersection between the wheel plane and the ground plane. If the contact patch moves relative to the upright but the steering axis (defined by the strut or upper and lower ball joints) stays fixed relative to the upright, then the moment arm which causes the lateral force to produce a self-centering torque in the steering system changes. With symmetric camber and kingpin inclination, the mechanical trail on the outside tire shrinks and can eventually become negative. The trail on the inside tire becomes larger. Depending on Ackermann, static toe angle, and lateral load transfer, the self-centering torque through the steering system will generally reduce and may reverse. A similar effect can happen in airplanes when the control surfaces have too much aerodynamic boost. When it happens in the roll mode it is called "aileron snatch", so the reversal of control forces at the rim of a steering wheel will be referred to as "steering snatch" in this report. Cossalter gives an explanation and diagram of the trail change on a motorcycle when steering is applied while the bike is leaned into the turn.[38] Motorcycles do not exhibit steering snatch because they use large amounts of static mechanical trail (i.e. without steering and roll at the same time) and most importantly because they do not use large steering angles (more than a few degrees) when leaned over far. This lack of steering is due to relying mostly on camber thrust for lateral force and also the short wheelbases of most motorcycles. In certain situations, such as slaloms, there is a danger of steering snatch at the apex of each turn, when the bike needs

---

[38] Cossalter, Vittore.: <u>Motorcycle Dynamics</u>, pages 22,23

to reverse lean angle. If the slalom is negotiated too fast, there is a tendency for the rider to apply too much steering angle if the lean angle is increasing too fast. This usually ends in a "high-side" crash.

The shift in contact patch position relative to the upright is more pronounced when the wheel, and not just the kingpin axis, is significantly inclined, so steering geometry on a camber-car requires more careful design and analysis. Steering snatch due to kingpin inclination can be avoided on a camber car but requires a less-conventional suspension layout. Multilink suspensions (also known as "5 link") have complete freedom of the steering geometry, but the geometry changes when steered. If one positions the upper ball joint above the tire, then it can be placed directly above the lower ball joint in order to remove the kingpin inclination. This approach has the benefit of consistent geometry as the wheel is steered, but results in either a more compliant upright, a heavier upright, or some combination of the two because of the cantilever required. It also will limit the A-arm geometry because the wishbone will tend to interfere with the upright/wheel unless it is designed with a more complex shape to clear the tire, thereby requiring the wishbone to be heavier in order to regain stiffness. The Millikens did not report steering snatch on the MX-1, which had a kingpin inclination roughly equal to its camber angle. The MX-1 had a mechanical trail of about 2.6 inches in its final, best form and was tested to 1g lateral on a 200-foot diameter circle, after which it was recorded that the steering centered "okay". This vague comment from the normally very meticulous Milliken suggests that the steering forces may have gotten lighter than the 11 pounds per lateral g which he liked on the zero-camber configuration and lighter even than the 8 pounds per g which was measured on other high-camber tests and which he did not want to increase. The steering did not snatch, however, and there are many factors that could have contributed to this outcome. The combination of greater mechanical trail, less steering angle (due to the large turn radius), and the lack of tire grip all helped the MX-1 (cornering at 1g did not cause sufficient weight transfer to cause snatch). Another important factor that can help avoid steering snatch is the scrub radius. If a positive scrub radius is used with large kingpin inclination then the front of the car is lifted when the wheels are steered. This adds steering weight, most noticeable at low speeds. The steering on the previous Cal Poly SLO camber cars did not snatch and they had larger scrub radii (on the order of 2 inches) and significant caster (and so mechanical trail) to go along with the kingpin inclination.

Static negative camber on the front tires causes a lateral force and yawing moment that tend to counteract the yawing moment due to an impact with a bump in the road on one wheel. When the wheel hits the bump the increase in normal load on the tire increases the camber thrust on that corner and so produces a net lateral force at the front and a corresponding moment about the center of mass. The lateral force causes more lateral weight transfer, however, and this increases the lateral force such that the car tends to move away from the bump. The effect of negative camber on the rear tires is therefore stabilizing since the lateral force is in the same direction as in the front but the moment arm is reversed. Milliken notes that, from his experience with the MX-1, static toe-out of about 10% of the static camber angle tends to stabilize the wandering of a camber car.[39]

---

[39] Milliken, William F. & Douglas L.: <u>Race Car Vehicle Dynamics</u>, page 406

A camber car sees transient response benefits from faster lateral weight transfer. One way to do this is by sending forces through the suspension members themselves, rather than the springs, since the links are much stiffer than the spring on cars not using significant amounts of aerodynamic downforce. The kinematics of the suspension can be set to achieve this load path by placing the instant center of rotation in the correct place, which then puts the roll center at the right height above ground.

The instant center of rotation is the point about which a rigid body (the upright) is rotating at an instant in time. Perpendiculars to the velocity vectors on three or more points of the rigid body can be used to find the instant center, but the analysis is usually broken up into two planar representations of the suspension: front view and side view. An example of the instant center in front view is shown in Figure 21.
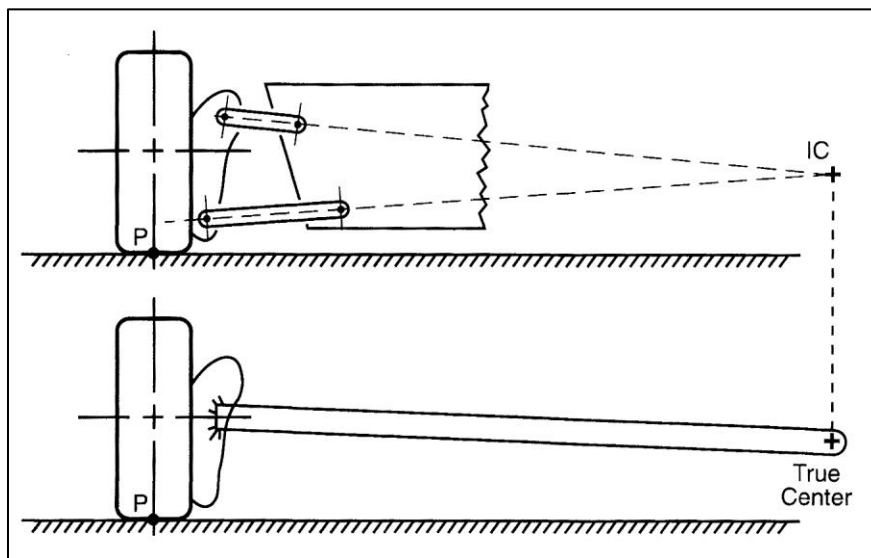
Figure 21: Instant Center vs. True Center[40]

The instant center will move as the wheel displaces on most suspensions. A swing-axle suspension, like that shown in the lower half of Figure 21 has an instant center that is also a true center and which does not move. There is only one suspension link in front view and the upright is rigidly attached to it so that it is constrained to rotate about one physical point. The advantage of a four-bar linkage like that in the upper half of Figure 21 is clear to see: it is much more compact while having the exact same kinematics for that instant in time. It can be much lighter and more rigid because there are no bending stresses and because the links are shorter, increasing buckling resistance. The construction of the instant center for suspensions with tension-compression members consists of drawing lines through those members and finding their intersection point. This is because the velocity of the upright where those members attach must be perpendicular to those (assumed rigid) links. The instant center affects the distribution of forces in the mechanism; in other words which links have more loading.

---

[40] Milliken, William F. & Douglas L.: Race Car Vehicle Dynamics, page 611

28

When the instant center is drawn for both sides of the car, another point can be drawn. This point is the roll center and represents the coupling point for the sprung and unsprung masses. In other words, a force applied at the roll center causes no roll of the chassis. A roll center is shown in Figure 22.
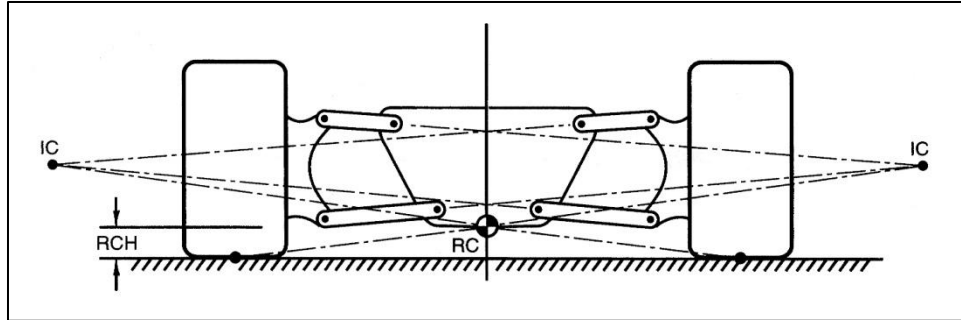
Figure 22: Roll Center Construction[41]

The roll center moves vertically and laterally with suspension displacement since the instant centers do as well. The roll center is found by drawing a line from the center of the contact patch to the instant center of that wheel. What this is mimicking is the true center of a swing axle suspension, where there is a force applied by the tire to a link with a pin connection at one end. Because of this end constraint it can transmit only forces and no moments to the chassis on which it is anchored. The true center is always above ground and since the contact patch is always on the ground the load path does not align with the load. In order to transmit the lateral load component through the slanted load path there must also be a vertical component, called a jacking force. This is shown in Figure 23.
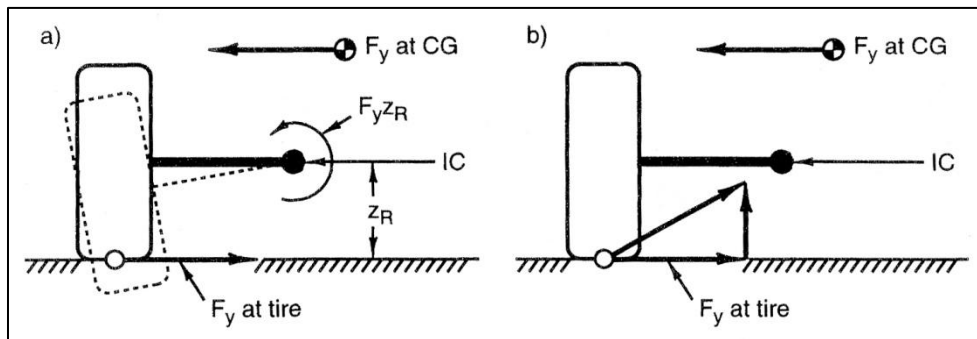
Figure 23: Vertical Jacking Force Due to Applied Lateral Force[42]

The instant center is shown above ground but can be below ground, as can the roll center. In that case the jacking force from the outside wheel is downwards. The jacking force on the inside and outside wheel would largely cancel if the two tires produced the same lateral force, but this is not the case due to lateral weight transfer, and especially on a camber car. Because of this, the sprung mass sees a net vertical force with the direction of the jacking force of the outside wheel (usually). This net vertical force must be reacted by an equal displacement of the springs on both the inner and outer wheels. There can still be net compression on the outside and

[41] Milliken, William F. & Douglas L.: Race Car Vehicle Dynamics, page 614
[42] Milliken, William F. & Douglas L.: Race Car Vehicle Dynamics, page 615

extension on the inside, but there is more extension and less compression than if the roll center was at ground level (meaning no jacking forces). Care must be taken to not let the sprung mass rise too much due to the jacking forces, lest the car overturn. This can be combated by using stiffer springs, which do not need to displace as much to absorb the jacking forces. These stiffer springs further speed lateral weight transfer if they also contribute to roll stiffness and are not the "third spring" acting only in heave (both wheels moving equally).

For the case of the roll center above ground the sprung mass moves up. The jacking force also has a complimentary reaction at the tire which adds load and therefore counters lateral weight transfer (when the roll center is above ground). This reduces the amount of load transfer the springs must support, thereby reducing body roll. Because of this effect the roll center can be used as the pivot point of an inverted pendulum consisting of the sprung mass of the car at the end of a massless rod which is equal in length to the distance between the mass center height and roll center height. The centrifugal inertia force is applied to the mass center and the tire forces are applied to the roll center, causing a roll couple. If the roll center and mass center coincide there is no roll, if the mass center is higher than the roll center the sprung mass rolls to the outside of the turn, and if the mass center is lower than the roll center the sprung mass leans into the turn.

Since jacking forces are transferred through the suspension links they react faster than elastic weight transfer (through the springs). Geometric weight transfer (through the links) therefore, can be used to speed transient response on a camber car which reacts favorably to lateral weight transfer. The jacking effect of a roll center above ground can also be used to raise the mass center for more total lateral weight transfer in steady-state cornering, but this rise must be kept in check so that the car does not capsize.

William F. Milliken did not like high roll centers on the MX-1 because they caused so much jacking that the camber was severely reduced, compromising the handling. This can be countered by stiffer springs, however. The other reason he did not like the high roll center was because a high roll center usually comes with a very short front-view-virtual swing arm length. This means that the instant centers are nearer to their respective wheels and the shorter radius means more camber change when the wheel is displaced vertically. If the front-view swing arm length is equal to half the track width, then there is no change in inclination relative to the road on either tire when there is pure body roll (inside and outside wheels displaced equally and opposite). If the front view swing arm length is shorter, then there is inclination gain on both inside and outside wheels- in other words the inside wheel loses negative camber and the outside wheel gains it. This sounds good but contributes to poor rough road handling and increases gyroscopic kickback through the steering wheel. A swing arm longer than half the track width loses inclination but is better over bumps. Milliken did not like large camber gain when he performed a turn reversal maneuver[43], which means starting out turning in one direction and then turning immediately in the other direction. Presumably this was because of gyroscopic effects as the car rolled, but this was tamed with a steering damper and a droop-limiting device which caused Milliken to be surprised at how well the car handled rough roads despite the short swing arm. Optimal roll center height is still a compromise between faster lateral load transfer and

---

[43] Milliken, William F.: Equations of Motion, page 517

rough road handling (steering) effects, along with how stiff the springs can be made to control jacking without being unduly harsh over bumps.

Transient Response

When a step steering input is applied to a tire there is a delay before the steady-state lateral force is reached. This first-order delay is called relaxation length and represents how far the tire must roll to achieve 63% of full lateral force (one time constant). According to Cossalter the relaxation length to slip angle for motorcycle tires is generally between 0.12m at 20kph and 0.45m at 250kph, increasing slightly with load.[44] He then states that the relaxation length for camber thrust is much less, and has been shown in some tests to be almost negligible.[45] Pacejka, however writes that the relaxation length for camber is about equal to the one used for slip angle and on the order of magnitude of the wheel radius,[46] but this appears from context to be referring to conventional car tires with squared-off shoulders.

If the response time to camber for round-section tires is negligible, then the incomplete block diagram shown in Appendix A gives a starting point to model the transient response of a static-camber car or a conventional car. Tire properties, vehicle mass properties, and suspension settings must be determined before it could be used to provide transient response estimates. The model assumes symmetrical camber gain on bump and rebound. For an operational model, it is strongly suggested to break the car into four tires rather than front and rear axles, so that all the nonlinear effects of load and camber can be taken into account.

The camber car responds faster because it has more paths in the block diagram which increase lateral force than a conventional car does. For example, elastic weight transfer increases lateral force at the rear of a camber car, beginning the transition to steady state. On a conventional car the weight transfer decreases the cornering power and only the yaw displacement adds to it. This means that a camber car can be set up stiffer in roll (assuming the chassis is sufficiently stiff in torsion), speeding up the weight transfer and hastening the build-up of lateral force at the rear sooner than a conventional car. The conventional car would either need to be softer, which leads to issues on quick turn reversals if the yaw and roll get out of phase, or suffer from a slower build-up of lateral force at the rear (since the weight transfer interferes with the slip-angle-generated force). The camber-car advantage is present even if the relaxation length for camber is similar to slip angle.

The benefit to resisting roll couple with elastic elements (springs) is that the lateral force from the front tires can then be used to assist the rears via the rear roll stiffness percentage. The benefit to reacting the roll couple geometrically is that this happens faster than elastic weight transfer due to the stiffness of the suspension links and because of the positive feedback, but the track must have started to generate net lateral force through some other means (such as the weight transfer due to roll damping, which has less of a lag by virtue of being velocity-dependent than the displacement-dependent spring forces) before the geometric weight transfer can take over.

---

[44] Cossalter, Vittore: <u>Motorcycle Dynamics</u>, 2nd ed., page 56
[45] Cossalter, Vittore: <u>Motorcycle Dynamics</u>, 2nd ed., pages 58
[46] Pacejka, Hans B.: <u>Tire and Vehicle Dynamics</u>, 3rd ed., page 22

Because camber cars build-up lateral force on the rear axle more rapidly than a conventional car they reach yaw equilibrium sooner and should feel "tighter" on turn entry (less oversteer) than a conventional car. A similar affect can be obtained on a car with vertical tires by steering all four wheels. In this case the rears would need to turn in the same sense as the fronts. Many premium automakers today employ small amounts of active rear-wheel steering. These systems usually vary the phase of the rear wheel steering as speed changes. For slow speeds the rear wheels turn opposite the front to enable a tighter turning radius for parking lot maneuvers. As speed rises, the rear wheels turn less relative to the fronts until they begin to turn in the same direction at high speeds. This speeds the lateral force response from the rear axle, but by applying the input earlier rather than reducing relaxation length. This type of in-phase rear-wheel-steering also creates an understeering moment to make the car feel more stable to most drivers. Passive rear-wheel-steering, as is often done on multilink rear suspensions via body roll, do not speed transient response as much as active systems do because it takes time for the sprung mass to roll. The passive rear-wheel-steer delay has the same drawback as a passive dynamic camber system.

Milliken writes that the MX-1 had a time to 90% steady state of 0.182 seconds and that response time near maximum lateral acceleration was short and desirable.[47] Corrections for rear-end breakaway were necessary to reach maximum lateral acceleration but this was possible for sustained periods so the car was still stable enough despite fast response times. The response time quoted for the MX-1 on antiquated, treaded tires is only 75% longer than that for a 1993 Grand Prix car, if the example calculations in Race Car Vehicle Dynamics are based on reasonably accurate tire properties.[48] The MX-1 was therefore closer to a modern racing car in terms of response than it was to contemporary road cars. Camber cars are therefore at least as good in transient response as conventional cars, if not better.

Conclusions Regarding Vehicle and Suspension Design

For maximum steady-state lateral acceleration and fastest transient response, a car using round-section tires at a camber angle of -40 degrees is best.

Track width should be as narrow as practical while still achieving benign roll center behavior (movement during roll and bump) and the desired amount of suspension travel. Benefits of a narrow track include improved rough-road handling due to smaller yaw moment arms for impact forces[49] and less steering input needed to negotiate slaloms (the track effectively becomes wider). The mass center should be placed low enough that the car does not capsize except in extreme situations but high enough to increase lateral load transfer. Track width adjustments can be substituted for mass center height in order to reduce the total mass of the vehicle, which can be increased if extra chassis members are required to raise the mass center. The wheelbase should be used to set the longitudinal weight distribution. Using a mid-rear mounted powertrain to keep driveline mass to a minimum (no driveshaft) the differential would ideally be at the very back of the transmission so that there is no overhang past the rear axle line. This reduces the

---

[47] Milliken, William F.: Equations of Motion, page 520
[48] Milliken, William F. & Douglas L.: Race Car Vehicle Dynamics, page 257 & 258
[49] Milliken, William F. & Douglas L.: Race Car Vehicle Dynamics, page 408

polar moment of inertia (in yaw) and speeds transient response and stability because the tires effectively have more leverage to rotate the mass of the vehicle. The wheelbase length should then be set via moving the front wheels forward or backward to achieve the desired weight distribution. A longer wheelbase (for a given polar moment of inertia) increases directional stability and reduces longitudinal weight transfer, aiding handling when simultaneously turning and braking or turning and accelerating at the same time but hampering acceleration on a rear-wheel drive car.

A good ratio of mass center height to track width to design with initially is 0.25, which is where diminishing returns in maximum lateral grip appear in the Milliken simulations of Figure 13. This ratio results in a maximum (limited by inside wheel lift) lateral acceleration of 2g, found using the formula $a_{y,\max} = \left(\dfrac{2h_{cg}}{T} \right)^{-1}$, where $a_{y,\max}$ is the maximum lateral acceleration in g, h_{cg} is the height of the mass center, and T is track width (the same units of length must be used to measure both the mass center height and track width). This formula is derived from a front-view free body diagram of the car as a rigid body and summing moments about the outside tire. The moment arm for the inertial force is the mass center height and that for the weight is half the track width. For a Formula SAE racecar without aerodynamic aids, 2g is more than the tires can support and so gives a margin of safety against tipping over. In order to pass the 60 degree tilt test during tech inspection, corresponding to a lateral acceleration of 1.7g, the h/T ratio must be less than or equal to 0.285. The MX-1's mass center height is not reported but the h/T ratio was probably around 0.13 based on the track width and lateral acceleration given and the weight transfer in figures 10 and 11. A benefit to being able to use a higher mass center is that the ground clearance can be increased in order to clear bumpier or steeper roads as might be found on a rally stage on a mountain road.

Theoretically, more than 2g of lateral acceleration can be achieved with an h/T ratio of 0.25 if aerodynamic devices producing downforce are used. These could be either conventional wings or a wing split along the centerline of the car and using actuators with a control system to keep the load on the inside tire near zero while also preventing the car from overturning. This active system should never create lift as this reduces the total normal force on the tires and so also the lateral force capability. At low speeds, corresponding to tight turns, aerodynamic devices are ineffective but in this case control-moment gyroscopes could in theory be used to maintain weight transfer or even eliminate it for a conventional car, but this comes at a severe weight penalty and does not increase vertical load the way that aerodynamic downforce does. A better method for achieving very high lateral accelerations at slow speeds would be to use a fan and side skirts to evacuate air from under the car in the manner of the Chaparral 2J.

Weight distribution for all road-racing cars should be equal left-to-right to ensure equal cornering performance in each direction. This is even more important for a camber car because an imbalance side-to-side will cause the car to drift left or right when the car is pointing straight down the road. Correcting the drift requires a yaw that adds both tire-induced drag and aerodynamic drag, decreasing efficiency and top speed.

The best longitudinal static weight distribution depends on the load sensitivity of the tires. Using a very limited data set consisting of the two graphs in Figures 10 and 11 of the MX-1

tires at two different loads, maximum lateral force coefficient at -40 degrees of camber increases by more than 5% (from 1.05 to 1.11) when vertical load increases by 66% from 291 pounds to 492 pounds, meaning there cambered tires show positive load sensitivity. More than two points of data from the same tires are required to determine if the load sensitivity is concave up as well, however it is promising that mass center can be moved rearward to regain some of the longitudinal acceleration capability lost to camber without incurring a lateral acceleration penalty. In the absence of more data, the goal should be to have an equal front-to-rear weight distribution but err on the side of rear-heavy. This means that if different drivers weigh significantly more or less then the most forward the mass center should be is mid-wheelbase. The transient response benefits of a forward mass center can be replicated by the rear camber, a chassis stiffer in the torsional mode, and more rear roll stiffness.

Round-section tires and a narrow track provide aerodynamic benefits and weight reduction compared to wide, square-shouldered tires. According to William F. Milliken, a camber car could have about 60% of the frontal area of a conventional car while the narrow tires would open up more plan-view area for efficient under-car aerodynamics such as diffusers. The slanted sides also would make the car much more stable in yaw, which is something that modern sports-prototypes have trouble with (lifting off the ground and flipping once getting a little sideways). Tire pressures should be set at 30psi hot initially but testing should be used to find the pressures which result in the best handling. 30psi is the best value according to the research by Fonda[50] and is also close to the value which the Millikens found as optimal for the MX-1[51]. Cossalter shows camber and cornering stiffness dropping off with increasing pressure[52], however, so lower than 30psi may be better but should be very much dependent on the particular model of tire.

Bump steer should be minimized on any suspension system so that the wheels point in the direction the driver wants, but on a camber car there is a tendency to use large amounts of camber gain in bump, which can cause a different kind of bump steer: gyroscopic kickback through the steering system. On a smooth road the consequences of this can be kept to a minimum and by using a swing arm length (virtual or otherwise) of approximately half-track so that the camber angle changes very little relative to the road as the car rolls in a turn. If the wheel maintains its inclination relative to the road there is no gyroscopic kickback because the spin axis of the wheel does not precess in inertial space. On a rough road, a long or infinite swing arm increases the stability of the vehicle by reducing the gyroscopic kickback and the variation in camber thrust at each wheel. William F. Milliken wrote, after testing the MX-1, that a swing arm length approximately corresponding to swing axles (meaning a length of about half the track width) was "a very good configuration. In every respect, seems a desirable configuration."[53] Conventional Ackermann should be used due to the adverse camber of the inside wheel. Static toe-out of about 10% of the camber angle can be used to stabilize the car if the driver complains of wandering and also provides more Ackermann. Mechanical trail is not effective in this

[50] Fonda, Albert G.: "Tire Tests and Interpretation of Data",
[51] Milliken, William F.: Equations of Motion, page 520
[52] Cossalter, Vittore: Motorcycle Dynamics, 2nd ed., page 55
[53] Milliken, William F.: Equations of Motion, page 517

situation[54]. Control forces at the rim of the steering wheel of about 10 pounds per g of lateral acceleration provide the best feel in a performance car according to Milliken's MX-1 tests.[55] Kingpin inclination should be minimized if practical, and positive scrub radius and static mechanical trail should be set appropriately to avoid steering snatch while keeping the maximum self-centering force (at any steering angle) at the desired level. Positive scrub radius is advisable even without kingpin inclination, in order to reduce the low (or zero) speed control forces.

The suspension should be as stiff as possible to speed transient response while still being manageable over rough roads. The roll center should be above ground at all times, no matter the combination of wheel displacements. A higher roll center speeds transient response but requires stiffer springs to manage jacking and the loss of camber as a result. The roll center should be below the mass center height so that there is roll couple remaining to be distributed elastically between the front and rear tracks in order to tune the oversteer/understeer balance and in order to allow the front lateral force to hasten the build-up of lateral force on the rear of the car. A roll center higher than the sprung mass center would provide roll couple while also allowing a longer front-view swing arm for better rough-road handling (less camber change) since the car would lean into the turn and gain favorable inclination on all tires, however this high of a roll center would mean extreme jacking forces and large amounts of tire scrub. A good roll center height to begin designing with is at the level of the bottom of the chassis such that the roll center height is about equal to the ground clearance. Front-view virtual swing arm length should be approximately half-track.

When attempting to maximize the benefits from camber the drivetrain tends to become a limiting factor. The issue of transmitting drive torque to the wheels at large camber angles can be overcome with wheel hub motors or clever use of chain drives and gearboxes to circumvent constant-velocity joint angularity restrictions. An example would be two, counter-rotating motors (cancelling gyroscopic forces) with their axes parallel to the longitudinal axis of the car. These motors would drive sprockets on the uprights via chains (located so as to minimize the amount of tensioning adjustment required) and those sprockets would connect to a right angle gearbox which then drives the wheel hub riding in the wheel bearings. The chains would accommodate the small static toe angle necessary in the rear suspension. The right-angle gearbox would incorporate a speed reduction so that the outboard sprocket could be reduced in diameter, allowing more camber angle before contacting the ground. This would make the drivetrain able to handle any camber angle while being mounted higher for more ground clearance and better rough-road handling. It would also add anti-squat (if done properly), which could aid traction if kept at a reasonable magnitude. A yaw moment would be generated if this system was applied to a variable camber system but this could be used to advantage. Due to the high percentage of lateral weight transfer, a limited-slip differential is necessary to make best use of the limited longitudinal grip available by beginning acceleration as soon as possible after the apex of a turn. This could be either a torque-biasing type, clutch & ramp type, or spool. A high-ratio torque-biasing differential would be the best option for a car with a reasonable mass center height to track width ratio of about 0.25 because of the greater longevity of the gear mesh compared to the clutch type, because more torque is sent to the outside wheel, and because differential wheel

---

[54] Milliken, William F.: Equations of Motion, page 517
[55] Milliken, William F.: Equations of Motion, pages 515, 517, and 606

speed is allowed, unlike the spool. The spool would be best for cars with higher mass centers and little aerodynamic downforce, which would have the inside rear wheel almost completely unloaded in a turn. In such a case even a 3:1 torque bias to the outside wheel may be insufficient if the inside wheel has almost no traction.

The drawback to an extremely high negative camber configuration is poor braking and acceleration performance due to the inability to eliminate lateral force and so reach the peak longitudinal force point on the friction circle for the tires. Race tracks are combinations of tight turns, open sweepers, and straights. Aerodynamic downforce and camber can increase the speed at which both tight and open turns can be taken, but on the straights the camber is detrimental.

The static camber car responds more quickly to steering inputs than a passive dynamic camber car and can achieve the same steady-state lateral acceleration (assuming identical mass properties), but the dynamic camber car would have advantages on certain circuits where quick transitions are not necessary or do not make up a significant portion of the lap and where acceleration and braking dominate. An active dynamic camber system could improve transient response but would be difficult to control properly in all situations. To determine either the best compromise for static camber angle or the benefits to a dynamic camber system the affect of camber on longitudinal force must be known, but this data is scarce to non-existent. Friction circle diagrams are about all that exists, but this is usually based on conventional cars without significant camber. Keeping the load on the rear tires low with a long wheelbase and equal front-to-rear weight distribution would reduce the camber thrust and mean that the tires could operate closer to their peak longitudinal grip coefficient even with camber, but the lighter load reduces the total longitudinal force which would result. Without four-wheel drive there would still be a loss in longitudinal acceleration potential, perhaps even greater than with a rearward mass center. Braking would be improved with a rearward mass center because it would produce a more even dynamic weight distribution and the typical four-wheel brake system can make use of this.

Ideally, the camber would change from highly negative for best cornering to zero for best acceleration on turn exit and braking before the next turn.[56] Alternatively, the static camber angle can be reduced to strike a compromise for a particular track. Both of these methods were considered when designing the 2013 Formula Electric suspension.

Dynamic Camber

Active vs. Passive

An active suspension which can change the camber angle to the optimal setting for cornering and for acceleration or braking would have fast transient response, high steady-state lateral acceleration, and high longitudinal acceleration. The challenge is in the control system. If simply based on steering angle then corrective steering inputs to arrest spins would then reduce lateral acceleration by reducing camber or even reversing it if the camber was asymmetrical (both inside and outside wheels leaning the same way). A combination of steering angle, brake position, lateral acceleration, and throttle position may be the best method of control. If the

---

[56] Milliken, William F. & Douglas L.: <u>Race Car Vehicle Dynamics</u>, page 405

steering angle is reduced and throttle dropped, no action is taken. The control system would be looking for a reduction in lateral acceleration below a certain amount, throttle or brake application, and steering angle reduction all at once. The difficulty is still in discerning corrective inputs for a slide or spin versus accelerating out of a corner. GPS correlation of track position and turn proximity may be the ultimate answer, but this is not as versatile as a passive system.

A system that leaned all tires into the turn would also have likely feel odd unless calibrated very well since the sideslip response would occur too quickly in relation to the yaw response expected from a normal car. A system which varied the negative camber from zero to -40 would not have this issue, since no net lateral force would be produced by the active suspension, it would simply increase the cornering limits.

Varying the camber relies on the relaxation length for camber thrust being negligible in order to achieve fast transient response. An active system could counteract this somewhat with a higher camber angle to steering angle gain, but a passive system is fundamentally hampered by roll inertia. Passive dynamic camber has the tires vertical when there is no lateral acceleration and uses centrifugal force (initially from slip angle, then aided by the camber) to roll the car and generate favorable camber on the tires through suspension kinematics. This requires time for the roll angle to establish itself and so has a much longer response lag, even if the relaxation length is short for camber. A passive system does not need a complicated control system, however, and in certain situations it performs well. Examples of these cases would be fast, sweeping turns where the control inputs are smooth and relatively low-frequency. Here the suspension does not have the problem of the roll and yaw getting out of phase, as would be the case in a slalom. There is also a benefit to the passive system when correcting a spin, since the camber does not change as fast as the steering input. The main drawback, then, is in turn reversal. Too high a frequency causes the car to be leaning out of the turn and so poorly cambered. If the frequency is high enough and the motion well damped then this problem can be kept to a minimum since the amplitude of the camber will be small and the weight transfer small as well (assuming zero geometric roll resistance so that there is maximum roll couple to be used for steady-state roll angle and camber thrust). Depending on how much of the track is made up of fast, wide-open sweepers, the passive setup may be fine, as long as there are not many quick turn reversals required.

Both the active and passive dynamic camber systems will be heavier than simple static camber setups and this must be taken into account when the gains in longitudinal grip from camber reduction are found through testing. Weight increases for the passive system due to the increased complexity of the suspension mechanism and drivetrain (large amounts of axle plunge) compared to a static camber setup and mass is added to the active setup by the actuators, control system, power source, and drivetrain.

A system under manual control and separate from the steering would theoretically accomplish the desired effect but would put too much work load on the driver if the "camber switch" was anything other than a bi-polar one: vertical or full negative camber and only to be activated before or after a corner, not entering or exiting a turn. In those transitions the friction circle would not be fully exploited as it would be in an independently-controlled, active system.

Polynx

The initial suspension concept was a passive dynamic camber system which has the tires vertical when not turning but which generates a large negative camber angle on the outside tire and a small positive camber angle on the inside tire when turning. The difference in camber angles is in recognition of the fact that the lightly-loaded inside tire does not benefit from camber as much as the heavily-loaded outside one. A single spring and damper unit is installed on each corner and an additional spring and damper connects the inside and outside wheels on each axle in order to provide additional spring rate in ride and pitch. This minimizes the pitch angle and therefore keeps the wheels more vertical during acceleration and braking so as to maximize longitudinal force.

The desired camber change happens in response to the opposing displacements of the wheels when the sprung mass rolled, similar to the effect of a front-view swing arm length of less than half the track width. The issue with using a conventional suspension (such as dual A-arms) with a short swing arm length is that it usually comes with a high roll center, which reduces the roll couple and so the roll angle which the suspension relies on (though a higher roll center would increase the natural frequency in roll and so reduce the response time). The other issue with a conventional suspension design was that it was impossible to achieve the highly-unequal camber change between bump and rebound travel. As a result, a novel new suspension mechanism was devised.

This is a system incorporating a four-bar linkage with an extended coupler link forming a rocker arm controlling the path of the lower ball joint of the upright. Connecting to the upper ball joint is a link that connects to a floating node, which is a pivot on the end of a link that has its "ground" pivot point on the chassis. A third link connects to this floating node, but this third link has its other pivot point floating as well. This floating pivot point is shared with the lower four-bar linkage and is also the floating fulcrum for the rocker arm controlling the lower ball joint. This suspension falls into the category of VXI suspensions because it uses two floating pivot points and a "camber link" connecting to the upper ball joint. Figure 24 shows a basic sketch of the general concept but with equal inclination on the inside and outside tires rather than the approximately vertical inside tire that was deemed superior because it reduced the amount of plunge necessary in the driveshafts.
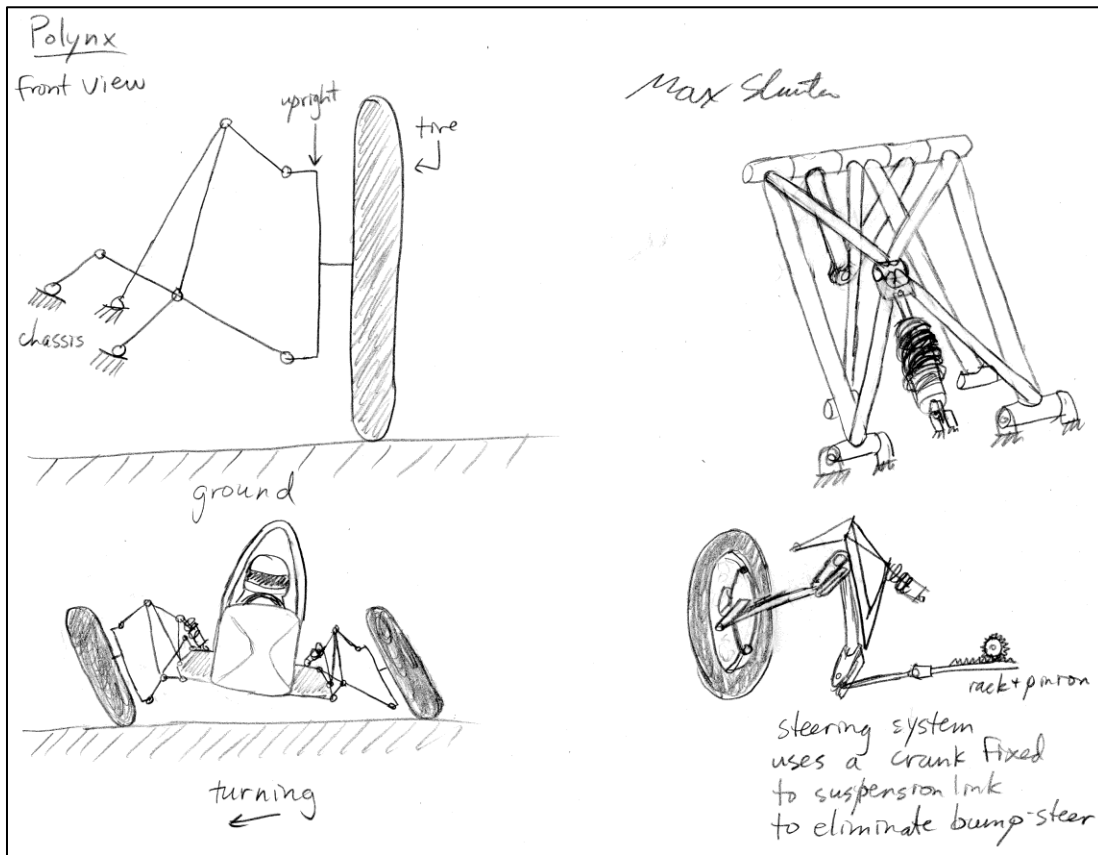
Mechanism Design

Figure 24: General Polynx Design

In order to minimize bump steer, an intermediate crank is used so that the steering linkages follow the suspension links' centers of rotation as camber changes. This crank is anchored to one of the suspension links which connect to the chassis. There is an inner tie-rod connecting one of the crank arms to either a steering rack or a lever at the end of the steering column (like a go-kart). Another tie-rod connects the other crank arm to the steering arm on the upright. This system eliminates bump steer in a straight line but not when the wheels are steered.

This suspension design was given the name Polynx as a reference to both Cal Poly and the number of links in the system. Polynx is a planar (in front view) mechanism with three pivot points on the chassis, but for certain kinematic profiles two of those pivots can be in the same spot, resulting in two rocker arms in the suspension, reducing the number of joints and increasing the rigidity. The three-pivot version allows more complicated wheel paths such as short-travel, high camber change ones, but can also be used to achieve a high-travel suspension with little camber change. The two-pivot design provides a convenient position for a direct-acting coil-over shock absorber (coil spring concentric over a linear damper). Figure 25 shows a CAD rendering of the steering system on a 2-pivot Polynx system but without the spring-damper unit installed.
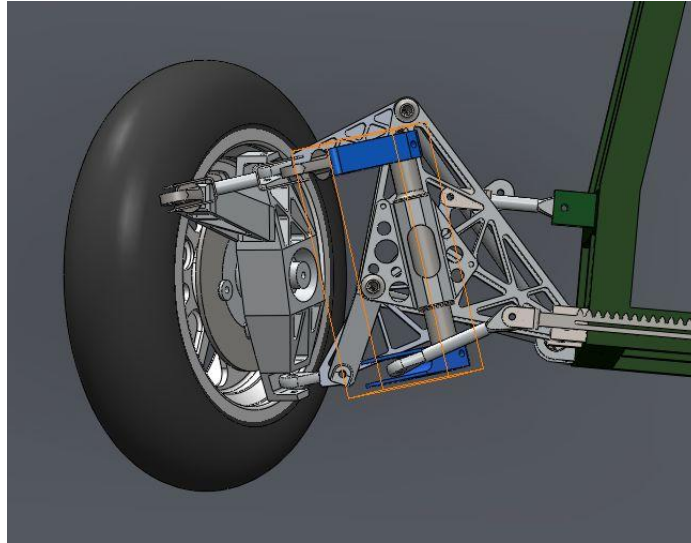
Figure 25: Steering Mechanism Shown on a Simplified (2 Pivot) Polynx Suspension

The roll center of the Polynx configuration chosen for the FSAE camber car is fixed relative to the chassis and is at ground level at static ride height in order to increase the steady-state roll angle without causing jacking of the sprung mass or lateral tire scrub.

With the extreme camber change and low roll center the driveshafts must change length significantly. One solution would be wheel-hub mounted electric or hydraulic motors. What was settled upon, primarily due to familiarity, was a system using conventional, Rzeppa-type constant velocity joints and a shaft that can change length by means of ball-bearing splines.

Driveshafts were also to be used in the front for inboard brakes because the current Formula Electric wheels are too small to fit the brakes inside them and larger wheels would be heavier and require heavier, larger tires. Mounting the brakes on the inside of the uprights, as was already done on the previous Formula Electric cars, would interfere with linkages. These driveshafts will add weight and so cancel the weight advantage of the small motorcycle tires, but the inboard brakes relieve the suspension links of the need to react brake torque and so they can be made lighter. Full-size motorcycle tires would be large enough in diameter to fit brakes in and would allow the camber angle to be shared better between the inner and outer constant-velocity joints, therefore permitting more camber. Running inboard brakes does show that a four-wheel-drive Polynx version is possible. The main drawback of the inboard brakes is a smaller maximum steering angle, but this should only affect very tight parking maneuvers which are not important for track performance. This version of Polynx would be better suited to vehicles larger than FSAE cars, where the weight penalty of tires large enough to fit outboard brakes in the front would not be such an issue. Inboard brakes are a logical choice in the rear because the drivetrain is already there for propulsion.

Design Direction Change

As the time to manufacture the Polynx suspension drew near, it was decided that the Formula Electric team did not have the resources to manufacture the Polynx suspension for the 2013 competition. Additionally, the team did not wish to redesign the electronic stability control system to account for the inherent torque-vectoring that the dynamic camber system included

due to the change in rolling radius when the tires lean. Along with the complex drivetrain (plunging shafts and high-angle constant-velocity joints) necessary for Polynx, the necessary changes to the electronic yaw & traction control system and the manufacturing difficulty prompted the decision by the team to abandon the Polynx suspension system and adopt an approach of optimizing the much simpler static camber setup.

The suspension team still desired to know more about camber and the specific characteristics of the small motorcycle racing tires being used (due to their light weight). Therefore, the design goals became to design a suspension system that could accommodate any camber angle between approximately -30° and +6°. This would enable testing of many different camber configurations so that the optimal static camber angles on the front and rear could be determined for the competition. The second main goal of the adjustability was to simulate the Polynx suspension's steady-state cornering grip by performing skidpad tests with asymmetric camber of -24° on the outer wheels and +2° on the inside wheels.

Final Design: Static Camber

Kinematics

The front-view swing-arm length was set at approximately half the track width, in accordance with Milliken's recommendations. The roll center static height in the front was set at about 2 inches above the ground. This was largely determined by the minimum clearance between the inner suspension pivot point and the ground, as well as the necessity for the suspension links to clear the brake rotor. The rear roll center height is about 0.25 inches higher than the front to speed transient response by having more geometric weight transfer in the rear than the front. The front-view suspension pivot points are shown in Figure 26 for the front suspension and in Figure 27 for the rear suspension. Dimensions are in inches and the solid, horizontal, black line is the ground level. The dotted, vertical line is the centerline of the chassis. The shorter, dotted lines represent the springs and connect to triangles which show the rocker pivot geometry. The four lower points are the inner pivot points for the two pseudo-A-arms.

The steering link inner pivot (on the steering rack) is positioned 0.012 inches lower and 0.114 inches further outboard than the inner pseudo-A-arm pivot points. This was the best position for minimum bump steer as determined by SolidWorks after the upright geometry had been set for simplicity of manufacturing, and with the knowledge that the steering link had to clear the brake rotor and the steering rack had to be mounted low in order to allow the driver's legs to pass over it.
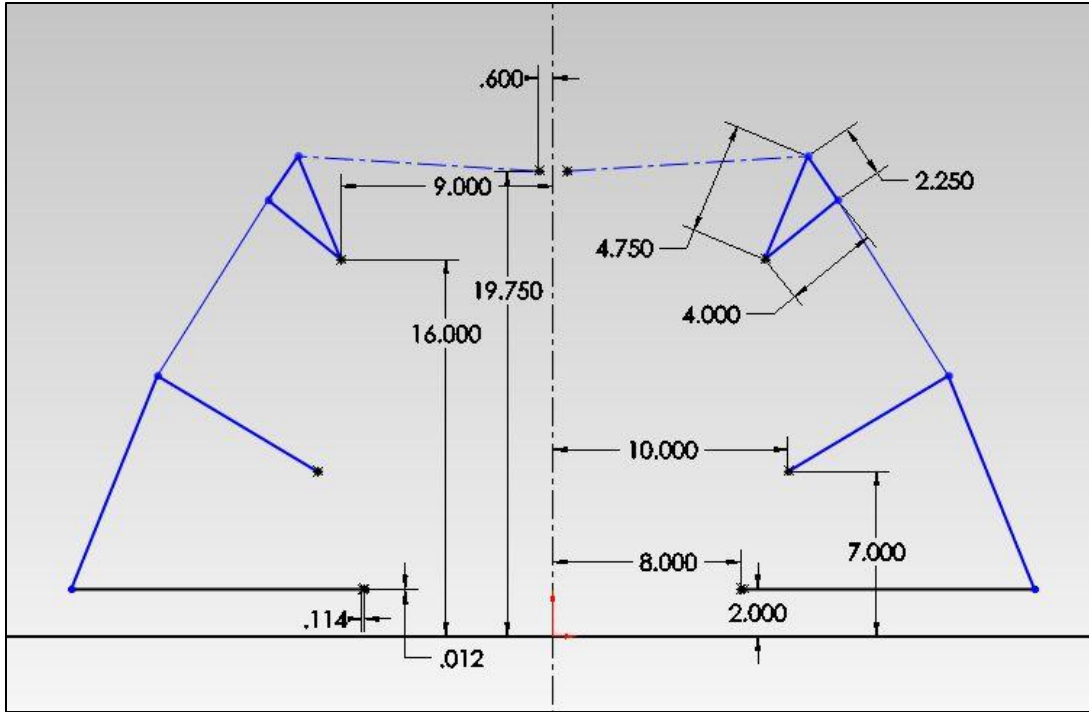
Figure 26: Front Suspension Pivot Point Front View Geometry
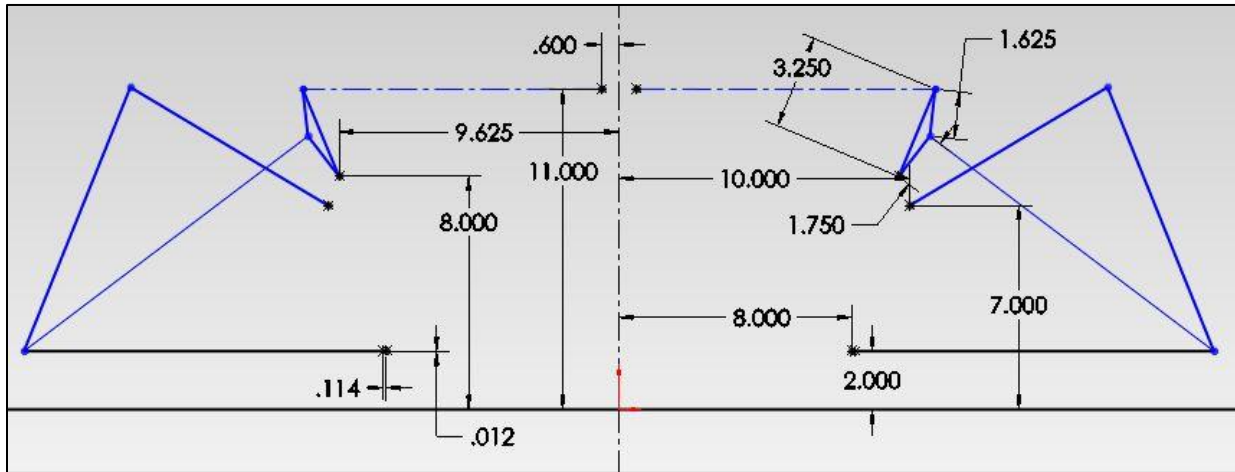
Figure 27: Rear Suspension Pivot Point Front View Geometry

Both the front and rear suspensions have only one spring per corner (no heave springs) and there are no anti-roll bars because they would add weight and complexity and their purpose can theoretically be fulfilled by changing spring rates.

The static camber angle is -22 degrees on all four wheels because it is near the limit of the constant velocity joints being used. Joints that would allow higher angularity would be heavier, and more complicated drivetrain layouts were rejected by the drivetrain team as too much work.

There is no anti-dive or anti-squat built into the suspension because the undamped oscillations caused by the coupling of longitudinal and jacking forces through the suspension members tends to reduce the braking or acceleration capabilities.

The side view geometry of the front suspension is very important because it sets the steering geometry. The pseudo-A-arms define upper and lower virtual ball joints at the intersection points of lines projected along the suspension links in those pseudo-A-arms. In the rear the side view geometry is set in order to reduce the maximum forces in the links between braking/driving and turning. This is accomplished by adjusting the splay angle of the links. Side view geometry is shown in Figure 28 for the front suspension and Figure 29 for the rear.
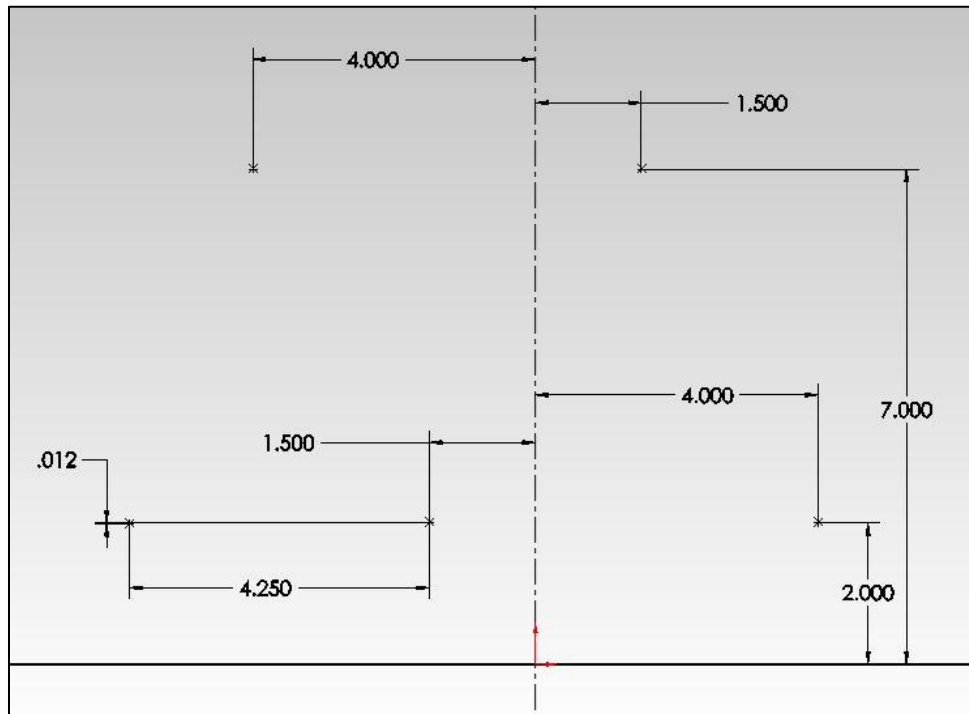
Figure 28: Side View of Front Suspension Points

The vertical centerline is the center plane of the rocker arm and coil-over spring mount. The solid, horizontal line is represents the ground level. The front pushrod is in the plane of the rocker arm when the wheels are pointed straight-ahead but the rear pushrod is slanted because the rocker arm had to be moved rearward to clear drivetrain components.

Figure 29: Side View of Rear Suspension Points

Upright geometry is more complex, especially on the front where the clevises are angled. The front view geometry of the front upright is shown in Figure 30 and the front view of the rear upright is in Figure 31.

Figure 30: Front View of Front Upright Geometry

44

In the front view sketches of the uprights and tires the wheel offset of +0.45 inches can be seen, as well as the 0.75 inch thickness of the hub and the 0.158 inch or 0.177 inch protrusion of the inner bearing race from the outer face of the upright. In Figure 30 the angle of each clevis block is shown (24 degrees for the bottom and 6 degrees for the top), as well as where the pushrod clevis spherical bearing is located (the 1.296 inch line at the top of the upright). The 0.75 dimension is the distance between the two plates of the clevis (in other words, the throat). The solid, horizontal line is the ground level in both drawings.
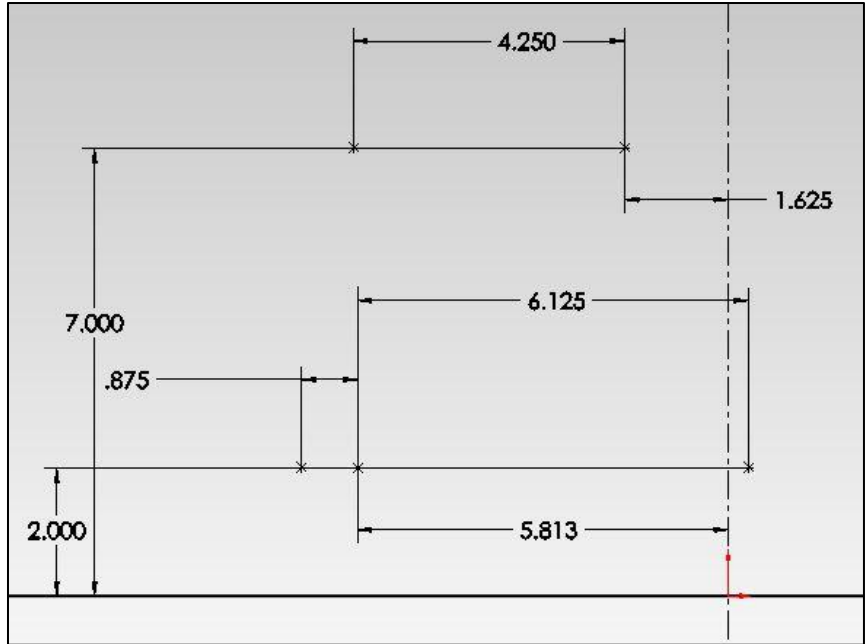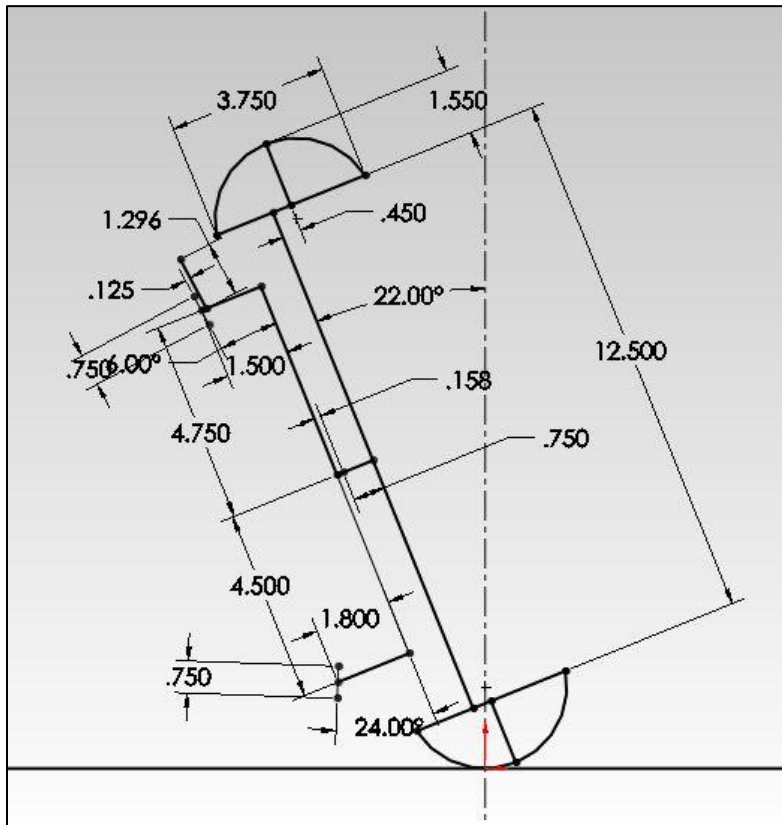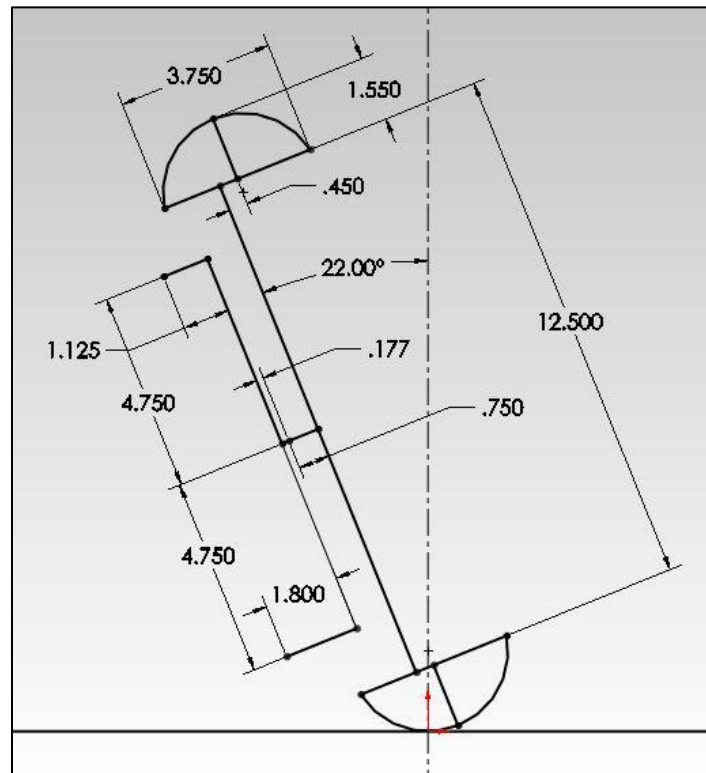

Figure 31: Front View of Rear Upright Geometry

The side view of the uprights is harder to show because of the three-dimensionality of the parts. The lower pivot point shown in Figure 30 is only for the pseudo-A-arms. The steering arm is mounted in the same clevis but is not in line with the lower pivot points. This geometry is seen in Figure 32, and the construction of the upright will be discussed in a following section.

Figure 32 is a top view of the left front upright's lower clevis block, but the part is the same on the right side, just flipped over so as to be mirrored. The part is also the same for the high and low camber parts. The offset of the bolt hole for the steering rod end (0.906 inches) is necessary for the correct Ackermann with a front-mounted rack. The front-mounted rack is necessary to allow a one-piece steering column, and a rear-mounted rack would have required multiple universal joints or a right-angle gearbox. This is a common issue, characteristic of the small size of FSAE cars.
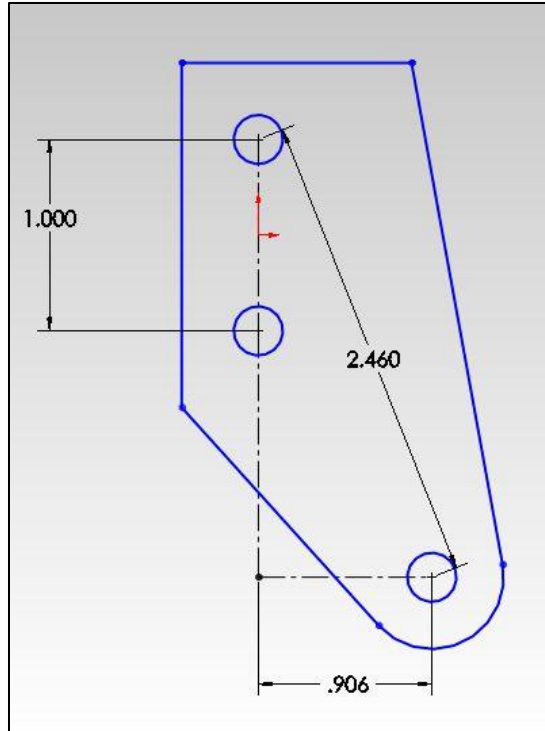
Figure 32: Top View of Left Front Upright Lower Clevis Plate

Figure 33 shows the top clevis block for the high camber front uprights. The upper and lower plates of the top clevis are different from each other and are different for the high and low camber configurations because the length of the plate must be adjusted to meet and weld to the outer face of the upright when the angle of the top clevis changes for high or low camber.
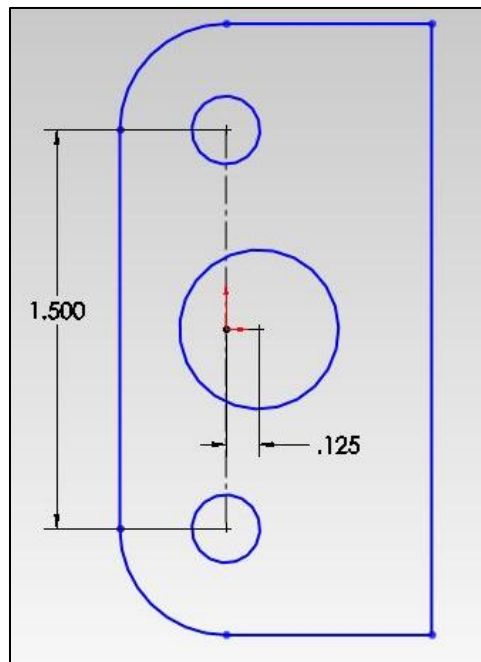
Figure 33: Top View of Left Front, High Camber Upright

46

The 1.5 inch spacing between the bolt holes for the pseudo-A-arm rod ends in the top clevis, as well as the relative location of the hole for the rotating clevis bushing tube (the large hole in the middle) do not change between high and low camber parts.

The four spherical bearing center points are symmetrical about a plane perpendicular to the clevis plates and containing the wheel spin axis. This plane is also perpendicular to the road when the wheels are pointed straight-ahead, meaning the upright is not leaned forward or backwards in side view. Caster is achieved entirely by the top-view angles of the suspension links.

The side view geometry of the rear upright is easier to show, but the rear hub and constant velocity joint are not normal to the plane containing the suspension points. As a result, the vertical spacing shown in Figure 34 is not exactly to scale. The fore and aft location of the spherical bearing center points relative to the vertical centerline is correct, though. This centerline passes through the axis of wheel rotation. The view is once again from the left looking right, with the front of the car being out of the picture frame to the left of the page. The toe link connects to the forward-most point and the pushrod to the rear-most. The other points are for the pseudo-A-arms.

Figure 34: Side View of Rear Upright Geometry

The theoretical center-to-center lengths for each link are shown in Table 1, calculated using CAD and the desired steering geometry and kinematics.

47

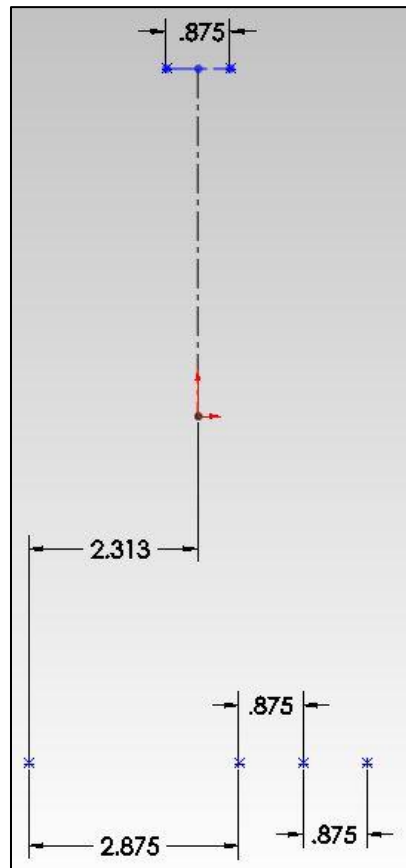| Link Name	Center-to-Center Length (inches)	
	-22˚ Camber	0˚ Camber
Front Lower Rear	13.030	13.368
Front Lower Front	12.591	12.941
Front Upper Rear	8.277	12.433
Front Upper Front	8.861	12.829
Front Pushrod	8.134	10.136
Steering	13.932	14.286
Rear Lower Rear	12.629	12.833
Rear Lower Front	12.629	12.833
Rear Upper Rear	8.469	12.574
Rear Upper Front	8.469	12.574
Rear Pushrod	12.386	11.735
Rear Toe	12.369	12.577

The multilink system allows much more freedom in steering geometry than dual A-arms do. This is because the steering axis is defined by the instantaneous centers formed from the two pairs of lateral control arms, rather than constrained by two physical pivot points on the A-arms. This allowed the scrub radius to be reduced significantly from the previous suspension despite the wheels and tires being too small and narrow to house any steering or brake components. The previous (A-arm) suspension had more than 2 inches of scrub radius and about 30 degrees of steering included angle which combined for significant steering kick-back and also lifted the front of the car an amount equal to about 50% of the ride height, shifting weight rearward when steered. The multilink has a scrub radius of approximately zero with a -22 degree camber configuration with a steering included angle approximately equal to the camber angle. Front-end lift has been reduced to nearly zero, partially due to the placement of the pushrod on the top of the upright. As the upright turns the pushrod changes its angle and effectively shortens which cancels-out the effect of the rising front upright so that the sprung mass remains at the same height. Self-centering on the new suspension is achieved via mechanical and pneumatic trail rather than the front-end lift used previously and this means steering weight changes are in theory more dependent on speed and lateral acceleration.

According to research, the inside tire must be turned about 6 degrees more than the outside one in order to produce maximum grip with a large negative camber angle. To achieve this, a goal of 100% geometric Ackermann was set. About 80% was achieved because more resulted in too much nonlinearity on the inside wheel, causing structural issues (large loads in the links) and link interference. A graph of the Ackermann is shown in Figure 35. The steering angle of the road wheels were calculated using CAD. The toe angle was defined to be the angle between the straight-ahead and the line formed by a plane containing the circumference of the tire intersecting the plane of the road.

The amount of Ackermann shown in the graph is supplemented by the static toe-out of about 2 degrees on each wheel for stability. Therefore, the effective Ackermann is closer to 100% than it appears. In the rear, the static toe-out can be set to produce nearly the optimum slip angles on both the inside and outside tires for the most common turn radii while still being close

to 10% of static camber as recommended by Milliken. When slip angles develop in the rear, the turning center shifts forward and the theoretical Ackermann no longer applies.
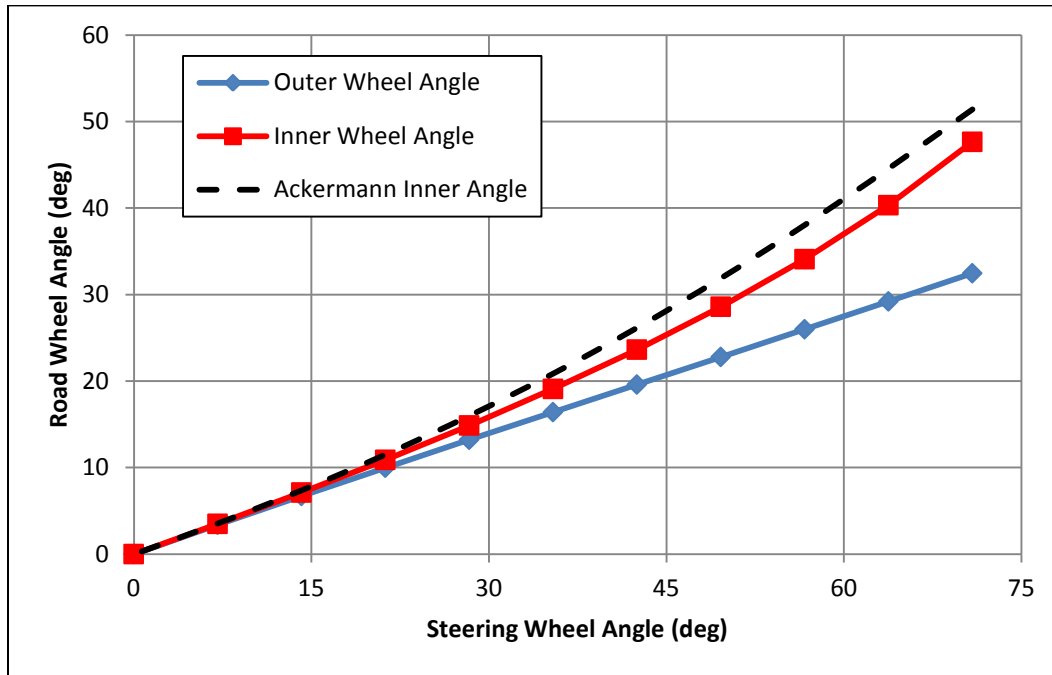

Figure 35: Ackermann of the Front Multilink Steering System

The steering link's outer pivot was positioned on the front of the upright so that the rack could be mounted in its forward location without forcing the steering link to cross over the lower lateral control arms. Crossover is not possible because the outer steering rod end must be mounted low in order to clear the brake rotor. The inner steering arm location which was found to have the least bump steer with the desired upright configuration (steering arm mounted low as part of the pseudo-A-arm clevis) was determined using front-view sketches of the front suspension in its maximum bump, maximum droop, and static positions. This location necessitated a rack and produced the bump steer curves shown in Figure 36, which shows that there is practically zero bump steer in a straight line. The short outer steering arm length means that the inner steering link pivot point does not need to move very far to achieve large steering angles. That then reduces the bump steer when the wheels are turned.

The steering ratio of about 2 (two degrees of steering wheel turn per degree of road wheel steering) means that the driver's arms do not cross-over each other, even in the tightest turns, and that he or she does not need to reposition his or her hands on the wheel. This is safer, more comfortable, and can help the driver go faster around a corner because of the enhanced ability to correct spins compared to a slower ratio. In order to keep the steering weight manageable, the mechanical trail was set at a value of about 0.4 inches when the wheels are pointed straight-ahead. This resulted in an expected steering weight of about 11 pounds per g of lateral acceleration for large-radius turns, measured at the rim of the 9.375" diameter steering wheel. A benefit of the fast steering ratio is that the steering rod's inner pivot point moves less for a given turn radius than it would with a slower ratio. This reduces the bump steer when negotiating turns

on a rough road, improving stability and the speed at which the turn can be taken. The steering weight is similar to that on the MX-1 which William F. Milliken found satisfactory.[57]
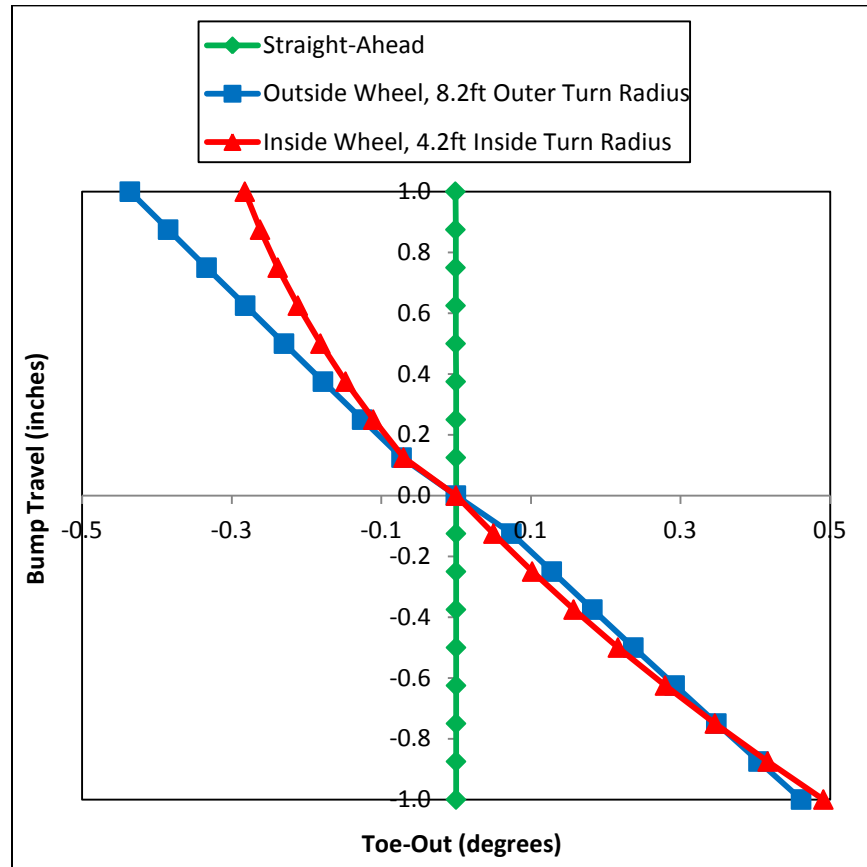
Figure 36: Bump Steer for Multilink with Rack & Pinion Steering

Due to the complex geometry involved, a full analysis of steering force variation with steering angle and lateral acceleration was not completed in the short time available for the suspension re-design after the abandonment of dynamic camber and before manufacturing had to begin. Since the kingpin inclination was similar to the MX-1 and the previous Cal Poly camber-cars it was believed that the steering would not snatch, although the steering weight would likely decrease at high lateral acceleration. To add more self-centering in those high-g situations the brake calipers were placed on the front of the upright so that their inertial forces exert an understeering yaw moment on the road wheels. This did not prove to be enough and the steering snatch at large steering angles during testing, however it is not known how much steering angle was applied when the snatch (very abruptly) occurred because the frame geometry is not exactly as-designed so the drop-down clevises do not act as steering stops as they were supposed to. Therefore, it may be that the steering is going too far, a conclusion seemingly supported by two failures of the front suspension (which will be discussed in the design verification section), although improper handling of the rod ends during construction is also suspect. The conclusion from the initial test drives is that the large steering angles, negligible scrub radius, and small

---

[57] Milliken, William F.: <u>Equations of Motion</u>, page 515

50

static mechanical trail combined to cause the steering snatch. The scrub radius which was thought to be a good feature because it reduced the front-end rise with steering also increased the zero-speed steering weight to unacceptable values. This shows the importance of considering the interactions between all the steering geometry factors in order to design a good steering system.

The large steering angle is still desirable, so other measures should be taken on a future version of the suspension in order to eliminate steering snatch. A larger, positive scrub radius (perhaps 1 inch) and smaller steering included angle would be the most important changes. This could be achieved by moving the lower pseudo ball joint inwards, accomplished by increasing the plan-view included angle of the lower pseudo A-arm links, specifically by moving the lower, aft inboard pivot point rearwards on the chassis and leaving the lower, forward pivot point where it is. An additional benefit to this change in geometry is that it would reduce the peak load in that suspension member, which occur during braking and when cornering at high lateral accelerations with full steering lock. To reduce the kingpin inclination even more, the spacing of the pseudo-A-arm rod ends in the upper clevis of the front upright should be increased, along with the spacing of the inner pivot points of the upper pseudo-A-arm, thereby positioning the virtual upper ball joint further outboard. Offsetting the upper and lower clevises in the upright, and the upper and lower inboard pivot points may also allow the mechanical trail to be made more consistent throughout the range of steering travel. The geometry of the steering arm on the upright and possibly the rack position will need to be modified to keep the correct Ackermann and steering ratio.

With the multilink design the brake rotor does not necessarily need to be positioned on the inner face of the upright, but since the caliper would not fit in the wheel, the spindle would be severely cantilevered out from the bearings and so would need to be stronger and heavier to handle the bending stresses, and the bearings would need to be larger. Therefore, weight is reduced by locating the brakes on the inner face of the upright (as seen in Figure 37), which is where they were on the previous suspension. This outboard brake configuration eliminates the complex plunging shafts necessary for the front inboard brakes on the Polynx design, but means that the bottom front links are very highly stressed while reacting the brake torque in addition to the longitudinal force.

The motion ratios for the front and rear spring systems are slightly less than 1:1, meaning that the spring and damper compress slightly less than 1 inch per inch of upward wheel travel. This ratio was chosen to provide the most leverage for the spring without exceeding the limits of the damper stroke. The leverage is important to provide a stiffer suspension so that it does not bottom out. This could also be achieved with stiffer springs but it was desired to save money by using springs already in inventory. The spring rates are equal front and rear at 200 pounds per inch because the weight is distributed approximately equally between the front and rear axle. A slightly higher rear natural frequency helps provide a level ride and increases driver comfort. An anti-roll bar could be used on one end to tune the understeer/oversteer balance through changing the roll couple distribution without affecting the ride. If the weight distribution was slightly rear-biased this would not be necessary because the stiffer springs which provide a higher rear natural frequency also increase the rear roll stiffness and balance the handling. Geometric anti-roll must also be taken into account when choosing spring rates.

Ride height is 1.25 to the bolt heads for the front lower suspension points which are the lowest point on the car. Rake angle is zero. The low ride height is necessitated to reduce the angle of the outer constant-velocity joints. A higher ride height was desired in order to increase the mass center height (and so the lateral load transfer which camber relies on) along with improving performance over rough roads by preventing the chassis from scraping the ground over bumps.

The desired weight distribution for the car was 55% rear to provide a good compromise between lateral grip and longitudinal grip but the actual weight distribution turned out to be slightly less than 50% rear when the driver was in the car. The wheelbase of the car shrank from 66 inches to 62 inches because the chassis was longer than necessary in the midsection and it was not desired to move the front wheels forward along with the rear because it was believed that would result in too rearward of a weight distribution while increasing the turning radius. In hindsight, extending the wheelbase via moving the front wheels forward would have been better because it would have improved driver compartment ergonomics as well as returning the weight distribution to the desired value. The track width was set at 48 inches based on a projected mass center height of 12 inches which turned out to be much higher than the actual value, which was about 8 inches.

The tires are PMT rear tires for small racing motorcycles. The size is 100/85-10 on all four corners. These are what have been used previously on the Formula Electric car and what the current wheels fit. They are lightweight and are probably the best option in their size. Larger tires and wheels from a full-size sports motorcycle would allow more camber but would not fit in the 2012 to 2013 budget. They would also have considerably more inertia.

Component Design & Analysis

The final design for the suspension is based on the traditional multilink (or 5-link) concept. Six individual links constrain the upright in all six degrees of linear and rotational freedom. In such a system four of the links replace the pair of A-arms in a conventional system. A fifth link controls the toe angle of the wheel (and would be called a steering tie-rod on the front suspension). The sixth link is either the spring itself or the pushrod (or pullrod) which connects to the spring through a rocker arm. In the design chosen there are pushrods for both the front and rear suspensions because the spring-damper units are too bulky to attach directly from the chassis to the upright without interfering with other components. Each of the six links per corner are simple, aluminum-alloy rods with right-hand female threads on one end and left-hand female threads on the other so that two heim joint rod ends can be threaded into each end and the center-to-center length of each link can be adjusted by loosening jam nuts and rotating the rod in one direction or the other without removing the heim joints from their clevises. For large changes in camber (which would exceed the limitations of the threaded lengths of the rod-ends), new aluminum rods can be made much more quickly and easily than welded steel A-arms, which was what the previous suspension used. Figure 37 is a CAD rendering of the full suspension in isolation. The left side wheels have been removed to show the uprights and hubs better.

Figure 37: Final Suspension Design

In the rear, the heim joints are oriented with their axes of full rotation oriented longitudinally so that the camber can be adjusted throughout an extremely large range without requiring changes to the upright or chassis. The rear links are splayed, forming a "V" in plan view, similar to an A-arm, in order to better react braking and drive forces. The consequence of this is that the heim joints are very near their maximum misalignment angle but this is acceptable because only a few degrees of static toe-in or toe-out are necessary for tuning the stability and response and both ride motion and camber adjustment are accommodated by the heim joint's axis of infinite rotation (about the bolt axis). The right rear upright and suspension links are depicted as-manufactured and unpainted in Figure 38.

Figure 38: Right Rear Suspension Corner

The pushrod from the rear spring and rocker is attached to the bottom of the rear upright because it allows the pushrod to be more in line with the resultant force vector from the lateral tire force and the weight than if it attached to the top of the upright. It also allows a lower spring and damper placement which means that the rocker arm mounts can share a chassis tube with the suspension points and therefore reduce the complexity and weight of the chassis. Locating the pushrod on the bottom of the upright also means it does not need to change length significantly with large camber changes, as would be the case with the pushrod mounted on the top of the upright. What this means in practice is that fewer rear pushrods need to be made since the turnbuckle adjustment can cover a large range of camber. By having the pushrod acting on the upright through its own clevis, rather than acting on an A-arm as on the previous suspension, all

53

the suspension links are two-force members in theory, and can therefore be lighter and/or have a higher factor of safety.

Both front and rear coil-spring-over-damper pairs are horizontally-opposed, as seen in Figure 37, so that forces due to brake dive, acceleration squat, and heave (all four wheels moving up or down equally) are canceled within the spring-damper unit mount and putting less stress on the chassis. These mounts each consist of two metal tabs which form clevises for the spherical bearing in each spring-damper unit. There are two holes in each tab, one for the left side spring-damper unit's bolt and one for the right side unit. The net forces resulting on the chassis at that point are lower than with separate mounts or with spring-damper units that are not directly opposed to each other and those forces only come about as a result of the lateral load transfer. The rockers are all oriented with their rotational axes longitudinal, and the springs act on the same side of the rocker as the pushrod does, therefore the pushrod and spring forces partially cancel (more or less, depending on the lever ratios for the pushrod and spring) and reduce the stress on the rocker arm pivot.

In the front, the heim joints must be oriented with their rotational axes vertical in order to accommodate steering. This then creates challenges when changing camber because this must be accommodated by the limited misalignment capability of the rod-ends. With the chosen front view swing arm length of approximately half track and roll center height at the center of the bottom chassis tube the pivot points fixed to the chassis do not need to change position or angle in order to retain similar kinematics when varying camber. The clevis angles on the upright do need to change angle, however, and this led at first to a three-piece design for the front upright, with a central section serving as a brake caliper mount and a locator for the wheel bearings, an upper clevis piece where the top two suspension links would mount along with the pushrod, and a lower clevis piece which would mount the bottom two suspension links and the steering link. There would be three bolt holes in the center section for each clevis piece. Two through-bolts would pass through both the clevis piece and center section, occupying two of the holes. One bolt would serve as a pivot point and in order to change camber the second bolt would be removed and inserted into the third hole in the upright and clevis piece. This would change the angle of the clevis and the location of the outer pivot point. The change in location of the pivot point was beneficial to steering geometry (with the initial steering rack placement) and front-view kinematics. Only two angle positions were necessary to cover the desired range of camber when using relatively compact heim joints.

The three-piece design was abandoned when the steering system was finalized. A major goal was to use a single-piece steering column (rather than one or more universal joints) to reduce the backlash and deflection in the steering mechanism as much as possible. To achieve this, the steering rack had to be mounted very far forward do to the short wheelbase (required for acceptable weight distribution). The initial rack placement behind the front wheel centerline would have required a gearbox or several universal joints. With the front-mounted rack, the steering link's outer pivot point had to be much closer to the tire than the other suspension links' pivots in order to achieve the desired Ackermann effect. The result of this was that when the lower clevis was changed to the low-camber configuration the steering arm would hit the tire. Since the same clevis piece could not be used for both configurations, it was decided to move to a single-piece, sheet-steel, welded upright that would be lighter and stiffer than the three-piece

one. Two different uprights would be required per side, however: a high-camber one and a low-camber one.

The biggest issue that came up before manufacturing was that the rack was several inches too wide for the desired inner steering link pivot point. There was not enough time or budget to obtain or make a new rack, and changing the steering geometry so significantly was unacceptable. The suspension points could not be changed because the chassis subsystem team did not wish to change the floor of the chassis to be wider or to bend around the rack (the frame rails had to extend further forward for driver leg protection, a problem common to FSAE cars but not on full-size racing cars). This design constraint meant that special steering rack clevises were required to achieve the correct steering geometry. These allow the rack to mount on top of the lower frame rail while the clevis itself extends down to the correct position. This then creates the possible problem of the clevis hitting the frame when steering, but due to the steering ratio selected there was sufficient clearance simply by extending the bottom control arm tabs by about 0.5 inches (meaning the frame rails are narrower while the lower control arm pivots stay in the same spot). The clevises therefore also act as steering stops to prevent the heim joints from binding and failing. These clevis pieces were milled manually from blocks of 7075-T651 aluminum alloy and use a circlamp design similar to a two-piece shaft collar. Four ¼"-28 bolts clamp the clevis to the 7/8 inch diameter steel rack, and provide a sufficient level of friction to transfer the expected loads with a healthy margin of safety when torque properly. These clevises also circumvent the problem of the steering rack being too wide, which prevented the rack from being mounted at the correct height with clevises on the ends and the frame going around the rack housing. A final benefit is that the rack can be slightly further forward (and higher) that it otherwise would be, which decreases the steering column angle and increases driver comfort. Figure 39 shows the actual steering clevises and they can be seen in the CAD rendering of Figure 37 installed on the rack.

Figure 39: Anti-Bumpsteer Steering Rack Clevises

Ideally, the driver and roll hoop would be moved back, with the motor controller area shortened. This would allow the chassis proper to end just ahead of the front suspension

55

attachment points, permitting the steering rack to be positioned at any height without interfering with the driver's range of motion. Before setting the width of the suspension pivot points, the rack would be chosen (if a rack was to be used) so that the problem of the rack being too wide would not occur. This would then allow much lighter, simpler clevises to bolt to the end of the rack and not apply any torsional moments about the long axis of the rack. Eliminating these moments reduces the friction in the gear mesh and eradicates the problem of angular backlash in the rack. This angular backlash was not discovered until the steering clevises, with their longer lever arms to amplify the motion, were installed. If the rack had a slot with a linear bearing that would prevent rotation of the rack this would not be an issue. Fortunately, the front wheels do not transmit forward thrust and so the rack will "take a seat" in one orientation and stay there once in motion. The angular backlash does cause toe changes and irritating steering slop at near-zero speed.

The front pushrod mounts to the top of the upright, and this placement was determined initially by the need to clear the brake rotor but more importantly is the need to accommodate large changes in camber while also allowing large steering angles up to 45 degrees (the heim joints could not therefore be oriented as they are on the rear suspension). Ordinary heim joints and ball joints did not have the right range of motion and/or were too bulky and heavy (although a suspension designed only for a single, large negative camber angle could likely use a traditional automotive ball joint). The solution was to use a clevis that holds the spherical bearing on the end of the pushrod and which also rotates within the upright. This rotation is accommodated by fiber-reinforced PTFE flange bushings from igus. The thrust face of the bushing mates with a face lathed into the 303 stainless-steel clevis and there is a 3/8" shaft protruding from that face and going through the bushings. This keeps the clevis aligned properly. In the high camber configuration the pushrod's force is almost directly in normal to the thrust face of the bushing but the low camber configuration will put significant side-loads on the clevis and the smooth rotation of the clevis is essential for steering. This clevis was turned on a lathe from a large rod of stainless steel stock and then put into a mill to make the clevis mouth. Because the machining was done accurately, the bushings have met and exceeded all expectations of smooth rotation under combined loading. The bushings are pressed into a machined tube that was welded into the top clevis of the front upright between the top control arm pivot points. This tube adds rigidity to the upright and because of the small size of the bushing it can be a small diameter. This therefore allows the top control arm pivots to be closer together for a more consistent steering axis as the upright is steered. The pushrod and rocker geometry is positioned so as to reduce the front end lift when the front wheels are steered. The clevis is in between the two pivot points in the clevis in order to reduce the torque about the steering axis caused by the force in the pushrod. The igus bushings are an essential component to this design and were sourced from Rebel Racing Products. Figure 40 shows close-ups of the clevis and the bushing area. A circlip and washer keep the clevis from coming out of the bushing when all weight is off of the tire, such as if the car were driven off a jump or if it were on a jack. The circlip only needs to support the weight of the upright and wheel and is unloaded in normal operation.

Figure 40: Front Pushrod Rotating Clevis and Bushing Area

Figure 41 shows the high-camber front uprights and links assembled.

Figure 41: Front Uprights and Links

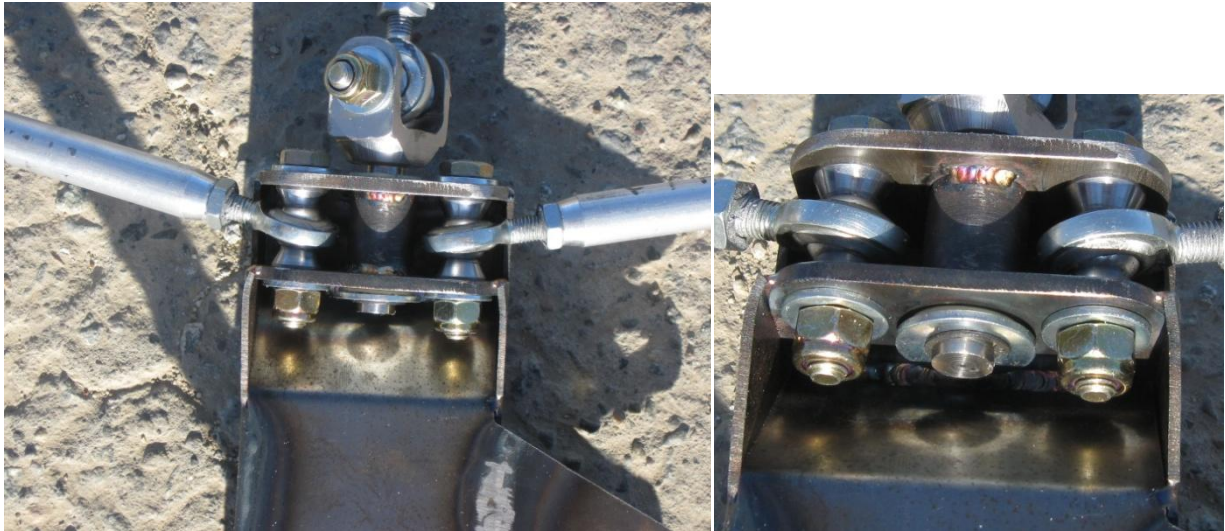Figure 42 shows the installed rotating clevis piece for the front pushrod.

Figure 42: Installed Rotating Clevis

Figure 43 shows the lower control arm pivots and the steering rod attached to the front upright. It also shows the precision, 4340 steel, high-angularity heim joint cone spacers which were outsourced to a machinist with a CNC lathe because nearly 100 of these small but precision components were required and the Formula Electric team did not have the time or skill to manufacture them.

Figure 43: Front (High Camber) Lower Control Arm Pivots, Steering Pivot, and Heim Joint Spacers

Figure 44 shows all of the suspension corners laid-out together with the steering clevises.

Figure 44: Suspension Corners and Steering Clevises

The analysis of the suspension system was completed using free-body diagrams of each upright. The forces at the tire contact patch were known from the car's expected mass properties and the maximum longitudinal and lateral accelerations desired. With 6 two-force members, each corner of the car is statically determinant and, using the known geometry, the forces in each link can be found by solving the sum of forces and sum of moments equations simultaneously. Simplifications to the geometry were made in hand calculations, which began with a front-view free-body diagram and then used the front view forces as the resultants for each pseudo-A-arm while satisfying the longitudinal force and moment equilibriums. A second, more accurate analysis was performed (after the car was constructed) using a MATLAB program with inputs being the coordinates of each pivot point obtained manually from inspection of a SolidWorks 3D sketch for one steering angle at a time. The results from this study supported the hand calculations and did not show any overloading. A more advanced analysis would incorporate the use of vector loop equations (and the Newton-Raphson method due to the nonlinear trigonometric functions involved) to find the exact geometry in MATLAB for any steering angle or camber angle, then solving the load equations for each case and finding the maximum tensile and compressive loads each link will encounter. To ensure the links are not extremely heavy or bulky it must be acknowledged that the car cannot reach maximum lateral acceleration at the same time as maximum longitudinal acceleration because of the friction circle effect. Therefore, when the front suspension is steered the assumed braking force must be reduced while the lateral force is increased and in a straight-ahead configuration the opposite is true. A reasonable factor of safety can be ensured by maintaining the expected ratio of cornering to braking force but by increasing each by the same amount. The front braking analysis must take into account the outboard brakes, which require the links to react both a force and a torque on the upright since

59

the wheel bearing reacts the force from the caliper but the two are separated by the radius of the brake rotor. The maximum deceleration assumed was 1.6g and the maximum lateral force was assumed to be 2g with a car weight of 550 pounds (which turned out to be very close to the actual weight) with a 180 pound driver.

It was discovered that the largest load during cornering at small steering angles was in the pushrod, with very little in the lateral links. This is due to the angle of the pushrod in front view. In the braking analysis and in the maximum-steering cornering simulation, forces through the front, lower links were determined to be on the order of 2,000 pounds and less than 1,000 in the rear suspension links. As a result, larger, ¼" heim joints would be necessary on the front bottom links, although the #10 rod ends initially specified would suffice on the top links and in the rear. To simplify the manufacturing, it was decided to use ¼" heim joints and bolts throughout the suspension, a decision which was wise in hindsight considering the rough handling the links received. The marginal weight gain from the larger rod ends was determined to be an acceptable trade-off for simplicity and the extra safety margin. The spherical bearing rod ends are EM4 (right hand thread) and EML4 (left hand thread) from Rod End Supply, sourced through Rebel Racing Products because they offered to sponsor the team by providing these rod ends at a much reduced price.

6061-T6 aluminum alloy was chosen for the suspension links because the largest loads are compressive and the extra yield strength of the more expensive 7075 alloy would not help modulus-controlled buckling, since the elastic modulus of 7075 and 6061 is essentially the same. An Euler buckling model was used, with an effective length of 14 inches, which is longer than the greatest center to center span of all the links. A pin-pin connection was assumed since the links have spherical bearings at each end. Thread pullout strength for 6061 was also determined to have a factor of safety of about 2 after a test showed a tensile force of 3,000 pounds was required to strip the internal threads out cleanly using a heim joint. A subsequent test using 7075 allow resulted in failure of the heim joints at the load expected based on manufacturer data. The 7075 internal threads showed no distortion and were still usable. The extra strength of the 7075 alloy is therefore primarily beneficial for maintaining thread quality over more fatigue cycles. 7075 was not in the original budget but some additional funds were procured in order to make the more highly stressed front, lower, aft links from the stronger alloy. Rods of 0.5 inch diameter were chosen for most of the links and but a diameter of 5/8 inch was necessary for the front suspension's lower rear control arms which sees large enough compressive forces under braking that the smaller diameter rods would buckle.

1/16" sheet steel was chosen for the outer walls of the uprights because it is easier to weld to the 1/8" metal used for the clevises and the thick bearing race tube than thinner metal (which would still have met strength requirements). It also has better dent resistance to keep the uprights safe from unexpected impacts during construction and from cones or rocks on the race track. The clevis pieces are thicker because they see out-of-plane loads. The front, top clevis must react the pushrod force and this is done in the form of shear in the welds between the bushing tube and the clevis pieces. The flat clevis pieces are therefore loaded in bending, although the support span is short, being boxed in on three sides and with the tube itself adding rigidity and linking the top and bottom flat clevis piece. The front, bottom clevis uses the thicker metal because it is not boxed in as much because the lower links would hit any additional webs

of metal and restrict steering angle. The steering arm is two cantilevered pieces, but the majority of the loads on them are in-plane where the section modulus is much greater. For the out-of plane loads, the cantilever distance is short and the heim joint spacers add rigidity when the bolt clamps them in. The thicker material adds minimal weight (since the clevis tabs are small) but increases the rigidity of the steering system and makes the upright more durable. 4130 normalized chrome-molybdenum steel was chosen for a higher safety factor and because the chassis is made from 4130 tubes so the team will be accustomed to welding it. The rear upright was originally designed as a CNC-machined aluminum part but the large waste as well as the unreliability of the availability of CNC machines in the required timeframe caused the decision to move to a boxed, sheet steel weldment similar in construction to the front.

The uprights both were constructed using jigs (shown in Figure 45 and Figure 47) consisting of steel plates with through-holes. Aluminum blocks bolted to the plate and then upright pieces were bolted to the aluminum blocks and held in place for welding. The base of the uprights were bearing race tubes made on a lathe and which had a lip on the inside diameter for locating the FAG (front) and SKF (rear) tapered-roller wheel bearing races when they were pressed into the tube until hitting the lip. A lip on the outside diameter mated with a sheet of steel which formed one side of the main box of the upright. All the sheet metal for the uprights was cut precisely on a water-jet machine and bent using a press-break. The SolidWorks sheet metal tool was crucial for constructing the upright in CAD and then converting the pieces to flat patterns with bend lines. Protrusions from the edges of the sheets mated with slots in other pieces to locate the sheets relative to each other and to help hold them together for welding. The uprights were self-jigging in this regard. This and the bearing cup lip are shown in Figures 45 and 46, depicting the high-camber front left upright.

The front, high-camber jig could be used for both left and right uprights without modification while the rear jig could also be used for both left and right uprights but this required relocating the clevis tab spacer blocks on the bottom. The blocks were taken off the jig plate and used to make the top and bottom clevis sub-assemblies. These were made from a piece of square 4130 tube cut diagonally to make a right angle. This was used to box the clevises and make it easier to weld up the rest of the main upright box. Care was needed to ensure the bottom clevises were mirrored, as they are asymmetrical. The welding process involved putting one block with two tabs on, welding both of those tabs, then inserting another block and tab and welding that until a series of three clevises were welded on one end of the angle piece. Those were then bolted to the jig plate along with the fourth clevis block and tabs. The outer tab for the fourth clevis was welded and then the clevis blocks were removed from the jig plate so the inner tab of the fourth clevis could be welded. Finally, the blocks were put back on the jig plate along with the simpler top clevis piece and the rest of the sheet metal so that the whole upright could be welded. The first piece to weld is around the bearing tube on the inside of the inner face sheet. Then the rest can be done in any order. Revisions to the jig that would be made with the knowledge gleaned from actually making an upright would include windows in the jig plate to allow some welding of blind joints without taking the clevis pieces off the jig so much.

The front upright also began with making the top and bottom clevis pieces, then bolting them to the jig along with the bearing tube and inner face sheet, welding the inner face sheet to the bearing tube, and then welding the rest of the sides of the upright on.
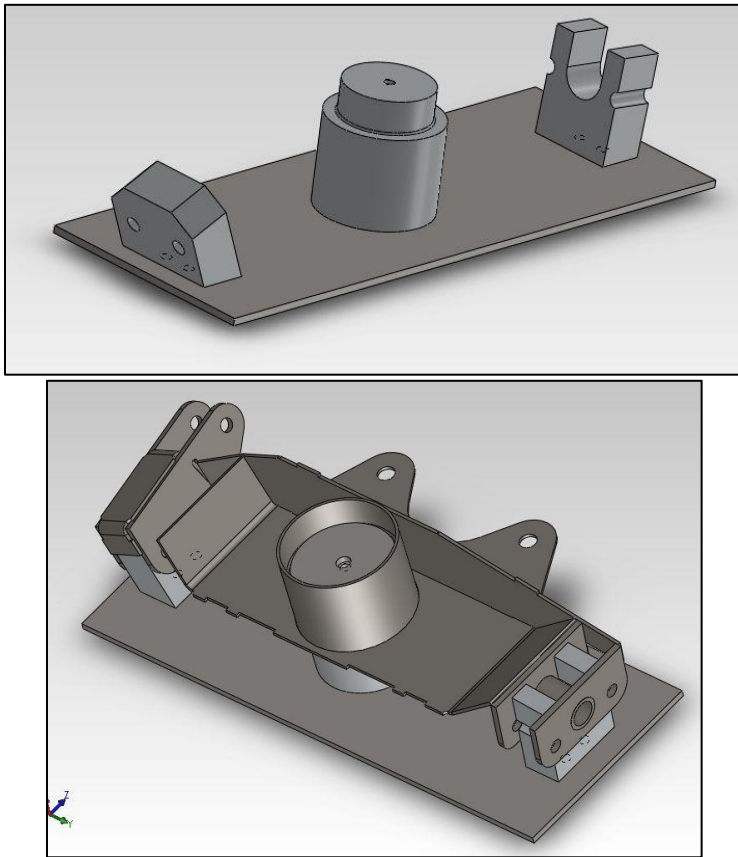
Figure 45: Front Upright Jig and Partially-Constructed Left Front Upright

The low-camber front uprights require a different hole spacing in the jig plate as well as different top and bottom clevis blocks. The same jig plate could have both hole patterns cut in it so only one would be required. The center aluminum round piece which locates the bearing tube can also be reused.
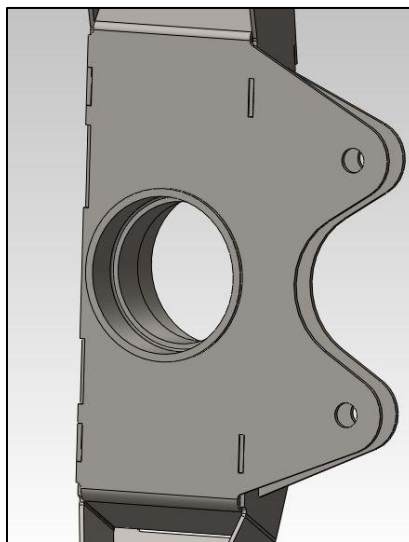
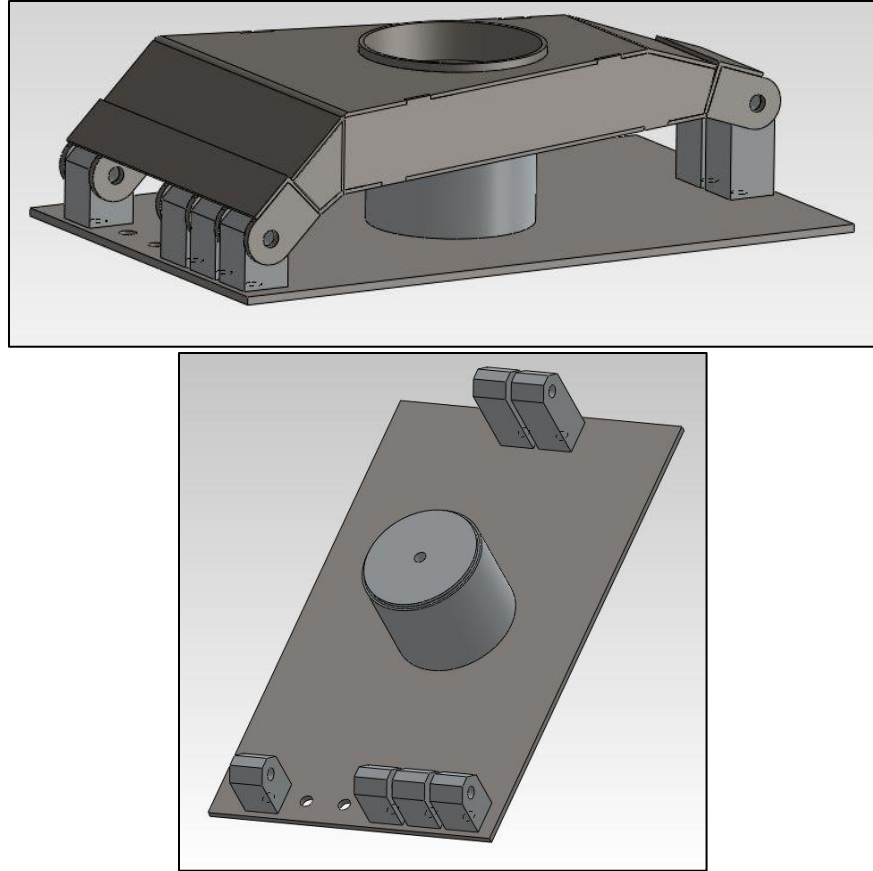**Figure 46: Tongue-and-Groove Joints for Self-Jigging**

Figure 47: Rear Upright Jig

The suspension rockers are simple weldments consisting primarily of two triangular sheets of 1/16" 4130 steel sheetmetal and a tube connecting the two. The pivot points on the chassis will have two ½" inside diameter by 3/8" long igus L280 flange bushings pressed into a 0.95" wall thickness, ¾" outside diameter 4130 steel tube. These bushings are lighter, cheaper, and smaller than ball bearings and do well when dirt gets in them. A 303 stainless-steel sleeve will go around a ¼" bolt and have the ½" diameter bearing surface. The stainless steel sleeve will be clamped by the bolt between two 4130 steel tabs welded to the chassis. Stainless steel is one of the best (lowest friction and wear) materials for use with igus L280.

The most challenging part of fabrication involved accommodating an inaccurate chassis and a change in the chassis necessitated by an incomplete SolidWorks model of the drivetrain. Jigs were fabricated to place the suspension tabs in the correct relative positions (particularly important in the front for the steering geometry) and these helped very much when welding. The simple 1/8" 4130 steel tabs had to be re-made and notched in back to accommodate a complete re-do of the rear half of the chassis, since a tube was interfering with the inner constant velocity joint. This meant the suspension tabs had to rotate and become longer to compensate. The rockers and springs also had to move but these are more flexible. In the front, one side is nearly perfect because of the jig being used before the upper chassis tube was welded in, but the other side has the top suspension point too high. Nothing could be done other than to move the suspension point up as well because the angle of the clevis was important. Figure 48 is a rendering of the front tab jig. It is made out of 6061-T6 aluminum alloy and can be used for both

right and left sides of the car by switching which holes the center piece connects to. The bottom tabs clamp onto the square frame rail that makes up the floor of the chassis. The tops go over the round tube that runs from the front roll hoop to the front bulkhead.
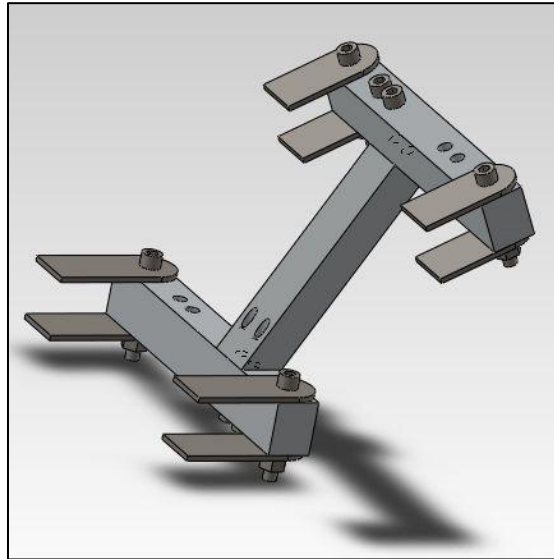

Figure 48: Front Suspension Tab Jig

Recommended Revisions

- Reduce the kingpin inclination to avoid steering snatch.
- Do not use drop-down clevises on the steering rack. Place the inner steering link pivot point on the axis of the rack in order to reduce the stress on and friction in the gear mesh. Obtain a steering rack that is narrow enough for the desired kinematics or change the kinematics to suit the rack being used. Make the chassis go around the rack if necessary, or else move the driver back so that the chassis can end in front of his or her feet.
- Increase the magnitude of the scrub radius to at least an inch positive or negative to reduce the steering weight due to tire scrub at very slow speeds.
- Use bearings instead of bushings for the rocker arms. The bushings require too much precision on the running surface of the inner race. Bearings come with the precision machining already done.
- Put more extensive jigging in the budget so that the chassis can be made to fit the suspension points and not the other way around. Link the left and right jigs of the front suspension and rear suspension together so that each is kept in the same plane. Include rocker arm pivot points and spring pivot points in the jigging, along with steering rack mounts in the front. Linking the front and rear suspension jigs together is not a high priority because the wheelbase can vary within the current manufacturing tolerances without significant changes in the front-to-rear weight distribution.
- Make go-no-go gages/jigs for the links to make the suspension geometry more accurate (though the pushrod and toe-links will likely need to be adjusted on the car). These would be simple steel or aluminum plates with holes milled in them. One rod end would be screwed in almost all the way and then bolted (with one

spacer cone) to the plate. The link would then be turned to adjust the center-to-center length until a bolt could be put through the other rod end into the desired hole in the jig (using another cone spacer to ensure the bolt is normal to the jig.

- Use 7075 aluminum alloy and alloy steel rod ends for all links, if the budget allows, in order to increase fatigue life and safety margins.

Design Verification

Structural Testing

Tests were carried out on the link assemblies using the model 1331 Instron Servo Hydraulic Load Frame in the Cal Poly Composites Lab. Initial tests were done for thread pullout, and more extensive tests done following a very unexpected failure of the right front suspension on the maiden drive and which occurred during a relatively low-speed turn and without impacting any obstacles. The driver was completely unhurt and the rest of the car was fine.

Link loads are known to a high degree of confidence because the 6 link system is statically-determinant and the heim joints closely approximate a zero-moment joint (friction means they can support a small moment and the threaded holes in the links cannot be perfectly concentric with the rod, causing a moment). Therefore, overloading was not believed to be the cause. Most heim joints were bent or broken and it was not known which joint broke first. One probable cause is the improper handling of the links during the construction of the car. Against the protestations of the suspension team, links were stepped on such that the aluminum rod bore weight as a beam in bending. Links were also allowed to fall, sometimes with the weight of the upright on them, and be caught by the misalignment cones, which produces a large bending moment in the links, and, more importantly, the threaded section on each rod end. Additionally, the threaded sections sometimes rested on the squared-off edge of the steel table while supporting the weight of the car. In the future, much more care should be taken during assembly and the suspension should be either assembled completely (on a corner-by corner basis) or taken off entirely.

Due to the simple-to-manufacture design, a new link was made the day after the failure (only one was damaged) and all heim joints were replaced on that corner, with the car running briefly that night with the suspension functioning properly. Some of the rod ends from the failed corner which did not appear to be damaged were tested the next day, along with several brand new joints. At the end of the school year another test ended in a suspension failure, this time the other front corner with the old heim joints. The driver reported steering snatch but it is not known how much steering was applied when it happened, since the frame is not as wide as it should have been in order to have the rack clevises act as steering stops. The car had made many turns at moderate speeds before the failure, and since the side with new heim joints did not break it is not known if the cause of both failures was the mishandled heim joints, too much steering available, or errors in calculating link loads

Link buckling strength did not agree with Euler buckling calculations for a solid aluminum rod with pinned ends and a length equal to the center-to-center distance between the heim joint balls. The longer rod in Figure 49 showed a buckling strength of about 2250 pounds, which is about what the Euler calculation is for an aluminum rod with pinned ends and a length

equal to only the aluminum part of the link, not the actual support span. The calculation for the actual center-to-center distance gives a result of about 1750 pounds, close to where the short link went nonlinear. The longer link assembly failed when the aluminum rod buckled in the first mode shape.
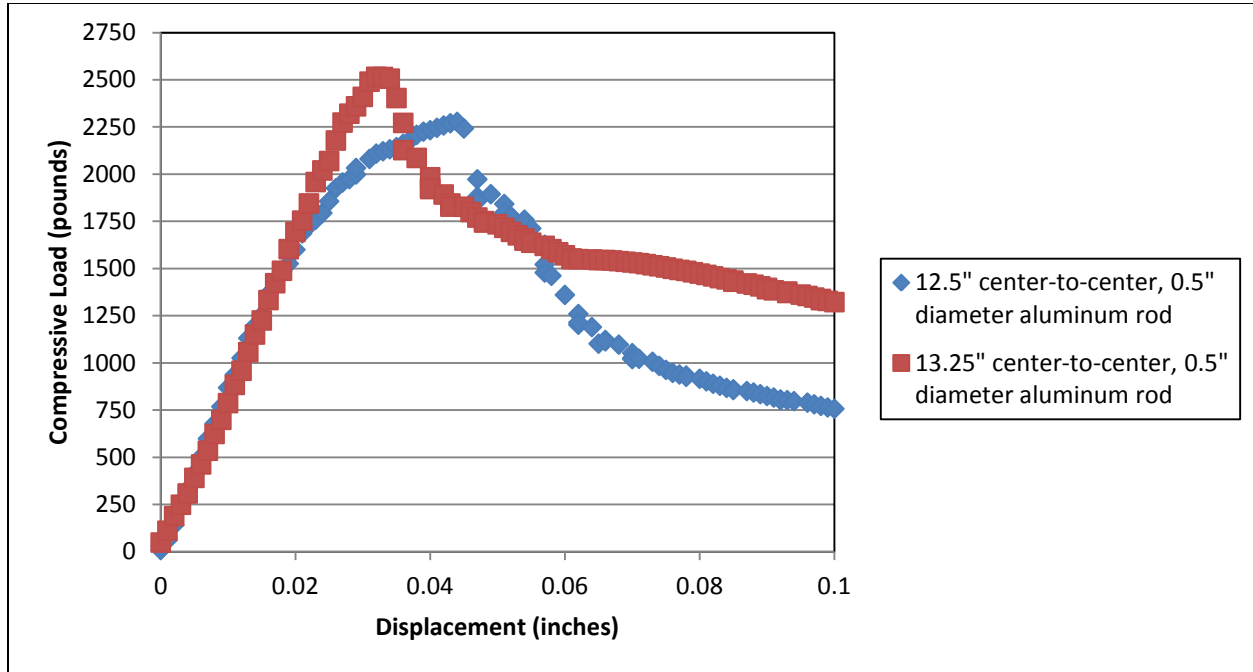

Figure 49: Link Buckling Test Results

The shorter link departed from a linear load-displacement curve at about 250 pounds below the Euler buckling strength for the center-to-center distance. The failure mode was bending of one of the heim joints at the threaded shank, just above the face of the aluminum rod which it was screwed into. The exposed thread length was greater than that of the longer link, but the heim joints were new. The rod ends on the long link were ones that appeared unbent but which were from the failed right front corner. This suggests that there is a critical length for exposed heim joint threads below which the aluminum rod fails and above which the heim joint fails. In both cases the 6061-T6 aluminum threads were still usable after the test, supporting the tensile testing in Figure 50 which shows that the pullout strength of these 0.5 inch diameter 6061 rods was about 3000 pounds. 7075 threads were also tested using a piece of 0.75 inch diameter scrap but with the same ¼-28 threads. The 7075 thread pullout strength could not be measured because the heim joints would break first. The link was so strong that it was used for at least half a dozen tensile and compression tests, even up to 4000 pounds, without damaging the interior threads.
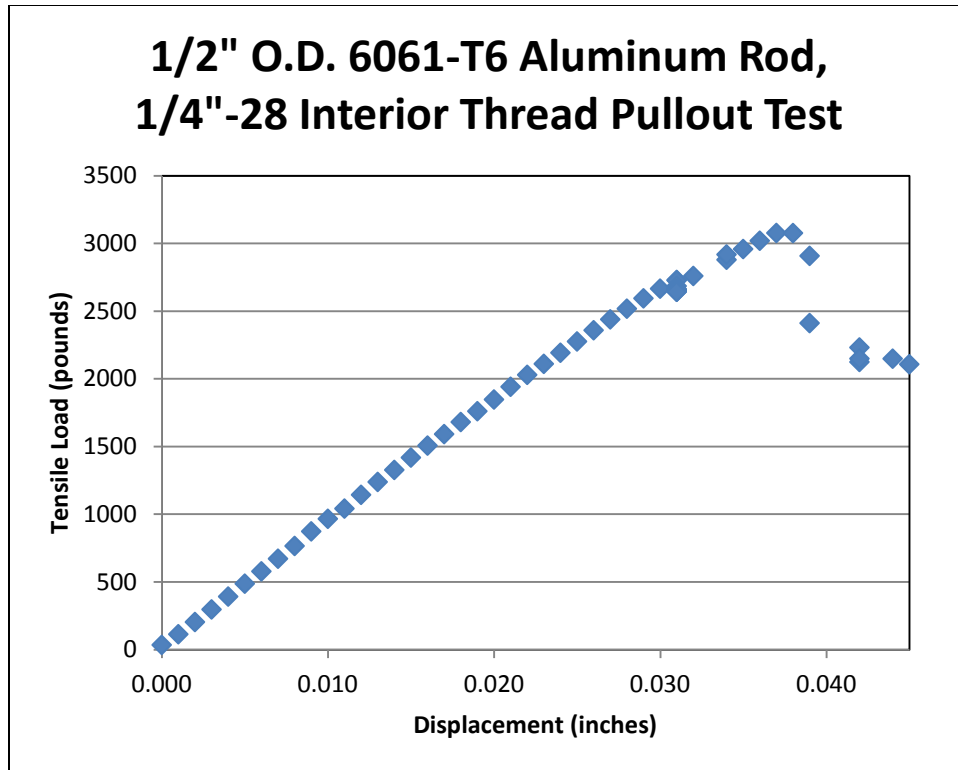
Figure 50: 6061-T6 Aluminum Alloy Thread Pullout Test Data

The buckling of the rod ends themselves was then tested, with results shown in Figure 51. It can be seen that exposing twice as much total shank length results in a lower effective modulus for the link, because the series where both heim joints were extended shows a shallower slope to the load-displacement curve. Also apparent is that the new heim joint took about 1500 pounds, or about 66%, more load than the "old" heim joint which came from the failed front right corner but which appeared undamaged. All of the rod ends in this test had performed either a tensile or link buckling test beforehand but emerged seemingly undamaged. Any undetectable necking from tension or bending from compression could cause early buckling. The softer release of load from the old heim joints means they were probably slightly bent. The reason why the 0.649 inch thread exposure was chosen is that this was as far into the 0.75 inch diameter 7075-T651 link that one of the rod ends would go, even though the others would go further. This was one of the joints in the double exposure test. A slight bend could cause the joint to not go all the way into the rod. The new heim joint failed nearer to its theoretical compressive strength limit (3400 pounds) than its Euler buckling strength (24000 pounds), though the end condition for the length of the shank was more complicated than pin-pin, having the spherical bearing housing at one end and a rigidly fixed to a very stout aluminum link (about 6 inches long) at its other end with another pin connection at the end of that. This buckling failure was very rapid and energetic, releasing more load in a split second that the other joints held at their peaks. The nonlinearity of the loading curve could be plastic deformation due to straight compressive loading rather than bending. Figure 51 and Figure 50 show that predicting the buckling strength of a link is difficult.
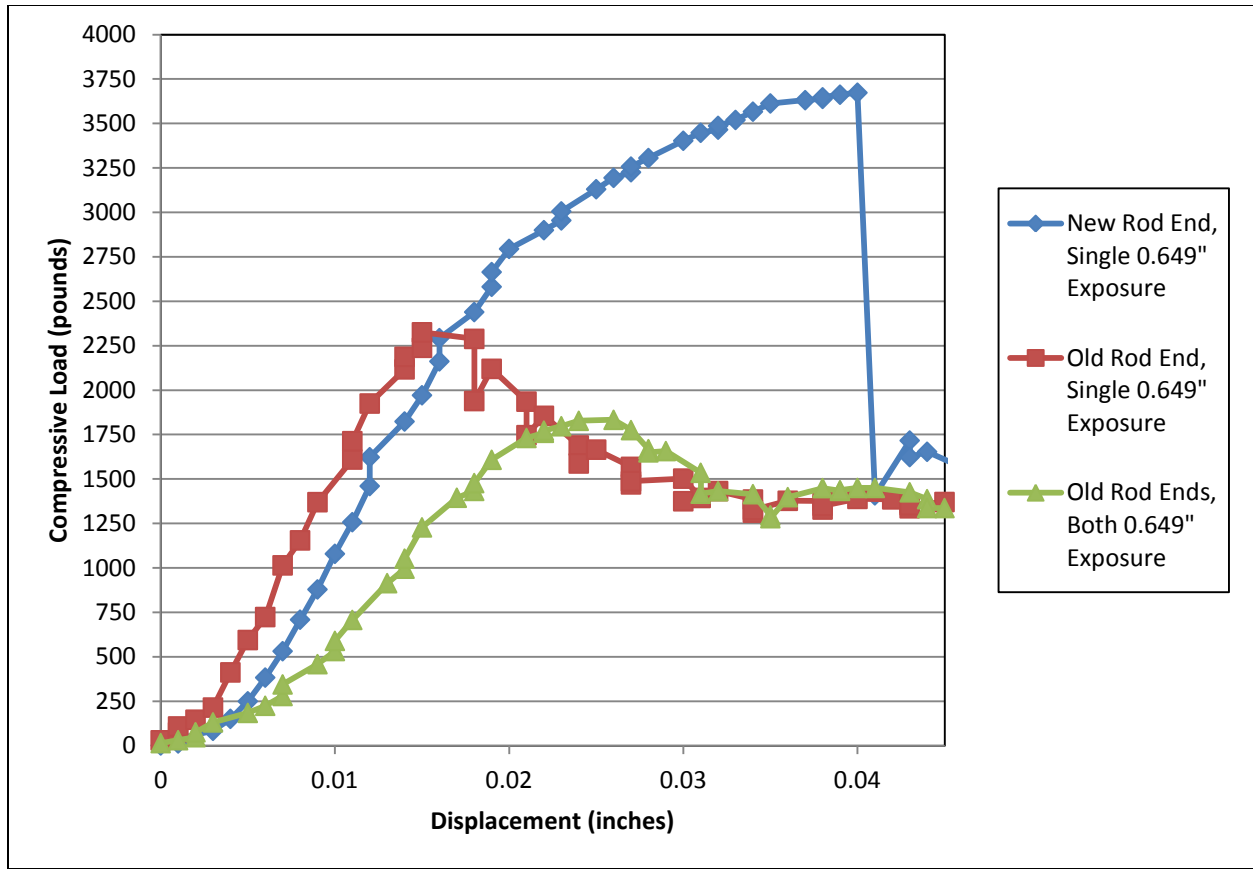
Figure 51: Rod End Shank Buckling Test

The tensile strength of the heim joints was twice what it was expected to be after preliminary tests using similar looking rod ends found in a box of spare hardware from previous Formula Electric cars. These broke at only 2300 pounds, or 700 pounds short of the 6061-T6 aluminum thread pullout strength. Fortunately, the heim joints obtained through Rebel Racing Products met and exceeded their claimed ultimate strength of 3820 pounds. This can be seen in Figure 52. The new heim joint was subjected to multiple pulls because the spherical bearings began to slip out of the hydraulic grips on the first two runs. Clamp pressure was set low on the first run in order to minimize the distortion out-of-round of the spherical bearing, which would cause more friction in the rod end and change the stress state in the housing, possibly even binding enough to change the end conditions on the links. For run 2 the clamp pressure was raised but the grips still slipped. Run 3 had the spherical bearing inserted further into the clamps, where the knurling was deeper, and this resulted in a good enough grip to break the joint on the third run at a peak load of 3940 pounds. The joint behaved remarkably linearly (elastically) up to 3800 pounds, almost exactly its rated load. This means the joint has a lot of usable strength when new, despite its low price and high angularity capability. The rod end from the failed suspension corner went to a higher ultimate load of 4070 pounds, but departed from the linear region at only 2500 pounds, perhaps due to damage in the accident or due to slippage in the clamps since it occurs near where the trend of the second run becomes nonlinear. The spherical bearing may have been located in a slightly different location in the clamps which did not have as much grip. Strain hardening due to accident damage would have resulted in a longer linear region and a lower ultimate strength, which is likely what occurred for the new heim joint after three loading

68

cycles. The first three plots have been shifted so that they all begin at zero displacement, so any hysteresis due to strain hardening cannot be seen. The rod end was not visibly deformed so the plastic deformation was small and apparently the joint does not lose much ultimate strength from the process. Therefore, peak loads greater than those due to the maneuvering forces of the vehicle could produce some strain hardening, but the joint should still function normally and have a greater elastic limit afterwards. There is about a 1000 pound margin before the onset of strain hardening in the link with the highest load, which occurs in the front links during braking.
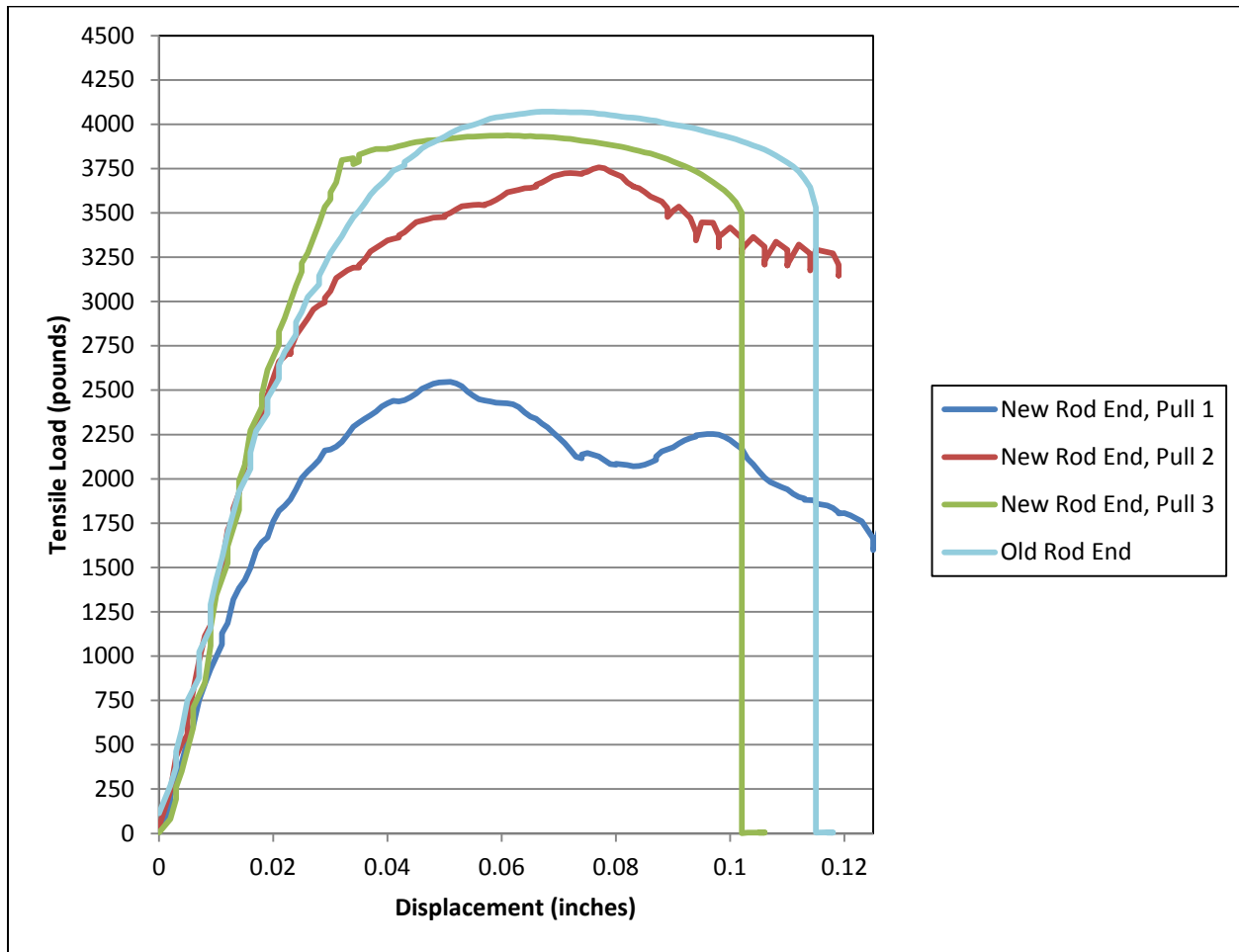

Figure 52: Tensile Strength of Heim Joints Sourced Through Rebel Racing Products

Testing Procedure

Research suggests that -40 degrees of camber is best for lateral acceleration but 0 degrees is best for longitudinal acceleration. The intermediate goals of testing are to determine the correlation between camber and lateral grip and the relationship between camber and longitudinal grip. This data will then be used towards the final goals of developing a formula to determine optimum camber angle for a particular track and determining if Polynx would have produced more lateral acceleration.

The testing procedure is to first perform left and right skidpad tests with the high camber (-22 degrees) setup, measuring maximum lateral acceleration using a 3-axis accelerometer aligned to the

vehicle axes and mounted to the car at the location of the mass center when viewed from overhead. Multiple laps will be driven in each direction and only the maximum sustained lateral acceleration will be used to determine performance. The lateral acceleration will be corrected for the roll of the car by using the data from the vertical channel, which should be 1g if the car is flat. After skidpad tests, maximum thrust will be determined with the same accelerometer via straight-line acceleration tests.

After the high-camber tests the right side suspension corners will be switched to the 0 camber configuration. This will simulate the Polynx dynamic camber design. A right skidpad test will then be performed to determine how much, if any, the inside tire is hampered by the negative camber.

Next, the left suspension will be reconfigured to low camber and the same skidpad and longitudinal acceleration tests will be performed as were with the high camber configuration. If available, square-shouldered tires would be used at this point as another comparison. The longitudinal grip is expected to increase but the lateral acceleration to decrease.

To cancel-out any asymmetries in the chassis and suspension points, the right suspension will then be changed back to a high camber setup and a left skidpad test performed. Following that, the left side will be reset to high camber as well so that the car is symmetric and can be driven for purposes other than camber tire testing.

After careful reading of the existing data on camber cars, it appears that there should not be a significant gain in lateral acceleration (on the order of 0.05g) when the inside tire is vertical as opposed to negatively-cambered. If there is, however, then Polynx is justified. The rest of the data will be plotted and curves fit to them so that the relations between camber and lateral grip and camber and longitudinal grip can be determined. To develop a formula for the optimal negative camber angle it must be known how longitudinal acceleration and lateral acceleration improve lap time at a particular circuit. A first attempt at this would involve going from steady-state turning through the arc length of a turn to full acceleration to full braking (the braking point would need to be back-calculated knowing the entry speed to the corner and assuming a constant deceleration) to steady-state turning, etc. and therefore ignoring transients. This would give a good idea of how important lateral grip and longitudinal grip are for lap time and the relations found with the test data would then be inserted into the lap time formula, leaving one variable of camber. Minimizing the lap time function would then yield the optimal camber angle. The relation between camber and lateral grip and the correlation between camber and longitudinal grip could be approximated as linear with just the two points of data, but the turnbuckle adjustment of the suspension links allows for several camber angles near each of the extremes to be examined as well. This would give information on how nonlinear the relationships are. A linear approximation may or may not be sufficient.

Further skidpad testing would involve shifting ballast to change the front-to-rear weight distribution and to change the mass center height. Additional tests would include a steering wheel position sensor in combination with the accelerometer so that transient response can be measured along with the oversteer/understeer balance. Linear potentiometers attached to the suspension rocker (with a known motion ratio) could be used to tune dampers and to study the lateral force response to weight transfer with negatively-cambered tires (effectively a relaxation length). The transient test results could then be used to refine the torque vectoring control system.

References

Milliken, William F. *Equations of Motion.* Cambridge MA, U.S.A.: Bentley Publishers, 2006. Print.

Milliken, William F., & Douglas L. Milliken. *Race Car Vehicle Dynamics*. Warrendale, PA, U.S.A.: SAE International, 1995. Print.
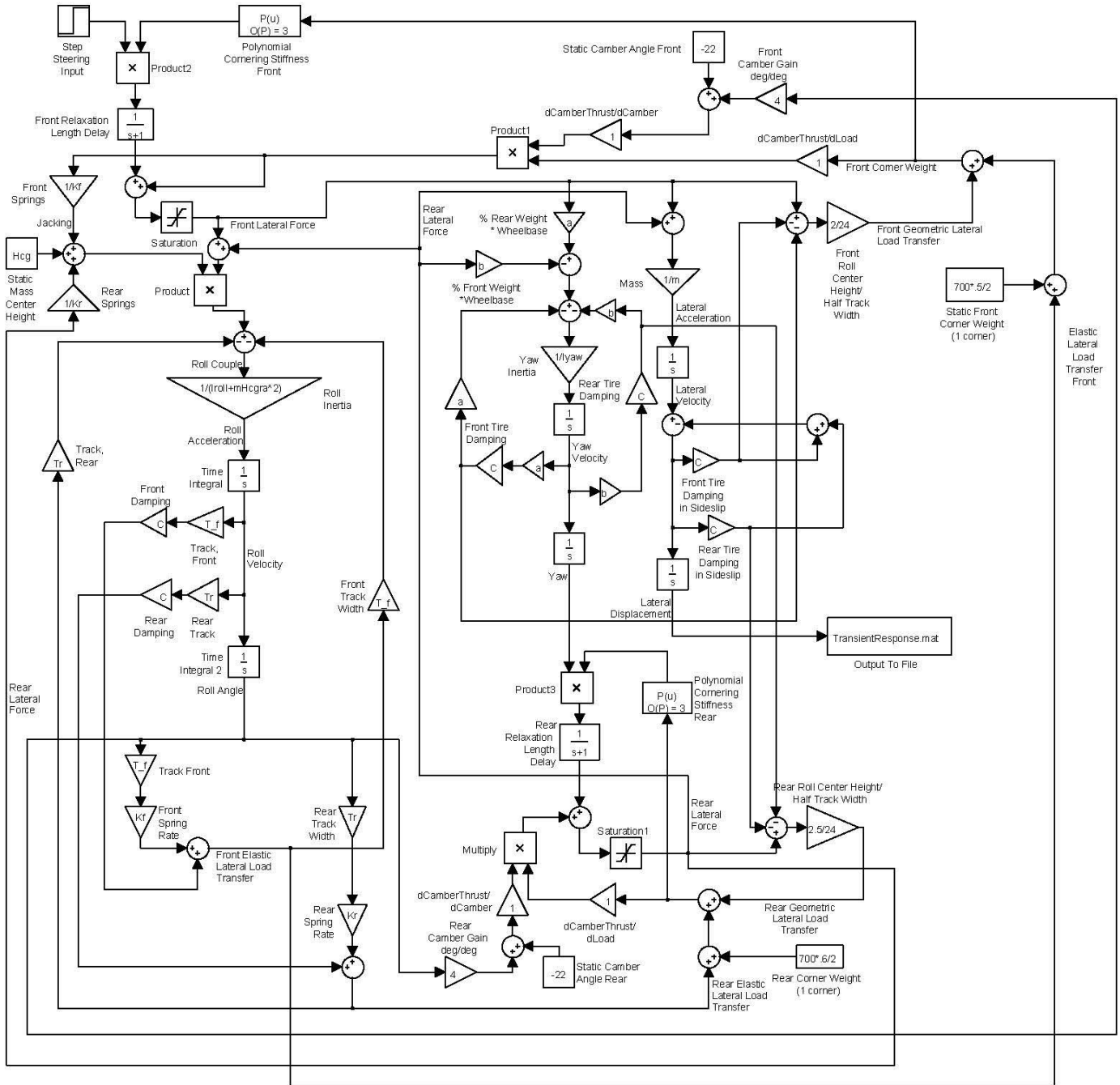
Pacejka, Hans B. *Tire and Vehicle Dynamics.* 3rd ed. Oxford, UK: Elsevier Ltd., 2012. Print.

Cossalter, Vittore. *Motorcycle Dynamics.* 2nd English edition. Lexington, KY, U.S.A.: Lulu, 2006. Print.

Fonda, Albert G. *Tyre Tests and Interpretation of Data*. Sage Publications on behalf of the Institution for Mechanical Engineers, 1956. PDF.

Formula Electric SAE Advisor: Professor Fabijanic, jfabijan@calpoly.edu, 805-756-5547

Appendix A: Simulink Modeling

Appendix B: Vendors

Aircraft Spruce
http://www.aircraftspruce.com/

Speedy Metals
http://www.speedymetals.com/

McMaster Carr
http://www.mcmaster.com/#

Online Metals
http://www.onlinemetals.com/

Rebel Racing Products
http://rebelracingproducts.com/

Rod End Supply
http://www.rodendsupply.com/index.php

Grainger
http://www.grainger.com/Grainger/wwg/start.shtml

Mid-South Minimoto
http://www.midsouthminimoto.com/

SKF Bearings
http://www.skf.com/group/products/bearings-units-housings/index.html

FAG Bearings
http://www.fag.com/content.fag.de/en/index.jsp

igus
http://www.igus.com/default.asp?c=us&L=en